Study Report SR457 [2021]

Positional material deterioration over the building envelope

Zhengwei Li and Nick Marston

Funded from the
Building Research Levy

1222 Moonshine Rd, RD1, Porirua 5381
Private Bag 50 908, Porirua 5240
New Zealand
branz.nz

ISSN: 1179-6197

Preface

This is the report prepared during research into building micro-environments and positional material degradation over the building envelope.

Acknowledgements

We would like to thank New Zealand Building Research Levy for financial support.

We would also like to thank

- Auckland Harbour Bridge Alliance
- Lauder Atmospheric Research Station (NIWA)
- Raukokore School, Waihau Bay
- Tai Poutini Polytechnic, Greymouth
- Unison Networks
- Vital Pet Food, Belfast

for allowing the installation of monitoring instruments and exposure racks on their premises

- Bryan Keen
- Nigel Kell
- Rob Causer
- Roger Stanford
- Sheng-Huei Huang

for their technical assistance

- Rob Francis of R A Francis Consulting Services Pty Ltd, Australia

for technically reviewing this report.

Positional material deterioration over the building envelope

BRANZ Study Report SR457

Authors

Zhengwei Li and Nick Marston

Reference

Li, Z. W. & Marston, N. J. (2021). *Positional material deterioration over the building envelope*. BRANZ Study Report SR457. Judgeford, New Zealand: BRANZ Ltd.

Abstract

This study characterised typical micro-environments, i.e. sheltered and exposed, on seven residential buildings across New Zealand. It revealed that environmental conditions on the building envelope were different from those of the surrounding atmosphere in terms of temperature, humidity, time-of-wetness, surface deposition, quantity of rain and UVA irradiation. Consequently, material degradation on the building envelope was different from that fully exposed to the atmosphere.

- For areas with light to moderate marine influences or strong geothermal influences, the corrosivity on the building envelope was lower than or similar to that of the surrounding atmosphere. The corrosivity in the exposed position was, in general, higher than or similar to that in the sheltered position on the same wall. This was supported by corrosion rate measurements with mild steel coupons and mild steel nails in H3.2 CCA-treated timber.
- For areas with severe marine influences, the building wall(s) facing towards the sea had a corrosivity higher than the surrounding atmosphere and the building wall(s) not facing towards the sea. The comparative corrosivity between the exposed and sheltered positions was complicated. The nails in the timber in the exposed position always had a higher corrosion rate than those in the sheltered position on the same wall. The corrosion rates of most mild steel coupons in the exposed position were higher than or similar to those of the coupons in the sheltered position on the same wall. However, the corrosion rates of some coupons in the exposed position on the wall(s) facing towards the sea were lower than those of the coupons in the sheltered positions.

This study improved our understanding of building micro-environments. It will provide in-depth information that may help inform the materials specification scheme used in relevant regulation documents as well as the design of simulated material performance testing methodologies.

Keywords

Building envelope, building micro-environment, sheltered, exposed, temperature, humidity, time-of-wetness, wind-driven rain, solar irradiation, surface deposition, corrosion, mild steel.

Contents

Figures

Tables

Executive summary

A wide variety of materials are used on buildings for cladding, decorating, fastening, framing and sealing purposes. Their resistance to environmental degradation is essential to the durability and performance of buildings. To ensure materials or functional components will meet or exceed the minimum durability requirements of the performance-based New Zealand Building Code (NZBC), a specification scheme has been established. This scheme relies on a reliable definition of the atmospheric corrosivity zone and the building micro-environment. Corrosivity zone information can be retrieved from the New Zealand atmospheric corrosivity map shown in NZS 3604:2011 *Timber-framed buildings*. Limited studies have been done to deliver a good understanding of building micro-environments for consistent building practice.

This study investigated the formation and characteristics of exposed and sheltered positions on seven residential buildings located within representative corrosivity and climate zones across New Zealand. These included Auckland, Rotorua, Waihau Bay (Bay of Plenty), Wellington, Greymouth, Christchurch and Lauder. Specific factors monitored over the building envelope included the following:

- surface temperature (and variation) (T)
- relative humidity (RH)
- time-of-wetness (ToW)
- surface (salt) deposition
- wind-driven rain
- UVA irradiation
- first-year metal corrosion rate (mild steel coupon and nail in timber).

This study revealed that the environmental conditions over the test building envelope were different from those of the surrounding atmosphere.

- The maximum surface temperature measured on the building could be up to 40°C higher than the maximum ambient temperature. It was dependent on the material type of the wall cladding, wall orientation and position on the wall. Meanwhile, the temperature on the building had a larger variation than that of the surrounding atmosphere.
- The time-of-wetness, defined as the period of T > 0°C and RH > 80%, showed a general trend of surrounding atmosphere > exposed positions on the building > sheltered positions on the building. ToW is extensively used in the atmospheric corrosion study and environmental corrosivity classification.
- The quantity of wind-driven rain on the building was significantly lower than that of the reference vertical rain. It had obvious dependences on wall orientation and prevailing/common wind direction.
- Surface deposition was dependent on the inclination angle and position of the collection surface. The horizontally inclined (0°) surfaces always collected more deposits than other surfaces no matter where they were installed, i.e. on the building or fully exposed to the atmosphere. On the building, the sheltered position always collected a larger amount of deposits than the exposed position on the same wall. This could be partly explained by the rain-washing effect. Surface salt deposition on the building also decreased rapidly with the distance from the sea.
- UVA irradiation on the building was lower than that in the surrounding atmosphere. For example, on the building in Wellington, the daily average UVA irradiation on the

south wall was approximately 6 times lower than that on the north wall and 10 times lower than that in the atmospheric environment.

This study revealed that these different micro-environmental conditions on the building may lead to material degradation that was different from that fully exposed to the atmosphere.

- The corrosion rate of mild steel coupons showed a dependence on inclination angle. The following corrosion rate trends have been observed.
  - On the test building: 0° >≈ 45° > 90°.
  - Fully exposed to the atmosphere: 0° > 45° >≈ 90°.
- The corrosivity of the surrounding atmosphere was greater than or similar to that on the building. This was particularly true in areas with light to moderate marine influences or geothermal influences (for example, Auckland, Rotorua, Wellington, Greymouth and Christchurch).
- In severe marine environments (for example, Waihau Bay), the comparative corrosivity between the building and its surrounding atmosphere was more complicated.
  - South and west walls (directly exposed to marine environment) > surrounding atmosphere >≈ north and east walls (not directly exposed to marine environment).

Surface deposition on the building could be correlated to mild steel corrosion rate. In general, a higher deposition was observed with a higher corrosion rate. However, surface deposition was not the only factor key to metal atmospheric corrosion on the building. In areas with light marine influences, environmental moisture may play a more important role.

This study revealed that material degradation over the building had an obvious positional dependence. The corrosivity in the exposed position would, in general, be higher than or similar to that in the sheltered position on the same wall. This was supported by corrosion rate measurements with mild steel coupons and mild steel nails in H3.2 copper chrome arsenate (CCA) treated timber. However, in severe marine environments, corrosion rates of some coupons installed in the exposed position on the wall(s) that were subject to direct marine influences might be lower than those of the coupons in the sheltered positions.

These experimental observations may help clarify whether current definitions and understandings of building micro-environments can support the materials specification scheme used in relevant regulation documents – NZBC Acceptable Solution E2/AS1 and NZS 3604:2011.

They also imply that, when designing a scheme for simulated material performance testing, environmental factors key to degradation must be identified and incorporated into the procedure. More attention should also be paid to sample arrangement details, purpose-built testing structure features and type of materials selected for testing.

Summary of experimental details and main findings

Building

- Auckland
- Rotorua
- Waihau Bay
- Wellington
- Greymouth
- Christchurch
- Lauder

Environment

- Atmosphere
- Micro-climate
  - Geothermal
  - Industrial
- Micro-environment
  - Exposed
  - Sheltered

Factor

- Temperature
- Relative humidity
- Time-of-wetness
- Rain
- UVA irradiation
- Surface soluble deposit
- Corrosion rate

Observation

- Environmental condition trend:
  - maximum surface temperature: building > atmosphere
  - surface temperature variation: building > atmosphere
  - UVA irradiation: building < atmosphere
  - rain: sheltered building position < exposed building position < atmosphere
  - time-of-wetness: sheltered building position < exposed building position < atmosphere
  - surface soluble deposit: sheltered building position > exposed building position
- Comparative corrosivity:
  - light to moderate marine area: atmosphere >≈ exposed building position >≈ sheltered position
  - severe marine area: building wall directly exposed to marine > atmosphere > building wall not directly exposed to marine
  - geothermal area: atmosphere > exposed building position >> sheltered building position

Implication

- Material degradation on building is position-dependent.
- Material specification scheme needs to be supported by a better understanding of micro-environmental characteristics and influences.
- Environmental factors key to material durability need to be identified and incorporated into accelerated or simulated test.
- Sample arrangement and testing structure features must be well controlled for accelerated or simulated test.

1. Introduction

The building and housing sector contributes approximately 8% to New Zealand's GDP by employing approximately 10% of our labour force (PricewaterhouseCoopers, 2016) to build and maintain our housing stock, which was valued at approximately $1,200 billion in 2020 (Reserve Bank of New Zealand, 2020).

Metals, polymers and timbers are widely used in building and construction for cladding, fastening, framing, sealing and decorating purposes. Their resistance to a variety of environmental attacks is essential to the durability and performance of buildings. The NZBC has clear and definite durability requirements for functional components used on buildings. For example, a minimum of 50-year durability must be met for components that provide structural stability or that are difficult to access or replace or where their failure may go undetected during service and maintenance.

To meet or exceed the minimum durability requirements, a scheme has been established for the specification of materials, functional components and protective measures. This has been adopted by NZBC E2/AS1 and NZS 3604:2011. This scheme uses a two-tier approach – atmospheric exposure zone (where the building will be constructed) and micro-environment identified on the building envelope (closed, sheltered and exposed). The exposure zone is defined by the New Zealand atmospheric corrosivity map. However, the understanding of building micro-environments and their influences on material degradation is relatively limited.

Micro-environments created on buildings by structural components and/or functional features are diverse. They can differ from surrounding atmospheric environments and also show large variations over the building envelope. Consequently, material degradation over the building envelope is dependent on position and location. This is particularly true for the sheltered and exposed positions that are defined by relevant New Zealand building standards.

Limited studies have been devoted to thoroughly investigate the generation and characteristics of representative building micro-environments, their influences on materials degradation and their implications for performance and durability. Some studies have been performed with purpose-built structures to determine the comparative corrosivity of sheltered and exposed conditions. However, the results obtained to date are not comprehensive and therefore cannot provide a sound base to understand the mechanisms behind and to consistently support the current material specification scheme.

Materials account for approximately 18–24% of new build costs (Deloitte Access Economics, 2018), and different grades of materials have large price differences. An improved understanding is needed of the representative micro-environments found on buildings, particularly in exposed and sheltered positions. This helps the industry make more-informed decisions about the use of fit-for-purpose materials and maintenance schemes, reducing risk of overspecification or under-specification. Over the longer term, this will lead to tangible savings, increase industry productivity and position the industry to "build right first time".

2. Literature review

In this section, the following aspects will be briefly discussed, these being based on findings from publicly available literature.

- Influences of individual environmental/climatic factors on material degradation.
- Monitoring of micro-climatic factors on the building envelope.
- Degradation behaviours of materials in open and sheltered environments.

2.1 Material environmental degradation

A variety of environmental factors such as climate and atmospheric pollution can contribute to material degradation as discussed in this section.

2.1.1 Temperature

Ambient temperature is not believed to be very important, especially for atmospheric corrosion. The material surface temperature is more important since it can directly affect relative humidity (RH), time-of-wetness (ToW) and degradation kinetics. An increase in temperature will, in general, accelerate mass transportation and electrochemical reactions. This tends to accelerate corrosion processes if environmental humidity is constant. That said, RH will normally decrease when the temperature is increased, leading to a decrease in ToW and the overall corrosion rate (Roberge, 1999). Therefore, temperature tends to affect atmospheric corrosion in more complex ways. An increase in temperature over the range of 20–40°C while holding the chloride content (160 mg/m^3) and RH (80%) constant has been observed to result in three distinct patterns with different metals (Griffin, 2006) over a relatively short period. These include:

- an increase of corrosion rate for iron
- a decrease of corrosion rate for zinc
- no change in corrosion rate of copper.

2.1.2 Humidity

RH is particularly relevant to atmospheric corrosion of metallic materials (Mansfeld, 1979). There is a critical RH (CRH) threshold below which corrosion will not occur since there is insufficient moisture to create an electrolyte layer on the metal surface (McCafferty, 2010). The CRH value is dependent on the surface condition of the metal and also the pollution level of the surrounding environment. The primary CRH for a clean metal in unpolluted air is approximately 66%. If the metal is covered with any corrosion products, a second CRH may exist. In the case of iron and steel, a tertiary CRH appears. At ~60% RH, rusting commences at a very slow rate and corrosion increases sharply at 75–80% RH. At ~90% RH, a tertiary increase in corrosion rate can be observed.

2.1.3 Rain

Rainwater is important to initiate and sustain corrosion since it maintains the humidity of the surrounding air above the CRH. If rainwater is retained in pockets or crevices of the growing corrosion products, it may also accelerate corrosion by supplying continued wetness in these localised areas (Cole & Ganther, 2006; Cole & Paterson, 2007). Regular rainwater washing could partially remove loose corrosion products, and consequently the fresh metal surface would be exposed to further attack.

On the other hand, rainwater can remove the accumulated dust and/or corrosive deposits such as salt particles partly or completely from the material surface. Rain-washing effects are particularly noticeable on inclined surfaces in marine environments (Ganther et al., 2011). A modelling study indicated that pollutants on a surface can be reduced to 10% of their original concentrations after a rainfall of 1.5 mm (Cole & Paterson, 2007). Another study found that, in areas with a monthly average rainfall of less than 100 mm, rain-washing effects would be limited (Chen, Chiu, Chan, Chang & Yang, 2013).

2.1.4 Wind

The speed and direction of wind, particularly the prevailing wind, will affect the formation and persistence of a water/moisture layer on a material surface. Wind can also affect particle accumulation on material surfaces (Klassen & Roberge, 2001; Cole, Paterson & Ganther, 2003; Schweitzer, 2006; Nguyen, Wang & Leicester, 2012). Wind can disperse airborne contaminants in larger areas. For example, in marine environments, strong prevailing winds can carry salt particles inland over long distances. However, winds with a speed exceeding a critical value have the ability to blow dry salt off metal surfaces (Cole, Lau, Chan & Paterson, 2004). They may also have a drying effect on a corroding metal surface. These may benefit corrosion resistance. In contrast, a low wind speed would favour accumulation of more pollutants, possibly contributing to a high corrosion rate. It has been found that better predicted results and/or correlations could be produced when wind was incorporated into atmospheric corrosion modelling (Oesch & Heimgartner, 1996).

2.1.5 Solar irradiation

Solar irradiation can affect ToW and subsequently the metal corrosion process. Light of certain wavelengths can stimulate photo-sensitive corrosion reactions on certain metals. The corrosion of carbon steel in sodium chloride solutions has been found to be increased by ultraviolet (UV) irradiation. This is because the conductivity of the corrosion product layer was increased in the presence of UV (Riazi, Danaee & Peykari, 2013). Potential interactions between UV light, airborne chlorides and oxidising agents such as ozone may produce reactive species that can be involved in corrosion processes. For example, it has been found that UV-induced photo-dissociation of ozone can generate reactive atomic oxygen, which can react rapidly with silver (Ag) to form Ag_2O, leading to more severe attack of the Ag surface (Chen et al., 2010). On the other hand, UV irradiation has been proved to be capable of suppressing pit generation and enhancing the passivity of AISI 304 stainless steel in solutions containing chlorides (Macdonald, Sikora, Balmas & Alkire, 1996; Moussa & Hocking, 2001).

UV light is the primary environmental factor contributing to degradation of polymeric materials, such as paints, sealants, adhesives and plastics, through auto-oxidation processes or photolytic rearrangements (Wypych, 2013; Yousif & Haddad, 2013). Signs of photo-induced degradation may include embrittlement (surface cracking), discolouration and loss of transparency.

Solar irradiation on a building envelope is not uniform and can be affected or (partially) blocked by architectural features, construction materials, functional structures, building orientation, urban morphology and/or building scale (Axarli, 2005; Martins, Adolphe & Bastos, 2014). For example, clear float glass can transmit a larger percentage of UVA radiation than polycarbonate and laminated glass, which has virtually zero transmission of wavelength shorter than 380 nm (King & O’Brien, 1995).

2.1.6 Chloride

Deposition of hygroscopic salts, such as NaCl and $MgCl_2$, can promote corrosion at low RH levels. The deliquescence relative humidity (DRH) values for NaCl and $MgCl_2$ are 76% and 33% respectively. However, considerable corrosion could be initiated and sustained down to 33% RH under NaCl and to 11% RH under $MgCl_2$ (Schindelholz, Risteen & Kelly, 2014).

Chlorides can directly participate in corrosion reactions and affect the morphology and composition of the growing corrosion products on steels (Ma, Li & Wang, 2009; Ghali, 2010). Chloride ions are known to compete with hydroxyl ions to combine with ferrous cations, leading to the formation of unstable and soluble iron-chloride complexes, which have a lower passivation effect than stable iron-hydroxyl species.

A direct relationship between airborne salt level (salinity) and atmospheric corrosion rate of mild steel has been observed (Qu, Yan, Zhang, Wan & Cao, 2002). Although the corrosion rate seems to be increased linearly with atmospheric salinity lower than 600 mg Cl^-/m^2/day, it tends to level off when atmospheric salinity is above this critical level (see Figure 1) (Alcantara, Chico, Diaz, de la Fuente & Morcillo, 2015).

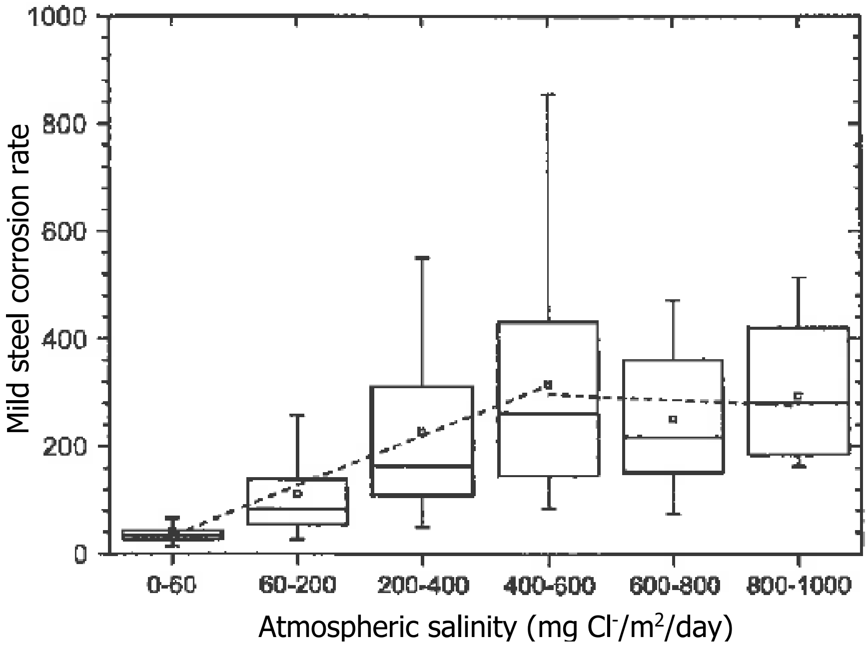

Source: Alcantara, Chico, Diaz, de la Fuente & Morcillo, 2015.

Figure 1. Correlation between atmospheric corrosion rate of mild steel and atmospheric salinity.

Most cities in New Zealand are coastal, and many buildings are within 5 km of the sea. Previous BRANZ studies suggest that sea salt-mediated corrosion rates at a distance of approximately 20 km and more inland in New Zealand were higher than those obtained on continental land masses (Duncan & Balance, 1988).

2.1.7 Hydrogen sulphide

Hydrogen sulphide (H_2S) is corrosive to most metals – for example, copper (Cu), iron (Fe), lead (Pb), silver (Ag) and zinc (Zn) – with the formation of sulphides and/or sulphates with poor protection (Lenglet et al., 1995; Tran, Fiaud, Sutter & Villanova, 2003).

In New Zealand, H_2S is often encountered within and close to geothermal areas – for example, within the Taupo Volcanic Zone of the North Island. Distribution and dispersion of H_2S is influenced by a multitude of factors, including surface terrain and weather conditions. H_2S has a higher density than air, and therefore it tends to accumulate and concentrate in low-lying areas with limited air movement.

2.1.8 Sulphur dioxide

Sulphur dioxide (SO_2) has a high solubility in water and can react with sunlight, oxygen, dust particles and water to form sulphurous acid (H_2SO_3), sulphuric acid (H_2SO_4) and sulphate (SO_4^{2-}) aerosol. The presence of sulphate ions on iron and steel leads to the formation of iron sulphate ($FeSO_4$), which can be hydrolysed to release sulphate ions in an auto-catalytic process (Badea et al., 2011). SO_2 can also lead to a decrease in the critical relative humidity for corrosion initiation. Therefore, SO_2 can cause direct damage to or accelerate the degradation of many building materials, such as stone, concrete, metal and organic coatings (WBK & Associates Inc., 2003).

2.1.9 Orientation

Under real servicing conditions, materials or components on buildings may face towards different directions at different angles. Orientation is one of the factors contributing to environmental material degradation (Jordan, 2010).

Table 1 shows that weathering steel samples fully exposed on the north side of a steel bridge in the Czech Republic corroded faster than those exposed on the opposite side. This difference has been attributed to the difference in ToW, which is affected by wind and solar irradiation (Kreislova, Knotkova, Krivy & Podjuklova, 2009).

Table 1. Corrosion loss of weathering steel samples on a steel bridge.

Position	Corrosion loss (μm)		
	1 year	4 years	9 years
South	16.8	19.3	17.5
North	21.6	43.6	58.5

Source: Kreislova, Knotkova, Krivy & Podjuklova, 2009.

2.1.10 Inclination

Materials are normally installed at different angles to the horizontal when used on buildings/structures or when exposed for performance testing (Wypych, 2013).

- 0° – provides a long wet period and gives a high degree of dirt accumulation.
- 5° – introduces some water drainage and slightly reduces dirt accumulation on the skyward surface.
- 45° – the most commonly used configuration for performance testing.
- 90° – normally results in the lowest surface temperature, solar irradiation and wetting period.
- Variable angle – allows samples to be exposed at an angle that can compensate for seasonal differences in the sun's position according to ASTM E782-95(2015) *Standard practice for exposure of cover materials for solar collectors to natural weathering under conditions simulating operational mode* and ASTM E881-92(2015) *Standard practice for exposure of solar collector cover materials to natural weathering under conditions simulating stagnation mode.*

The corrosion rates of carbon steel samples placed vertically (90°) and inclined at an angle of 30° with respect to the ground were measured after a 1-year exposure (see Table 2) (Griffin, 2006). The vertically positioned samples always corroded faster than the 30° inclined samples. This difference was particularly true for the samples closer to the sea.

Table 2. Corrosion rate ratio of vertical to 30° inclined samples.

Exposure location	Corrosion rate ratio – vertical versus 30° inclination
Kearny, NJ	1.25
Vandergrift, PA	1.26
South Bend, PA	1.20
25 m, Kure Beach, NC	1.41
250 m, Kure Beach, NC	1.25

Source: Griffin, 2006.

It was supposed that chloride deposits on the vertically positioned samples could not be cleaned as effectively as those on the 30° inclined samples. This would promote corrosion on the vertical sample surface. This mechanism could explain why the samples exposed 25 m from the sea have a larger corrosion rate ratio when compared with those exposed further from the sea. However, it is arguable that, although the vertical samples had a larger effective area for receiving sea salt impinging onto their surfaces than those positioned at 30°, these salt particles also had a larger probability of being lost from the surface.

BRANZ's study in an industrial area showed that the samples positioned at an angle of 45° could corrode at a rate approximately 2 times higher than those vertically positioned. Samples positioned at 5° always showed the highest corrosion rate among these three positions. It was believed that water and particulate matter could not be retained on the 45° inclined surface easily. Meanwhile, on the 5° inclined surface, a water layer contaminated with PM and other corrosive media could be retained for a much longer period, thus promoting corrosion.

The major pollutants found in the industrial area tested are SO_2, nitrogen oxides (NO_x) and/or particulate matter. The gaseous species could be involved in metal corrosion when dissolved into water, most commonly rainwater. As such, the retention of contaminated water on the surface would be a factor critical to metal corrosion.

The different influences of sample orientation on metal atmospheric corrosion in marine and industrial environments might be a result of the difference in type of corrosive media and their mechanisms contributing to corrosion.

2.2 Building micro-environment

2.2.1 Definition

Three micro-environments have been defined by NZS 3604:2011 (see Figure 2).

- Closed – dry, internal location, not subject to airborne salts or rain wetting.
- Sheltered – open to airborne salts but not rain washed.
- Exposed – open to airborne salts and rain wetting.

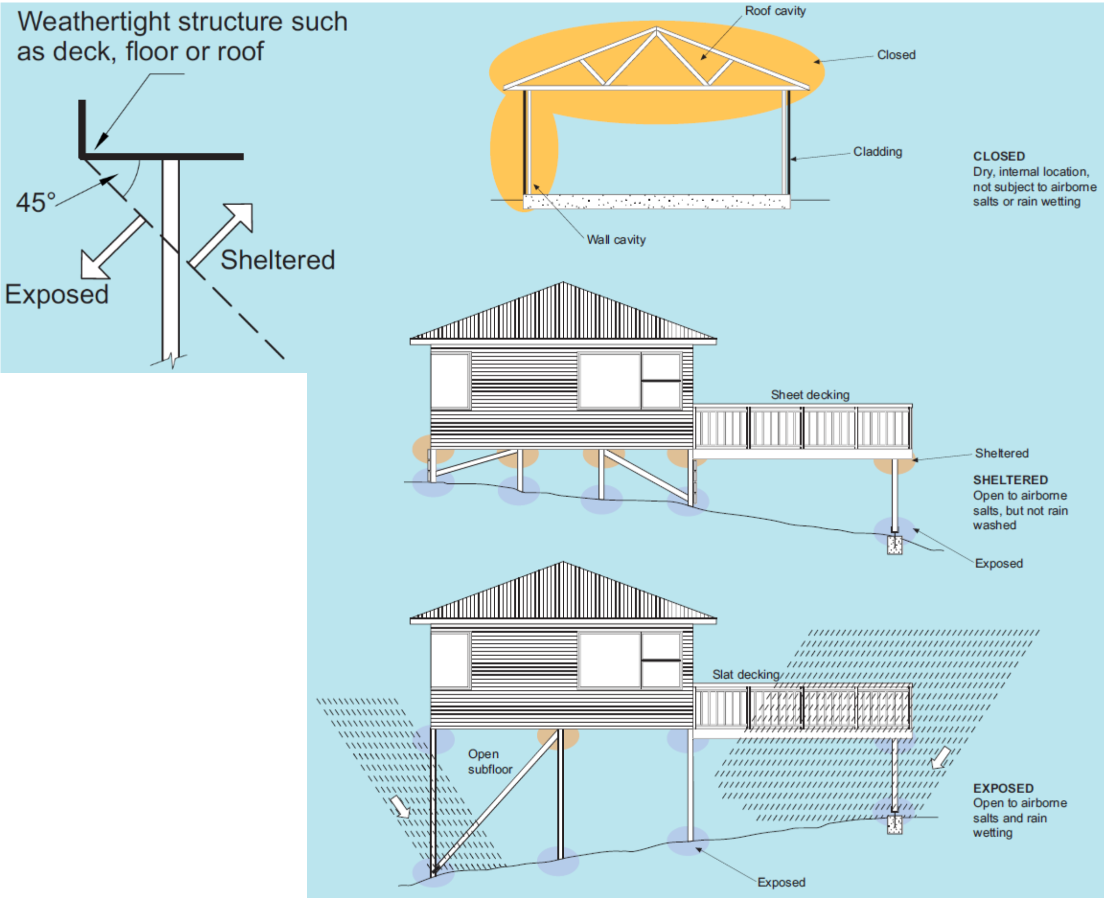

Figure 2. Schematics showing closed, sheltered and exposed micro-environments on buildings according to NZS 3604:2011.

Sheltered might be the most difficult or diverse among these three situations.

Note that the term "hidden" is also used by E2/AS1. It means concealed behind another element such that no part is visible. This micro-environment is somewhat similar to "closed" of NZS 3604:2011, but differences still exist.

2.2.2 Monitoring building micro-environment

Functional or structural components can change wind pattern, solar irradiation and/or rain collection on the building envelope. These changes can further impact surface deposition and accumulation of airborne pollutants and/or PM.

2.2.2.1 Wind-driven rain

It has been found that the actual rain load received by materials and components on building façades was heavily influenced by building geometry and design details – for example, the size of overhang (Ge & Krpan, 2007, 2009). The presence of an overhang can reduce the amount of wind-driven rain by approximately 4 times for low-rise buildings and 1.5 times for high-rise buildings. With respect to high-rise buildings, this wetting was significantly reduced for the location right underneath the overhang. The protection area provided by an overhang could extend beyond 2.5 m below the roof line for high-rise buildings and to half of the height for low-rise buildings. The width of the overhang has also been shown to significantly influence wall wetting wind-driven rain (Hubbs & Hircock, 2014; Mohaddes Foroushani, 2013).

2.2.2.2 Surface deposition

Airborne chloride deposition at locations both in the open and under a purpose-built shelter have been measured using the wet-candle technique (King & O'Brien 1995). The ratio of chloride levels in the open to the sheltered conditions is 3, 2.3 and 1.5 for severe marine, moderate-mild marine and mild marine environments respectively. Chloride levels in both open and sheltered locations also decrease rapidly with distance from the sea (see Figure 3).

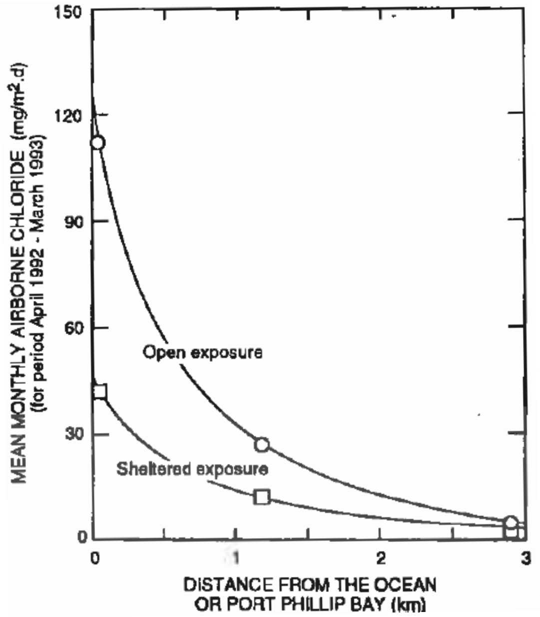

Source: King & O'Brien, 1995.

Figure 3. Correlation between airborne chloride deposition in open and sheltered locations and distance from the sea.

The concentration of water-soluble contaminants on a building's external surface could change with height (see Figure 4) (Tzanis et al., 2011). This change with height is particularly obvious with nitrate and sulphate.

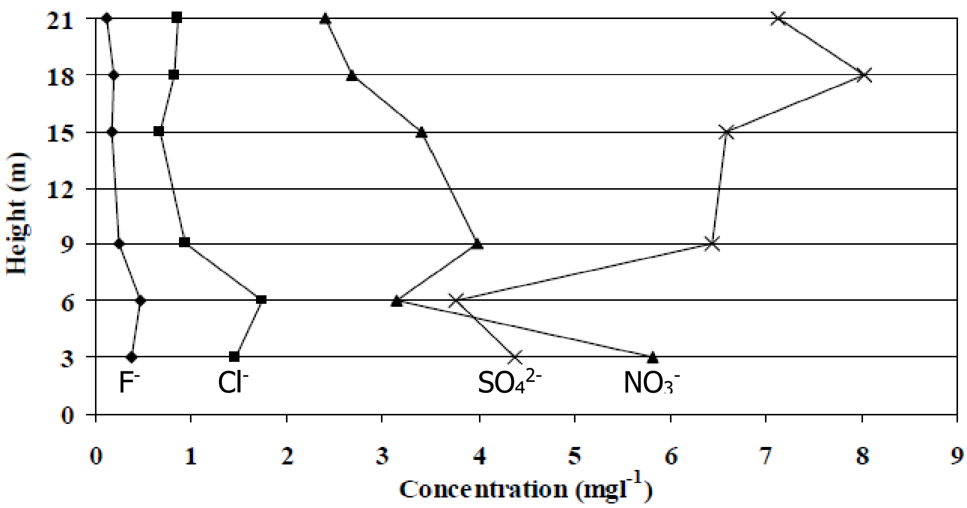

Source: Tzanis et al., 2011.

Figure 4. Changes of water-soluble anion concentrations on the surface of copper installed at different heights of a building.

2.2.3 Corrosivity of micro-environment

2.2.3.1 Implication of standards

Section 4 *Durability* of NZS 3604:2011 focuses mainly on the durability of metallic fastening and fixing components (bolts, nails, screws, nail plates and brackets). Materials specification in NZS 3604:2011 Table 4.1 to Table 4.3 appears to indicate that the exposed positions have a higher corrosivity towards steel-based fastening and fixing components when compared with the sheltered positions. For example, in zones B and C, structural steel fixings used in the sheltered positions can be protected with hot-dip galvanized zinc coatings. Meanwhile, only stainless steel fixings can meet durability requirements in the exposed positions.

Table 20 of E2/AS1 gives guidance on selection of materials for cladding, flashing and fixing applications. This table indicates that the sheltered positions are more corrosive than the exposed positions mainly due to the possible deposition of airborne salt particles on the building component surface. For example, hot-dip galvanized nails cannot be used in the sheltered positions on buildings in zone C but can be used in the exposed positions.

E2/AS1 and NZS 3604:2011 use the same approach for material specifications. However, their actual definitions of the corrosivity for specific building micro-environments are somewhat different.

2.2.3.2 Experimental observations

The atmospheric corrosion rates of zinc samples in exposed and sheltered locations within marine environments have been measured (see Table 3) (Leonard, 2003).

Table 3. Zinc corrosion rates in different marine environments.

Environment	Exposure	Corrosion rate (µm/year)
Mild marine	Open	1.0
	Sheltered	0.9
Moderate marine	Open	1.9
	Sheltered	3.9
Severe marine	Open	6.2
	Sheltered	15.2

Source: Leonard, 2003.

Note: Detailed description of mild, moderate and severe marine environments was not given.

In a mild marine environment, the corrosion rates measured in both open and sheltered locations were very similar – 1.0 and 0.9 µm/year respectively. In a severe marine environment, the corrosion rate measured in the sheltered locations could be approximately 2.5 times higher than that measured in the open locations.

This observation indicates that shelter could increase corrosion rate. However, this is only obvious when a large quantity of airborne sea salt particles is produced.

This could be further demonstrated by the correlation between metal corrosion rate and the level of airborne chloride (see Figure 5) (Griffin, 2006).

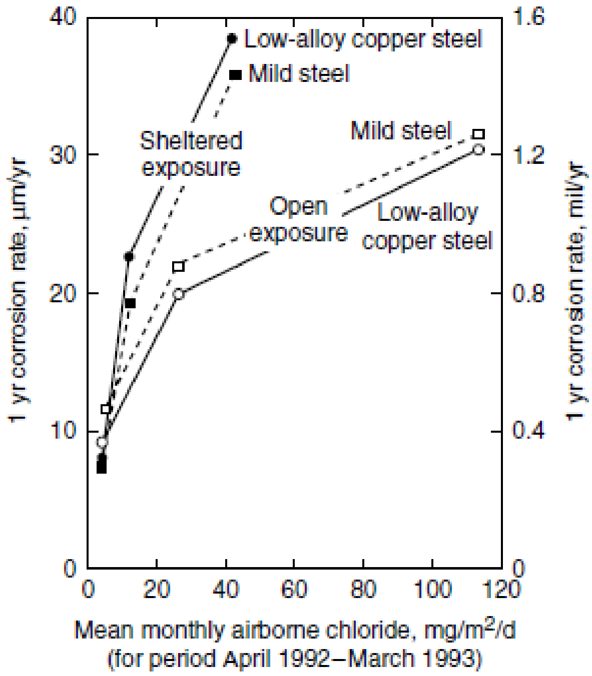

Source: Griffin, 2006.

Figure 5. Correlation between metal corrosion rate and monthly airborne chloride.

It is supposed that rainwater could remove some of the salt particles deposited onto the zinc surface. Shelters could decrease this positive rain-washing effect and therefore increase the accumulation of sea salt particles. These particles could contribute to the accelerated corrosion through some mechanisms.

However, salt deposition on a material surface is complicated and can be affected by many factors. These typically include:

- the condition of the sea
- the distance from the sea
- the speed and direction of prevailing winds
- the surface condition of material
- the quantity and frequency of rainfall.

Therefore, the exact influences of such a shelter on material degradation might not be simple.

Some studies have shown that large-scale open shelters – for example, aircraft shelters – that have free access to the atmosphere can reduce airborne chloride accumulation and then metal corrosion (see Figure 6) (Drozdz, Abbott & Jackson, 2007; Jett, Andrews, Barfield, Jett & Abbott, 2007).

This type of shelter could be different from the sheltered situation discussed previously in terms of changes in local environment, airborne contamination transportation and deposition. These have not been experimentally investigated, and therefore their actual influences on material degradation have not been clearly understood.

The type of atmospheric environment matters when discussing sheltering effects. For example, the corrosion rates of zinc in sheltered locations compared to open locations have been found to be reduced by 3.8 times, 2.4 times and 2.2 times in rural, urban and industrial environments respectively (Zhang, 2005). However, corrosion of zinc in sheltered locations would be increased by approximately 1.4 times when exposed to a marine environment. This increase was explained by the lack of rain to wash away the deposited sea salt particles on the sample surface. Note that the severity of this marine environment was not discussed in this reference.

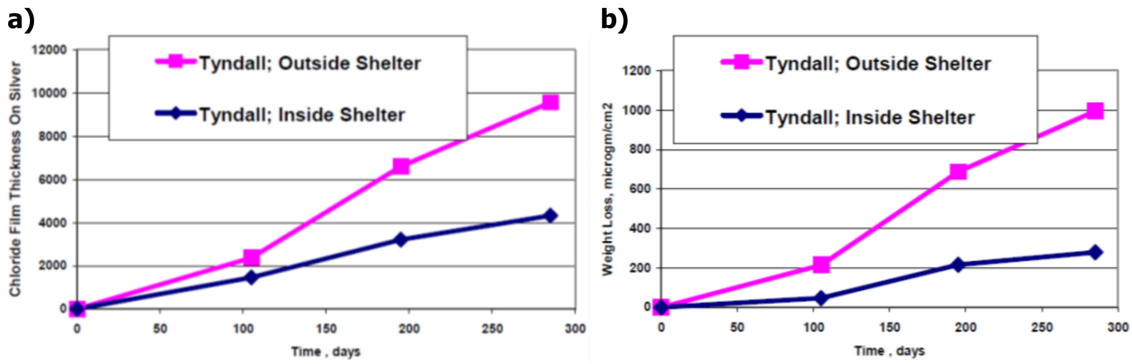

Source: Drozdz, Abbott & Jackson, 2007.

Figure 6. Chloride accumulation (a) and aluminium corrosion loss (b) under aircraft shelter.

Table 4. First-year corrosion rates of metallic samples exposed in sheltered and open marine-influenced environments.

Site	Exposure	First-year corrosion rate (µm/year)				
		Mild steel	Copper steel	Zinc	Zn-5%Al	Zn-55%Al
Navy Base (severe marine)	Open	31.8	30.3	6.94	3.22	1.47
		29.9	29.7	5.49	3.27	1.36
	Shelter	34.6	37.4	14.36	13.65	9.55
		36.2	39.8	15.95	12.70	10.77
Water Board (moderate-mild marine/rural)	Open	22.5	20.1	1.91	0.43	0.35
		21.3	19.4	1.85	0.43	0.34
	Shelter	17.9	21.3	3.76	1.29	0.58
		20.5	23.6	4.12	1.09	0.65
CSIRO (mild marine/urban)	Open	11.2	9.9	0.99	0.30	0.23
		11.2	10.0	0.96	0.27	0.25
	Shelter	8.9	8.3	0.90	0.70	0.41
		7.8	9.0	0.96	0.73	0.41

Source: King & O'Brien, 1995.

The corrosion rates of different materials exposed in sheltered locations have been measured at three marine environments in Australia (King & O'Brien, 1995). The first-year corrosion rates of mild steel and copper-bearing low-alloy steel samples exposed in the sheltered locations are not very different from those in the open locations (see Table 4). However, the corrosion rates of zinc, Zn-5%Al and Zn-55%Al samples exposed under a specially designed shelter are remarkably higher than those of equivalent in the open location. This indicates that different materials may respond differently to the environment modified by a physical shelter.

2.3 Summary

The limited research available on micro-environments showed that critical environmental conditions such as wind-driven rain and surface deposition can vary in different positions on a building. However, how the building micro-environments are formed and to what extent they can impact materials performance and durability are not clearly understood. For example, the exact influences of physical shelters on material degradation have not been thoroughly investigated.

Research has also shown that purpose-built sheltering structures for simulated tests in specific environments have the potential of exaggerating the influences of certain environmental factors (Carter, Linstrom, Flinn & Cramer, 1987). This could affect the degradation processes and/or mechanisms occurring on the surface of the material concerned when compared to the exposure – for example, on actual building envelopes. Thus, it would be practically challenging to establish micro-environmental exposure conditions similar to those on a building to investigate their actual influences on material performance and durability.

3. Objective

A survey of literature has shown that systematic investigation and quantitative characterisation of micro-environmental conditions on actual buildings would be valuable. The results of such a study would provide comprehensive comparative, trusted data and information to improve our understanding of the complex interactions between atmospheric environment, structure components and building materials.

This research therefore aimed to explore the formation and characteristics of typical micro-environments over actual building envelopes and their influences on material degradation and performance. It aimed to perform in situ monitoring of environmental conditions on buildings located within representative New Zealand atmospheric corrosivity and climate zones. Specifically, it sought to deliver a good understanding of the conditions of typical exposed and sheltered micro-environments over building envelopes. This includes the following:

- characteristics of the atmospheric environment in which the building is located – for example, climatic conditions, airborne pollutants and atmospheric corrosivity.
- micro-environmental conditions created by functional and/or structural features on buildings – for example, surface temperature, RH, ToW, wind-driven rain, solar irradiation and surface deposition.

This research then aimed to define the comparative corrosivity of specific micro-environments over the building envelope. Specifically, it quantified the interactions between materials and building micro-environments in terms of material nature, configuration and orientation. This should allow a micro-environmental corrosivity mapping over the building envelope.

This proposed micro-environmental monitoring and materials performance testing has two implications for material specifications:

- To ensure that materials and/or components, when chosen as acceptable or alternative solutions for construction, will meet or exceed the performance requirements of NZBC E2/AS1.
- To provide information and guidance for the establishment of effective and efficient schemes for maintenance of materials and buildings.

Overall, this study aimed to provide data and information that could improve our understanding of building micro-environments and help reduce inconsistent specification of materials and/or protective measures for building practice. This could then help reduce over-specification or under-specification, thus delivering buildings with reasonable construction costs and minimising premature failures.

4. Experimental

4.1 Monitoring site and building

Seven buildings were recruited for this monitoring. Their locations are shown in Figure 7 together with atmospheric corrosivity zone (NZS 3604:2011).

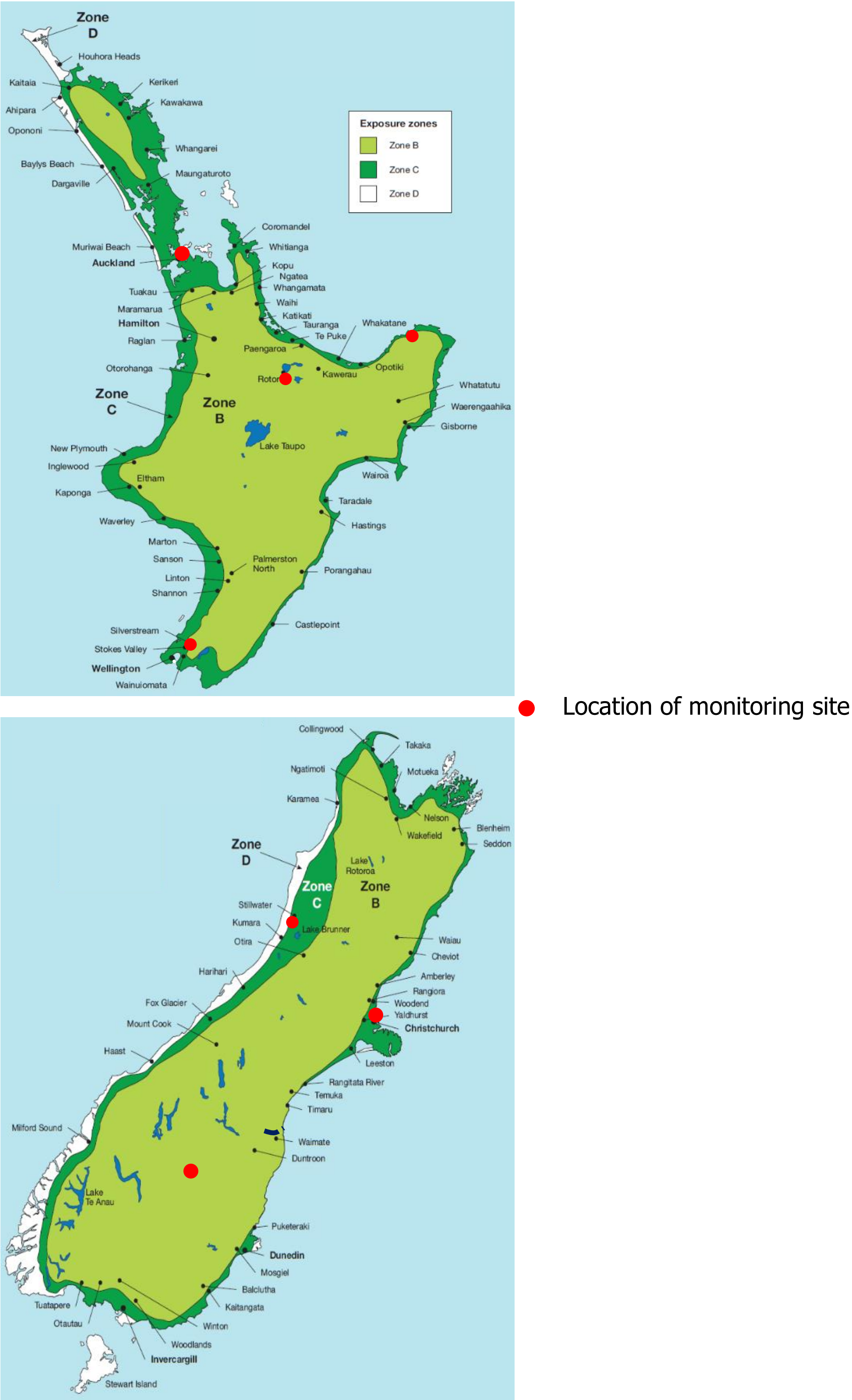

Figure 7. Location of monitoring buildings.

4.1.1 Auckland

Auckland is within the Northern New Zealand zone – a subtropical climate zone with warm humid summers and mild winters. Typical daytime maximum air temperatures range from 22–26°C in summer and 12–17°C in winter. This zone has an average of 2,000 annual sunshine hours and a prevailing southwest wind.

The test site is close to the Auckland Harbour Bridge and is subject to marine and traffic influences. The atmospheric environment could be classified as zone D (ISO 9223[1] C4 – High) according to NZS 3604:2011 atmospheric corrosivity map since it is within the area 500 m from the sea.

The test building (~13 × 11 m) has an A-shaped, corrugated roof cladding, white timber weatherboard wall cladding and a ventilated subfloor space.

4.1.2 Rotorua

Rotorua is within the Central North Island climate zone and is sheltered by high country to the south and east. It has warm, dry and settled weather during summer and cool and unsettled winters. Typical daytime maximum air temperatures range from 21–26°C in summer and 10–14°C in winter. This zone has an average of 2,000–2,100 annual sunshine hours and a prevailing southwest wind.

Rotorua is a large population centre in the Taupō Volcanic Zone with numerous geothermal features and systems. Surface geothermal activities are mainly confined to three areas: Whakarewarewa/Arikikapakapa, Kuirau Park/Ōhinemutu and Government Gardens/Ngapuna/Sulphur Bay.

The test site lies to the west of Sulphur Bay. Sulphur Bay is in the southeastern corner of Lake Rotorua and stretches from Motutara Point to Ngapuna. Puarenga Stream flows into Sulphur Bay and features geothermal activity at its mouth – fumaroles, mudpools and steaming grounds.

The test building is a rectangular shaped concrete building (~13 × 7 m). Its length is placed roughly along the southwest to northeast direction.

4.1.3 Waihau Bay

Waihau Bay is within the Northern New Zealand climate zone.

The test site, approximately 30 km northeast of Te Kaha, is exposed to severe marine influences. Whakaari/White Island, New Zealand's most active cone volcano, is approximately 63 km northwest. Continuous emissions could exert some influences on the atmosphere of some areas in the Bay of Plenty, including Waihau Bay. Its most recent eruption occurred on 9 December 2019. Therefore, this test site may have a combined influence of marine and volcanic activities. This is quite different from the Auckland and Rotorua test site.

The test building, approximately 60 m east of the coastline, is a regularly shaped, single-level construction with timber weatherboard wall cladding, painted long-run corrugated metal roof cladding and a low ventilated subfloor space.

[1] ISO 9223:2012 *Corrosion of metals and alloys – Corrosivity of atmospheres – Classification, determination and estimation.*

4.1.4 Wellington

Wellington is within the South-West North Island climate zone. This zone is quite windy due to its exposure to disturbed weather systems from the Tasman Sea. Typical daytime maximum air temperatures range from 19–24°C in summer and 10–14°C in winter. This zone has an average of 2,000 annual sunshine hours and a prevailing northwest wind.

The test site is within BRANZ's campus at Judgeford, Porirua. It is a sheltered semi-rural environment, separated by approximately 5 km from the nearest saltwater, a tidal estuary, and further protected from the open sea by gently rolling hills. It lies within zone C (ISO 9223 C3 – Medium) of NZS 3604:2011 atmospheric corrosivity map based on severity of exposure to marine aerosols.

The test building (~12.55 × 7.25 m) is an uninhabited, typical 1960–70s New Zealand residential house. It is rectangular shaped and has an A-shaped roof space covered with corrugated 55%Al-Zn alloy roof cladding. The wall cladding is fibre-cement weatherboard with a colour of light green. The house is supported on uniformly distributed timber posts and therefore also has a regular subfloor space. The length direction of this building is from east to west.

4.1.5 Greymouth

Greymouth is the largest town on the West Coast of the South Island. It is within the Western South Island climate zone. This climate zone features very high mean annual rainfall. Summers are mild with daytime maximum air temperature typically ranging from 17–22°C. In winter, daytime maximum air temperatures typically range from 10–14°C with frequent frost.

The test site at Puketahi Street is approximately 1.8 km away from the coastline.

The test building is an irregularly shaped, single-level building (~18.5 × 13.2 m) with weatherboard wall cladding, long-run corrugated roof cladding and a subfloor space. Its length is roughly along the north to south direction.

4.1.6 Christchurch

Christchurch is within the Eastern South Island climate zone, which is largely influenced by the lie of the Southern Alps to the west. In summer, daytime air temperature is moderate, typically ranging from 18–26°C. In winter, daytime maximum air temperatures typically range from 7–14°C. Prevailing wind is normally from the northeast, while southwesterlies are more frequent during winter. Mean annual rainfall in this climate zone is low.

The test site is located in Belfast and is influenced by light emissions from a pet food processing factory. It is approximately 6.4 km away from the coastline.

The test building is a regularly shaped, single-level building (~11 × 7 m) with brick veneer wall cladding, long-run corrugated roof cladding and a subfloor space. Its lengthwise orientation is approximately southwest to northeast.

4.1.7 Lauder

Lauder is within the Inland South Island climate zone. Its climate is largely influenced by the lie of the Southern Alps to the west. Maximum daytime air temperatures typically range from 20–26°C in summer and 3–11°C in winter. Severe frosts can happen frequently with occasional snowfalls in winter. The strongest winds are often from the northwest. Annual rainfall is low. Lauder has one of the cleanest and most pollution-free atmospheres in the world.

The test site is within NIWA's Lauder atmospheric research station (approximately 35 km from Alexandra).

The test building is a regularly shaped, single-level building (~13 × 7–11 m) with brick veneer wall cladding, metal roof tiles and a low subfloor space. Its lengthwise orientation is approximately southwest to northeast.

4.2 Atmospheric environment monitoring

The conditions of the atmospheric environment surrounding each of the seven test buildings were monitored and the data was used as a baseline for comparative analysis. This was achieved by installing a weather station by BRANZ or downloading data from the National Climate Database (i.e. a weather station operated by NIWA or MetService is close to the site). Table 5 shows the monitoring details at the seven test sites.

Table 5. Atmospheric environment monitoring details.

Site	Climatic factor	Weather station
Auckland	Hourly ambient temperature Hourly relative humidity Hourly wind speed and direction	Station on the bridge (height 67 m) that is very close to the test building
	Daily rainfall	Station agent number 37852 Installed within Rosedale wastewater treatment plant Approximately 9 km north of Auckland Harbour Bridge
Rotorua	Hourly ambient temperature Hourly relative humidity Hourly wind speed and direction Daily rainfall	Station agent number 41077 West of Sulphur Bay Very close to the test building
Waihau Bay	Hourly ambient temperature Hourly relative humidity Hourly wind speed and direction Hourly rainfall	BRANZ's weather station approximately 10 m east of the test building
Wellington	Hourly ambient temperature Hourly relative humidity Hourly wind speed and direction Hourly vertical rainfall Half-hourly UV irradiation	BRANZ's weather station approximately 100 m east of the test building
Greymouth	Hourly ambient temperature Hourly relative humidity Hourly wind speed and direction Daily rainfall	Station agent number 23934 Installed within Greymouth airport Approximately 1.8 km southwest from the test building

Site	Climatic factor	Weather station
Christchurch	Hourly ambient temperature Hourly relative humidity	iButtons
	Daily rainfall	Station agent number 4843 Installed within Christchurch airport Approximately 7.6 km southwest from the test building
Lauder	Hourly ambient temperature Hourly relative humidity Hourly wind speed and direction Daily rainfall	Station agent number 5535 Installed within NIWA Lauder atmospheric research station Very close to the test building

4.3 Building micro-environment

The environmental factors monitored on the test buildings include the following:

- Temperature – the surface temperature of the wall cladding.
- Relative humidity – the humidity of the air close to the wall cladding surface. Note that measurement of temperature and humidity was achieved by using programmable high-resolution 1-Wire Hygrochron iButtons.
- Time-of-wetness (ToW) – calculated based on hourly temperature and relative humidity measurements (T_{air} > 0°C and RH_{air} > 80%).
- Wind-driven rain – only monitored on the building in Wellington using a purpose-built rain collector together with a commercially available rain gauge (see Figure 8). The rain collectors were installed in two positions on the wall:
  - The boundary between sheltered and exposed positions.
  - Fully exposed position on the wall (i.e. lower end of the exterior wall).
- Surface deposition – to measure surface soluble deposits. In marine influenced areas, these may include primarily sea salt particles. This measurement was completed using a salt contamination meter (Elcometer 130T, Elcometer Ltd).
  - On the test building in Wellington, this measurement was performed on specially installed collection surfaces. These collection surfaces were installed at three angles: 0° (horizontal), 45° and 90° (vertical). Collection plates were made of different materials such as stainless steel, plastic and glass. This is to minimise surface condition changes during the testing period and to investigate material influences on dirt accumulation.
  - On the test buildings in Auckland, Waihau Bay, Greymouth and Christchurch, the measurements were performed directly on the vertical surface of painted timber weatherboards or window frames.
  - On the test building in Lauder, the measurement was performed on the vertical surface of an aluminium window frame.
- Solar irradiation – carried out only on the building in Wellington. It monitored UVA irradiation (315–400 nm) over the building envelope. Sensors (SKU 421, Skye Instruments Ltd) were installed at one location at the boundary between sheltered and fully exposed on each wall (see Figure 9). The data was collected half-hourly.

Note that:

- temperature and RH were not monitored on test buildings in Auckland and Rotorua
- surface deposition was not monitored on the test building in Rotorua.

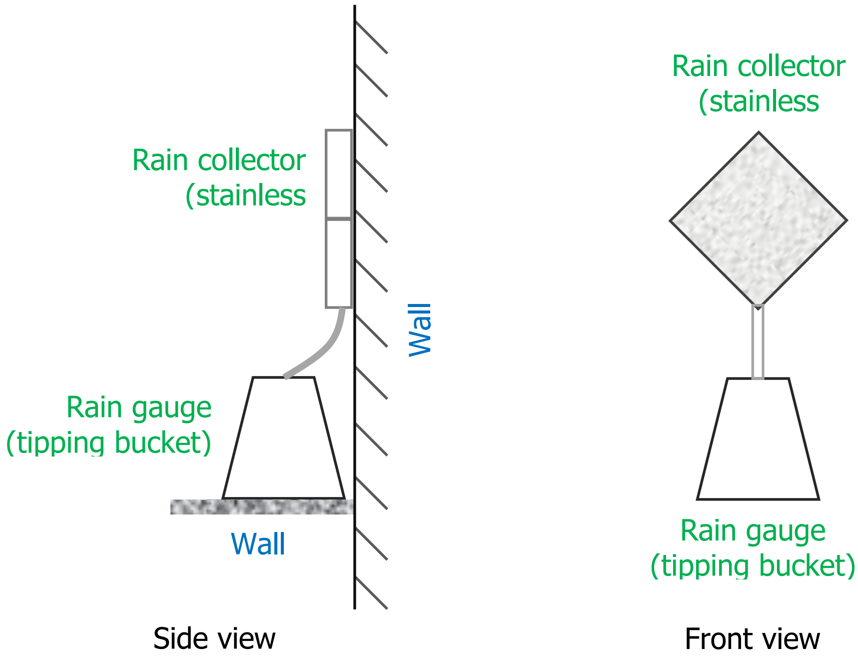

Figure 8. Schematic of the device for wind-driven rain measurement on the wall.

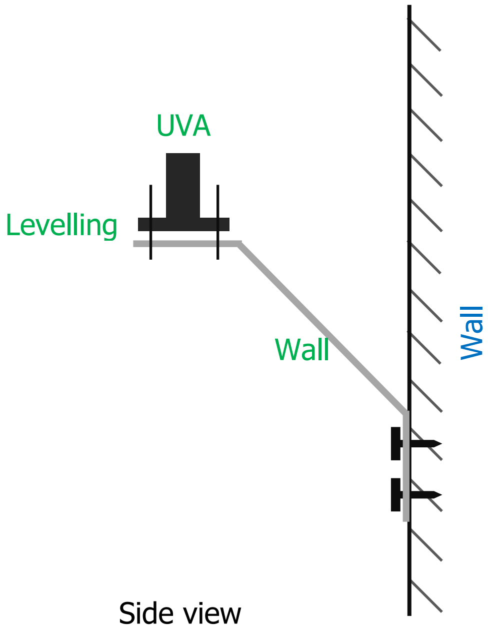

Figure 9. Schematic of UVA sensor installed on the wall.

4.4 Environmental corrosivity

Two types of samples were used to characterise the corrosivity of micro-environments on the test buildings.

- Mild steel coupons – steel plates with typical dimensions of ~120 × 80 × 1 mm (800 grit surface finish) used for position-dependent corrosivity characterisation on the buildings. These coupons were installed at three inclination angles relative to the ground: 0° (horizontal), 45° and 90° (vertical). Their back surfaces were completely sealed with wax, therefore only the front surface was exposed to the environment.

- Mild steel nails – clean nails (~3.15 × 75 mm) manually driven into H3.2 CCA-treated timber blocks (~20 × 20 × 100 mm) (see Figure 10).

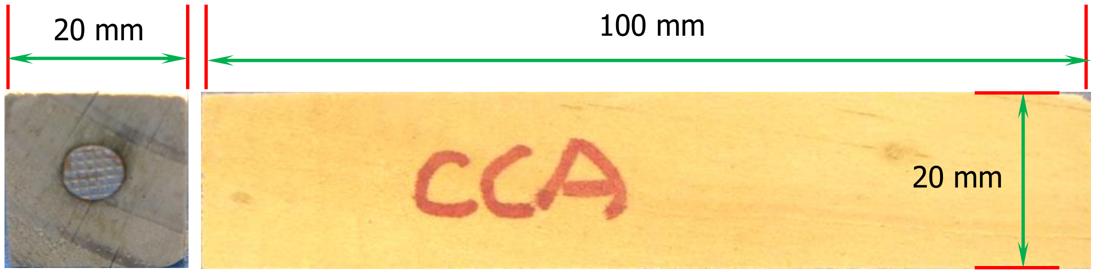

Figure 10. Mild steel nail driven into timber block for corrosion test.

Two groups of reference samples were exposed at each test site.

- The first group used mild steel coupons with typical dimensions of ~120 × 80 × 1 mm (800 grit surface finish). They were installed on the four sides of a rectangular rack (~0.6 m × 0.4 m), which was in the same orientation as the test building. On each side of this rack, three coupons were installed at 0°, 45° and 90° relative to the ground.
- The second group used standardised metallic coupons – mild steel (sand blasted to SA2.5 finish, ~150 × 100 × 3 mm), copper (800 grit surface finish, ~150 × 100 × 0.6 mm) and zinc (800 grit surface finish, ~150 × 100 × 0.6 mm). At most exposure sites, they were positioned towards the north at an angle of 45° at a height of approximately 3 m.

To determine the first-year corrosion rates, the corrosion products remained on the metal surfaces were cleaned thoroughly following the procedures recommended by ASTM G1[2]:

- Copper: 0.1 L/L sulphuric acid (H_2SO_4, specific gravity: 1.84, 98%) at 20–25°C.
- Mild steel: 0.5 L/L hydrochloric acid (HCl, specific gravity: 1.19, 38%) + 3.5 g/L hexamethylenetetramine ($C_6H_{12}N_4$) at 20–25°C.
- Zinc: 100 g/L ammonium chloride (NH_4Cl) at 70°C.

The chemically cleaned samples were rinsed with flowing water, dried with hot air and reweighed to determine their mass losses due to atmospheric exposure. Several clean, unexposed metal samples were subjected to the same cleaning process, and their mass losses were recorded for corrosion rate measurement correction.

[2] ASTM G1-03(2017)e1 *Standard practice for preparing, cleaning, and evaluating corrosion test specimens*

5. Results

5.1 Test building in Auckland

5.1.1 Atmospheric environmental conditions

The highest hourly ambient temperature was approximately 25.9°C while the lowest was approximately 5°C during the 1-year monitoring period (May 2017 – May 2018). Time-of-wetness and rainfall during this period were approximately 3,251 hrs (level $\tau 4$) and 1,323 mm respectively. The prevailing winds were from the west-southwest (WSW) and southwest (SW), although less frequently the wind would blow from the north-northeast (NNE) and northeast (NE) directions (see Figure 11). The maximum wind speed was approximately 24.2 m/s during this period.

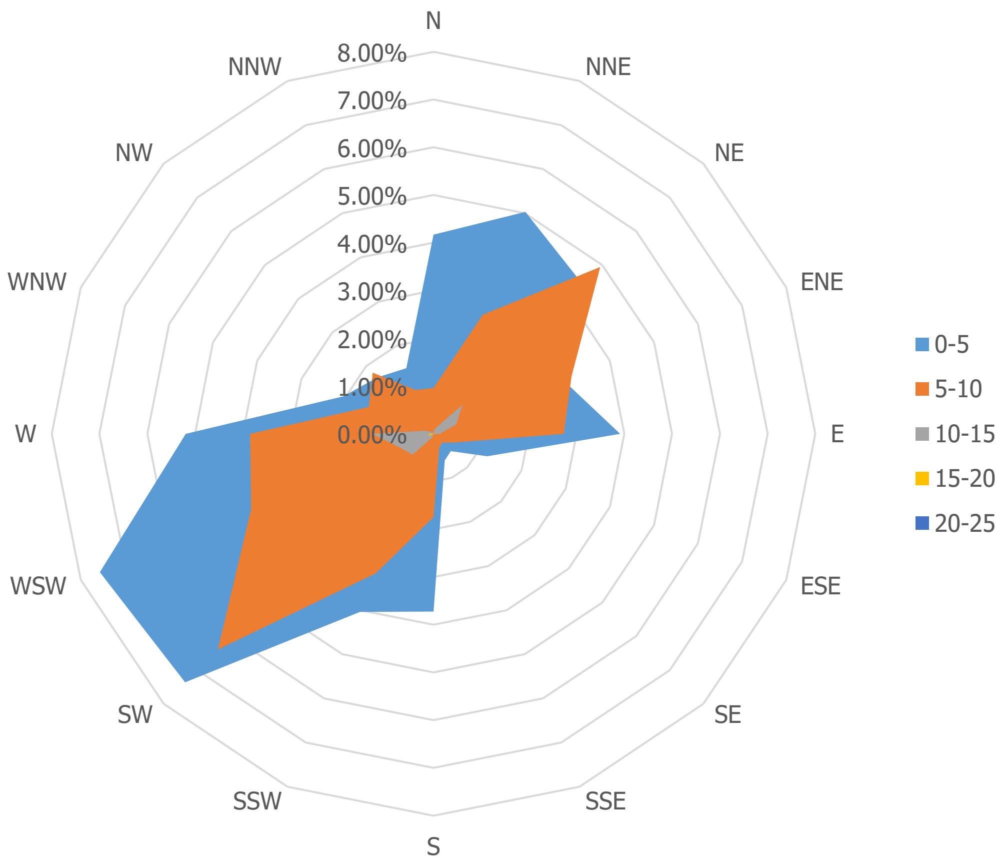

Figure 11. Wind speed (m/s) and direction during the 1-year monitoring period (percentage shown is count of wind speed).

Atmospheric corrosivity of this site was classified using the first-year corrosion rate.

- Mild steel – 163 g/m^2/year as ISO 9223 C2 – Low.
- Copper – 11 g/m^2/year as ISO 9223 C3 – Medium.
- Zinc – 9 g/m^2/year as ISO 9223 C3 – Medium.

These results indicated that the atmospheric environment surrounding this monitoring building was not very corrosive. The height of this site and the possible sheltering effects provided by the bridge and trees may be responsible for this relatively benign atmospheric corrosivity.

5.1.2 Surface deposition on the test building

Surface soluble deposition in the sheltered and exposed positions on the test building is shown in Table 6.

Table 6. Surface deposition on the test building in Auckland.

Wall	Position	Surface deposition (µg/cm²)				
		Aug 2017	Dec 2017	Feb 2018	May 2018	Yearly total
North	Sheltered	9.0–10.0	8.8–10.1	8.2–8.5	5.6–5.6	31.6–34.2
	Exposed	0.9–1.0	2.7–3.2	0.7–0.8	1.0–1.1	5.3–6.1
South	Sheltered	18.5–21.5	10.6–11.1	15.0–15.1	11.4–12.2	55.5–59.9
	Exposed	3.8–4.5	1.8–2.5	3.6–4.0	5.6–7.4	14.8–18.4
East	Sheltered	15.2–18.0	4.6–5.3	5.6–6.1	9.3–10.2	34.7–39.6
	Exposed	0.9–0.9	2.1–2.2	0.8–0.9	1.1–1.2	4.9–5.2
West	Sheltered	16.3–19.4	2.8–3.5	3.9–4.1	4.9–5.2	27.9–32.2
	Exposed	0.8–0.8	1.4–1.6	1.3–1.6	0	3.5–4.0

From Table 6, the following can be observed:

- The sheltered position on the south wall collected the highest total amount of deposits (55.5–59.9 µg/cm^2), approximately 2 times higher than the other three walls. Meanwhile, the north, east and west walls collected similar amounts of deposits during the 1-year monitoring period. This could be a result of the prevailing winds and the sources of air pollution. As shown in Figure 11, the prevailing wind at this site was from the west-southwest direction. The Auckland Harbour Bridge, a few metres west of the building, runs in a southwest to northeast direction. The sea salt particles carried by this wind could be partially blocked by the bridge. Some traffic-sourced dust and particulates could be carried to the south wall, which has a wide eave. However, most of these deposits, shown as black, appeared to be insoluble in water. Although wind could also be blown from the northeast, salt particles from the sea could be partially filtered by the trees sitting between the water and the building.
- The sheltered position under the eave or window awning collected more soluble deposits than the position fully exposed to the weather. The difference in yearly total was approximately 3–8 times.
- In general, a heavy surface soluble deposition was not observed on this building although it is close to the seawater. This agreed with the atmospheric corrosivity monitoring results and could be explained with the sheltering effect provided by the surrounding trees and the bridge.

5.1.3 Corrosion rates of mild steel coupons

The first-year corrosion rates of the mild steel coupons installed on the test building and the reference exposure rack are given in Figure 12.

From Figure 12, the following can be observed:

- For the mild steel coupons installed at 0° and 90°, the corrosion rates measured on the building were generally lower than those fully exposed to the atmosphere. The difference can be up to 2 times. For the coupons installed at 45°, the corrosion rates measured on the building were similar to or slightly higher than those fully exposed to the atmosphere.

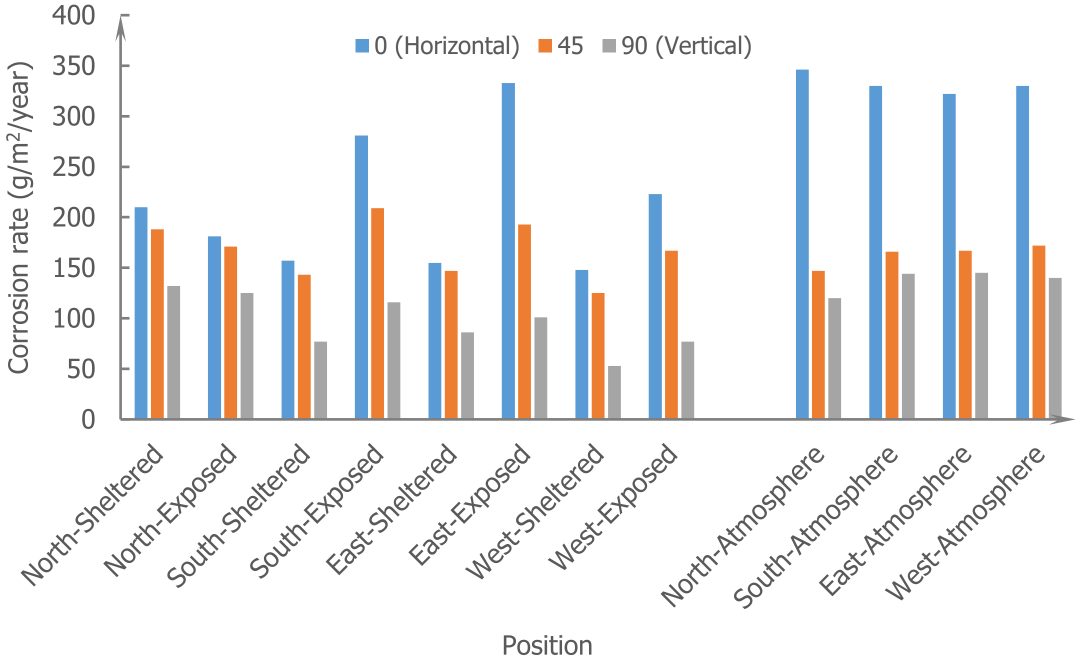

Figure 12. First-year corrosion rates of mild steel coupons on the test building in Auckland.

- When the corrosion rates measured in the sheltered positions on the building were compared, the north wall seemed to have the highest rates, while the other three walls had similar corrosion rates.
- When the corrosion rates measured in the exposed positions on the building were compared, the east and south walls seemed to have corrosion rates slightly higher than the other two walls.
- An obvious orientation effect was not observed with the corrosion rates of reference mild steel coupons fully exposed to the atmosphere during the 1-year period. It is supposed that airborne pollutants may disperse uniformly around the small reference exposure rack (~0.6 × 0.4 m). However, this uniform pollution distribution might not be expected on the test building, which has much larger dimensions (~13 × 11 m).
- The installation angle had a significant effect on the mild steel corrosion. The corrosion rate followed a general trend of 0° > 45° > 90°. However, a detailed analysis revealed the following:
  - When fully exposed to the atmosphere, the corrosion rates of the 45° inclined coupons were slightly higher than those of the 90° inclined. Meanwhile, the 0° inclined could be corroding approximately 1.9–2.4 times faster than the 45° installed. This gave a trend of 0° > 45° >≈ 90°.
  - When installed on the building, the corrosion rates of the 0° inclined coupons were slightly higher than that of the 45° inclined, which were approximately 1.4–2.4 times higher than that of the 90° inclined. This gave a trend of 0° >≈ 45° > 90°.
- On the south, east and west walls, the corrosion rates measured in the sheltered positions were lower than those in the exposed positions. The difference could be up to 2 times.

- On the north wall, the sheltered position had a marginally higher corrosivity than the exposed position (up to 16% higher).

5.1.4 Corrosion rates of mild steel nails in timber

Figure 13 shows the first-year corrosion rates of mild steel nails driven into H3.2 CCA-treated timber blocks.

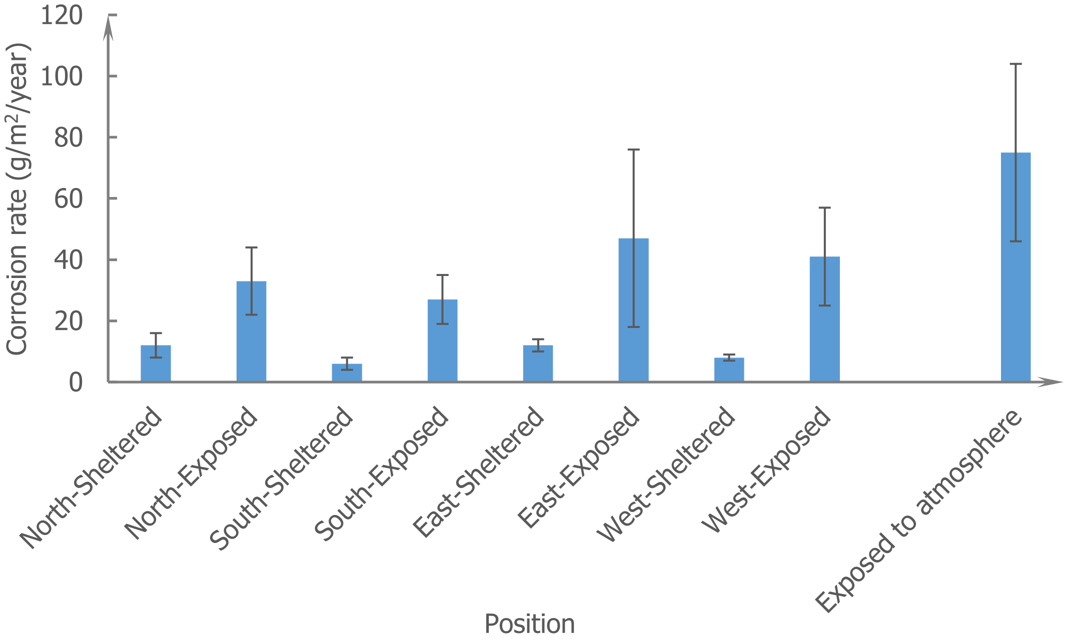

Figure 13. First-year corrosion rates of mild steel nails embedded into H3.2 CCA-treated timber blocks on the test building in Auckland.

From Figure 13, the following can be observed:

- The nails in timber blocks fully exposed to the atmosphere had a corrosion rate much higher than those installed in the exposed positions on the building. The difference could be approximately 1.6–2.7 times.
- On the building, the nails in timber blocks installed in the sheltered positions had a corrosion rate lower than those installed in the exposed positions, i.e. sheltered < exposed. The difference could be approximately 2.7–5.0 times.
- An obvious orientation effect on nail corrosion rate was not observed although the nails on the south wall seemed to corrode slightly slower when compared with those on the other three walls. Both sheltered and exposed positions on the south wall had the highest collection of salt particles. However, this did not lead to a higher nail corrosion rate.

5.2 Test building in Rotorua

5.2.1 Atmospheric environmental conditions

The highest hourly ambient temperature was approximately 28.3°C while the lowest was approximately -2°C at this site during the 1-year monitoring period (June 2017 – June 2018). Time-of-wetness and rainfall during this period were approximately 5,139 hrs (level τ_4) and 1,783 mm respectively. The prevailing winds were from the south-southwest (SSW) and north-northeast (NNE) (see Figure 14). The maximum wind speed was approximately 13 m/s during this period.

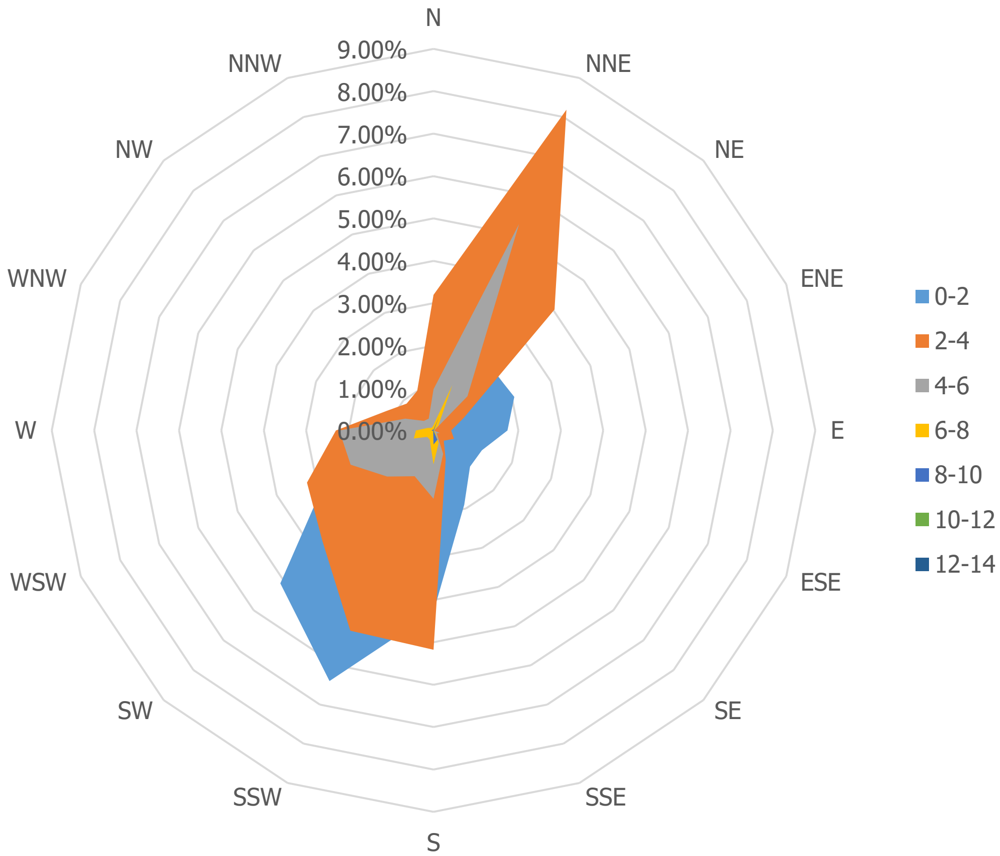

Figure 14. Wind speed (m/s) and direction during the 1-year monitoring period (percentage shown is count of wind speed).

Atmospheric corrosivity of this site was classified using the first-year corrosion rate.

- Mild steel – 1,262 g/m^2/year as ISO 9223 C5 – Very high.
- Copper – 205 g/m^2/year as ISO 9223 CX – Extreme. (Note that this corrosion rate is much higher than the upper limit of CX, 90 g/m^2/year.)
- Zinc – 48 g/m^2/year as ISO 9223 C5 – Very high.

These results showed that this site was extremely corrosive due mainly to its proximity to a large-scale geothermal source, Sulphur Bay.

5.2.2 Airborne sulphur-containing species

The average concentrations of airborne H_2S and SO_2 were analysed using specific passive tube sensors supplied by Gradko Environmental. This was carried out during a 3-week period from October to November 2017. H_2S and SO_2 were found to uniformly distribute around the building during this period with no concentration difference related to wall orientation, height or position (see Table 7).

This observation regarding height-related H_2S concentration was somewhat different from previous measurements done by BRANZ and other organisations in Rotorua. Previous BRANZ measurements in an open environment with a small-scale fumarole showed that the airborne H_2S concentration at ~3 m height was approximately 22 times lower than that at ~1 m height (Li, Marston & Stokes, 2018). This significant decrease of H_2S concentration with height was explained by its density, ~1.363 kg/m^3. Being slightly denser than air, it tends to concentrate in areas close to the ground.

Table 7. Concentration of airborne sulphur-containing species on the test building in Rotorua.

Wall	Position	Sulphur-containing species	Concentration (ppb[3])
Southwest	High-Exposed	H_2S	4.2
		SO_2	21.6
	High-Sheltered	H_2S	4.9
		SO_2	26.1
	Low-Exposed	H_2S	3.4
		SO_2	31.4
Southeast	High-Exposed	H_2S	4.1
		SO_2	28.3
	Low-Exposed	H_2S	5.1
		SO_2	27.2
Northeast	High-Exposed	H_2S	4.0
		SO_2	24.9
	Low-Exposed	H_2S	4.8
		SO_2	31.7
Reference	High-Exposed	H_2S	5.7
		SO_2	32.6
	Low-Exposed	H_2S	5.4
		SO_2	32.6

Notes:
- High position: approximately 2.65 m from the ground.
- Low position: approximately 1 m from the ground.
- Sheltered position was only available on the southwest wall.
- Reference site was approximately 50 m from the building.
- Monitoring was not performed on the northwest wall due to health and safety concerns.

The building is approximately 150 m away from the west boundary of Sulphur Bay, a large, complex geothermal system. In this area, H_2S and SO_2 could distribute in the dynamic air uniformly, particularly with a busy road running between the geothermal source and the test site. Therefore, the H_2S concentration gradient along height might be small. In addition, the barrier effect of a solid wall to wind/airflow might contribute to this reduced concentration gradient.

5.2.3 Corrosion rates of mild steel coupons

The first-year corrosion rates of mild steel coupons installed on the building and the reference exposure rack are given in Figure 15.

[3] ppb - parts per billion

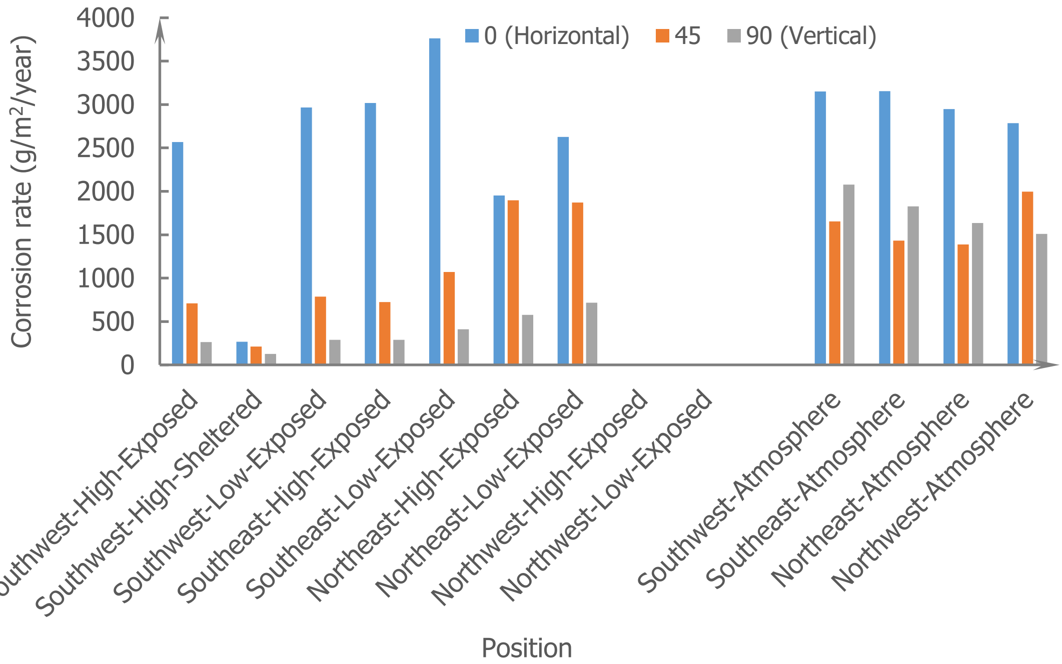

Figure 15. First-year corrosion rates of mild steel coupons on the test building in Rotorua.

From Figure 15, the following can be observed:

- The corrosion rates of mild steel coupons exposed to the atmosphere showed no obvious orientation dependence. This indicated that the dominant corrosive media (H_2S and SO_2) were distributing uniformly in the surrounding atmosphere.
- The 0° inclined coupons, either installed on the building or exposed to the atmosphere, had the highest corrosion rates. However, two correlations between corrosion rate and inclination angle were noted:
  - coupon fully exposed to the atmosphere: 0° > 90° > 45° (except northwest).
  - coupon on the building: 0° > 45° > 90°.

  This is different from the trend observed at other sites, such as Auckland.
- The coupons installed on the building were, in general, corroding slower than those fully exposed to the atmosphere. This is particularly obvious with the 45° and 90° inclined coupons on the southwest and southeast walls. The corrosion rates of the coupons that were 90° inclined and exposed to the atmosphere could be approximately 2.3–8.0 times higher those of the coupons installed on the building.
- It appeared that the coupons installed on the southeast and northeast walls, particularly those 45° and 90° inclined, had corrosion rates higher than those on the southwest wall. The southeast and northeast walls face towards Sulphur Bay, a larger-scale geothermal source. The wind from the northeast or north-northeast direction could carry sulphur-containing species to the test site.
- A weak height effect was observed with the metal corrosion rate on this building. The corrosion rates of the coupons in low positions were only 1.2–1.4 times higher than those of the coupons in high positions on the same wall.
- The mild steel corrosion rates measured in the sheltered position on the southwest wall were significantly lower than those measured in the exposed positions (high and low). This is applicable to coupons installed at all three angles. The largest decrease was observed with the 0° inclined coupons, and their corrosion rates could be decreased by approximately 10 times. Meanwhile, the corrosion rates of the 45° and 90° coupons could be decreased by approximately 2–3 times.

5.2.4 Corrosion rates of mild steel nails in timber

The first-year corrosion rates of mild steel nails driven into H3.2 CCA-treated timber blocks are given in Figure 16.

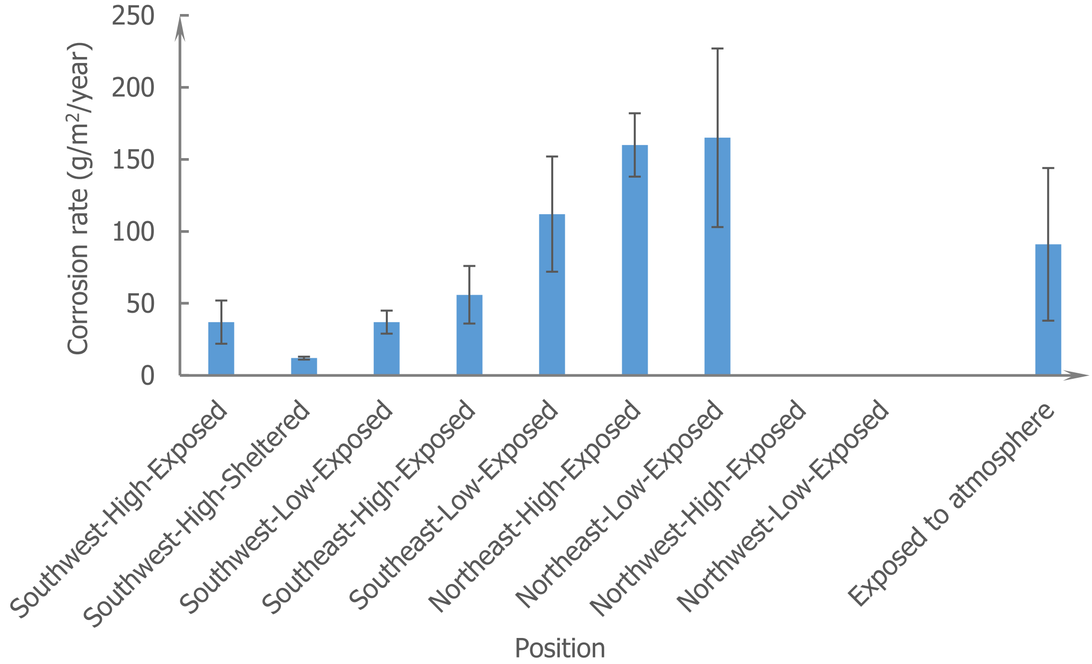

Figure 16. First-year corrosion rates of mild steel nails embedded into H3.2 CCA-treated timber blocks on the test building in Rotorua.

From Figure 16 the following can be observed:

- The nails in timber blocks exposed to the atmosphere had a corrosion rate higher than those on the southwest wall (approximately 2.5 times). However, this corrosion rate was lower than those of the nails on the southeast (except the high-exposed position) and northeast walls of the building.
- An orientation effect on nail corrosion rate was noted. The nails on the southeast and northeast walls were corroding faster than those on the southwest wall.
- The corrosion rate of the nails in the low-exposed position on the southeast wall was approximately 2 times higher than that of nails in the high-exposed position. On the southwest and northeast walls, corrosion rate was not related to the height.
- On the southwest wall, the nails in the sheltered position had a corrosion rate approximately 3 times lower than those in the exposed positions.

5.3 Test building in Waihau Bay

5.3.1 Atmospheric environmental conditions

The highest hourly ambient temperature was approximately 26.9°C while the lowest was approximately 2.5°C at this site during the 1-year monitoring period (February 2019 – February 2020). Time-of-wetness and rainfall during this period were approximately 5,526 hrs (level τ_5) and 1,284 mm respectively. The prevailing winds were from the west and east (see Figure 17). The maximum wind speed was approximately 8 m/s during this period.

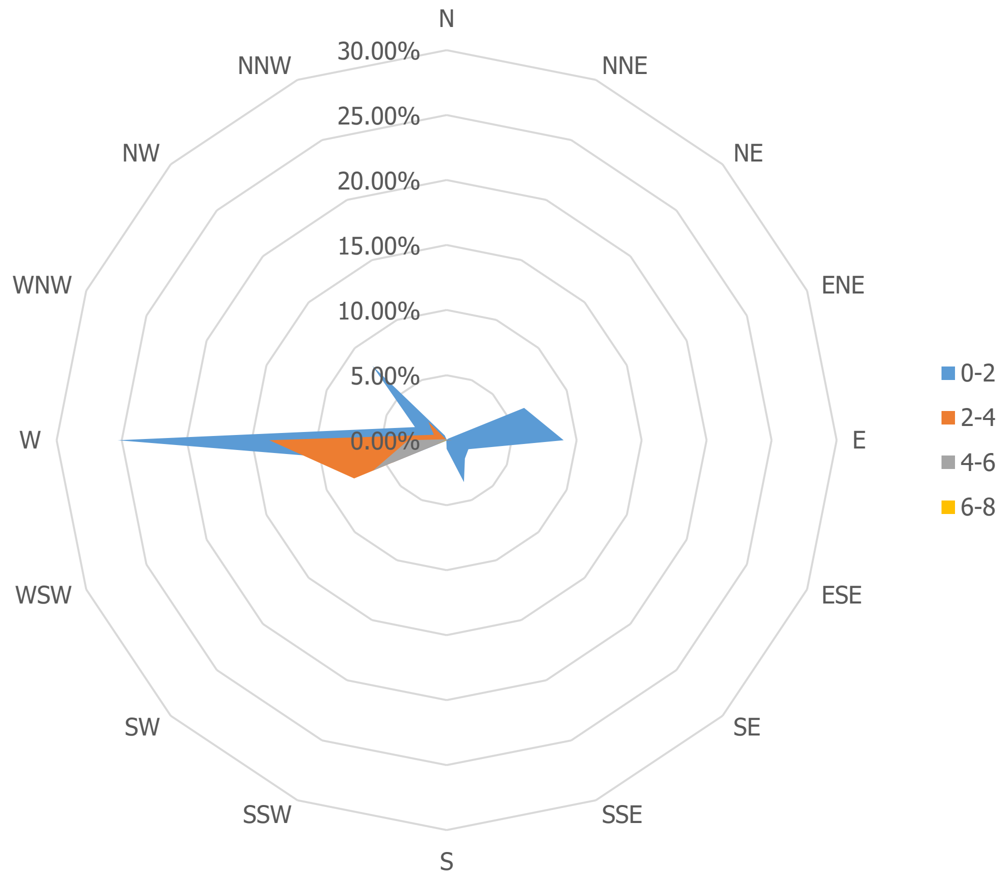

Figure 17. Wind speed (m/s) and direction during the 1-year monitoring period (percentage shown is count of wind speed).

Passive tube sensors were used to measure the concentrations of hydrogen sulphide (H_2S), sulphur dioxide (SO_2) and ammonia (NH_3) with the following results:

- 28 November 2016 to 21 December 2016: H_2S = 0.12 ppb.
- 31 October 2017 to 28 November 2017: H_2S <0.01 ppb, SO_2 <0.72 ppb, NH_3 = 2.96 ppb.

The passive tube sensors could not continuously measure the concentration of the airborne pollutant if not replaced at regular intervals. Consequently, the airborne H_2S or SO_2 concentration data collected gave averaged values for specific periods.

Atmospheric corrosivity was classified by the first-year corrosion rates of coupons that were positioned towards the sea at an angle of 45° at a height of approximately 3 m.

- Mild steel – 470 g/m^2/year as ISO 9223 C4 – High.
- Copper – 27 g/m^2/year as ISO 9223 C5 – Very high.
- Zinc – 25 g/m^2/year as ISO 9223 C4 – High.

These showed that this site was very corrosive due to its proximity to the sea and/or weak and/or seasonal geothermal/volcanic influences from Whakaari/White Island.

5.3.2 Environmental conditions on the test building

Table 8 shows the environmental monitoring results, and the following can be observed:

Table 8. Environmental conditions on the test building in Waihau Bay.

Wall	Position	Temperature (°C)		Average RH (%)	ToW (hours)	
		Average	Range		Value	Category
North	Sheltered	17.0	3.6–32.0	76	3,805	τ_4
	Exposed*	17.1	2.9–43.1	79	3,795	τ_4
South	Sheltered	16.8	2.9–35.3	77	4,096	τ_4
	Exposed	16.5	2.8–35.3	82	4,872	τ_4
East	Sheltered	17.3	3.5–38.6	80	4,650	τ_4
	Exposed	17.5	2.9–52.0	80	4,955	τ_4
West	Sheltered	17.2	3.7–49.4	77	4,111	τ_4
	Exposed	17.3	1.9–51.7	79	4,722	τ_4
Atmosphere		15.6	2.5–26.9	82	5,526	τ_5

* Data for the period February–May 2019 was lost since sensors were damaged.

- The average temperatures of all positions were similar, approximately 17°C. This is approximately 1°C higher than the average ambient temperature (15.6°C).
- The exposed position showed a larger temperature variation when compared with the sheltered position on the same wall. The exception is the south wall.
- The sheltered positions on the north, south and east walls showed a similar temperature variation that is smaller than that on the west wall.
- The exposed positions on the east and west walls showed a larger temperature variation when compared with those on the north and south walls.
- The exposed positions on all walls showed a larger temperature variation than the surrounding atmospheric environment.
- The highest temperature was measured in the exposed position on the east wall, 52.0°C. This is approximately 25°C higher than the highest ambient temperature.
- The exposed position had a slightly higher average RH than the sheltered position on the same wall.
- The total ToW values in the sheltered positions on all four walls were 3,800–4,650 hrs during the 1-year period and could be classified as category τ_4.
- The exposed positions on the south, east and west walls had a total ToW ranging from 4,700 to 4,960 hrs and could be classified as τ_4. Note that the ToW data for the exposed position on the north wall is incomplete.
- The sheltered position had a smaller ToW than the exposed position on the same wall. The difference was approximately 300–780 hrs.
- The ToW for the surrounding atmosphere was approximately 5,526 hrs, which was 570–800 hrs higher than that of the exposed positions on the building.

5.3.3 Surface deposition on the test building

Surface soluble deposits were measured on the painted timber weatherboard directly. From Table 9 the following can be observed:

- The sheltered positions on the north, south and west walls collected approximately 2–4 times more deposits than the exposed positions.
- On the east wall, the sheltered position collected smaller amount of deposits than the exposed position. It is supposed that the house could act as a barrier to the prevailing wind from the west, which carries salt particles from the sea.

Table 9. Surface deposition on the test building in Waihau Bay.

Wall	Position	Surface deposition (μg/cm²)					
		May 2019	Jul 2019	Aug 2019	Nov 2019	Feb 2020	Yearly total
North	Sheltered	22.0–23.9	23.8–25.7	25.6–29.6	26.9–29.4	15.6–15.8	113.9–124.4
	Exposed	4.3–4.9	2.8–3.2	10.6–10.7	1.5–2.1	11.3–12.0	30.5–32.9
South	Sheltered	30.3–31.2	25.6–27.2	49.1–50.0	33.4–35.7	25.4–28.1	163.8–172.2
	Exposed	6.0–6.3	19.0–19.3	35.0–42.8	1.7–1.9	27.7–27.8	89.4–98.1
East	Sheltered	10.7–11.8	9.4–9.9	12.4–12.9	14.8–17.9	16.5–17.8	63.8–70.3
	Exposed	10.4–12.1	9.9–10.9	18.2–19.9	14.8–15.6	16.2–21.2	69.5–79.7
West	Sheltered	14.7–15.9	15.8–17.1	19.0–21.4	16.8–17.2	23.1–25.3	89.4–96.9
	Exposed	5.4–6.2	4.0–5.0	11.0–12.7	3.1–3.2	3.8–4.0	27.3–31.1

The west wall is facing towards the sea, and the prevailing wind is from the west. Actually, the exposed position on the south wall collected the highest salt deposition among all four exposed positions. The west wall is directly exposed to the sea, but this does not ensure it will retain more salt particles than other walls. The cleaning and washing effects by wind and wind-driven rain should be considered.

5.3.4 Corrosion rates of mild steel coupons

The first-year corrosion rates of mild steel coupons installed on the building and the reference exposure rack are given in Figure 18. Note that the west-facing steel coupon exposed to the atmosphere was lost. The following can be observed:

- The corrosion rates of the mild steel coupons installed at an angle of 45° and on the reference rack ranged from 417 to 615 g/m²/year. These could classify the atmospheric corrosivity as ISO 9223 C4 – High. This category is the same as that determined by the mild steel coupon facing towards the sea at an angle of 45°.
- For the mild steel coupons exposed to the atmosphere, the installation angle seemed to affect their corrosion rates. The 0° inclined coupons seemed to corrode faster than the 90° inclined coupons. The normal trend, 0° > 45° > 90°, was not observed since the corrosion rates of the 45° inclined coupons could be higher or lower than those of the 90° inclined coupons.
- The mild steel coupons on the north and east walls were corroding slower than those exposed to the atmosphere and facing towards north and east. The coupons on the south wall were corroding faster than those exposed to the atmosphere and facing towards south. The highest difference can be approximately 4 times. On the west wall, the 45° inclined coupons were corroding faster than those exposed to the atmosphere, the 90° inclined coupons were corroding slightly slower than those exposed to the atmosphere.
- The corrosion rates of the mild steel coupons on the building showed a dependence on wall orientation: south ≅ west >> east ≅ north. The south and west walls had a much higher corrosivity than the north and east walls in both sheltered and exposed positions. The prevailing winds were from the west (sea) and east (farms on hill). The west and south walls would be exposed to the marine environment when considering the actual orientation of this building. The south wall surfaces received the highest salt deposits in both sheltered and exposed positions, as shown in Table 9. This may contribute to the high corrosivity observed on the

south wall. However, the high corrosivity on the west wall might not be well explained with salt deposition only.
- The 0° inclined coupons on the building, in general, had the highest corrosion rates, while the 90° inclined coupons had the slowest. The normal trend, 0° > 45° > 90°, was noted. The exception is the sheltered position on the north wall. This is different from the trend observed with the coupons exposed to the atmosphere.
- The corrosion rate of the 0° inclined coupon in the exposed position was higher than that in the sheltered position on the same wall. For example, the mild steel corrosion rate measured in the exposed position on the south wall was approximately 2 times higher than that in the sheltered position. The exception is the west wall, where the corrosion rate in the exposed position was slightly lower than that in the sheltered position, 1,333 g/m^2/year versus 1,487 g/m^2/year.
- The corrosion rates of the 45° inclined coupons in the sheltered positions were similar to (east wall), higher than (north wall, 1.5 times) or lower than (south and west walls, 1.3–2.0 times) those in the exposed positions.
- The corrosion rates of the 90° inclined coupons in the sheltered positions were similar to (east wall) or higher than (north, south and west walls, 1.1–1.4 times) those in the exposed positions.

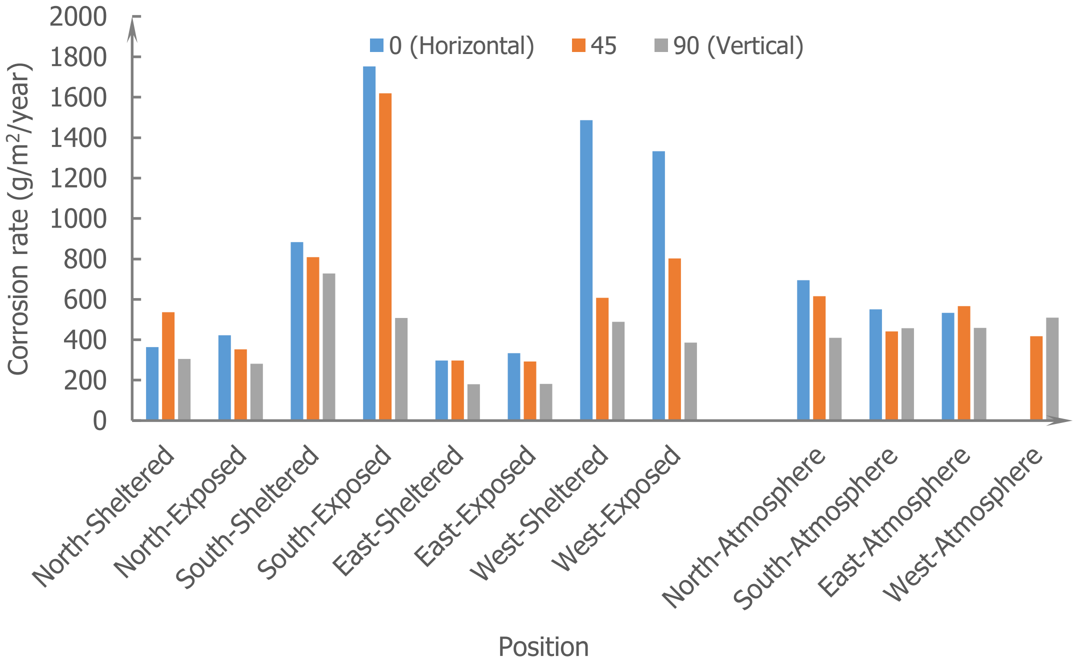

Figure 18. First-year corrosion rates of mild steel coupons on the test building in Waihau Bay.

5.3.5 Corrosion rates of mild steel nails in timber

The first-year corrosion rates of mild steel nails driven into H3.2 CCA-treated timber blocks are given in Figure 19.

From Figure 19, the following can be observed:

- The nails in timber blocks fully exposed to the atmosphere had a corrosion rate approximately 2–4 times higher than those installed on the building.

- An orientation effect on corrosion rate was not observed with those nails in the exposed positions. They had a corrosion rate of approximately 50 g/m^2/year. This is somewhat different from that observed with the mild steel coupons.
- The corrosion rate of the nail in the sheltered position on the west wall was 42$\pm$5 g/m^2/year. This was approximately 2 times higher than the corrosion rates of those nails installed in the sheltered positions on the north, south and east walls.
- The nails in the timber blocks in the exposed position had a higher corrosion rate than those in the sheltered position (approximately 2 times higher) on the same wall. This is particularly true for the north, south and east walls. On the west wall, the nail corrosion rate in the sheltered position was similar to that in the exposed position, 42 g/m^2/year versus 47 g/m^2/year.

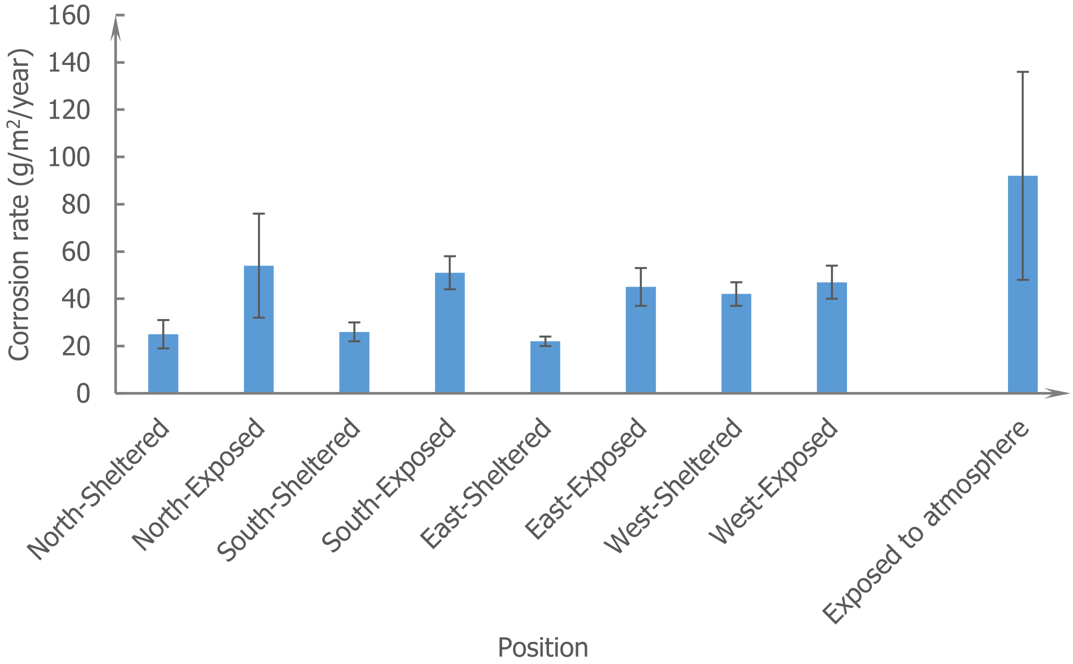

Figure 19. First-year corrosion rates of mild steel nails embedded into H3.2 CCA-treated timber blocks on the test building in Waihau Bay.

5.4 Test building in Wellington

5.4.1 Atmospheric environmental conditions

The highest and lowest hourly ambient temperatures were approximately 27.4°C and -0.3°C respectively during the 1-year monitoring period (December 2015 – December 2016). Time-of-wetness and rainfall were approximately 5,339 hrs (level τ_4) and 1,589 mm respectively. The prevailing wind was from the north-northwest (NNW), and the maximum wind speed was around 6.3 m/s during this period (see Figure 20).

Atmospheric corrosivity was classified using the first-year corrosion rate. Note that this monitoring was done during the period June 2015 – June 2016.

- Mild steel – 174 g/m^2/year as ISO9223 C2 – Low.
- Copper – 16 g/m^2/year as ISO 9223 C4 – High.
- Zinc – 7 g/m^2/year as ISO 9223 C3 – Medium.

These results indicated that the atmospheric environment around this monitoring building was probably sitting on the boundary of ISO 9223 C2 and C3.

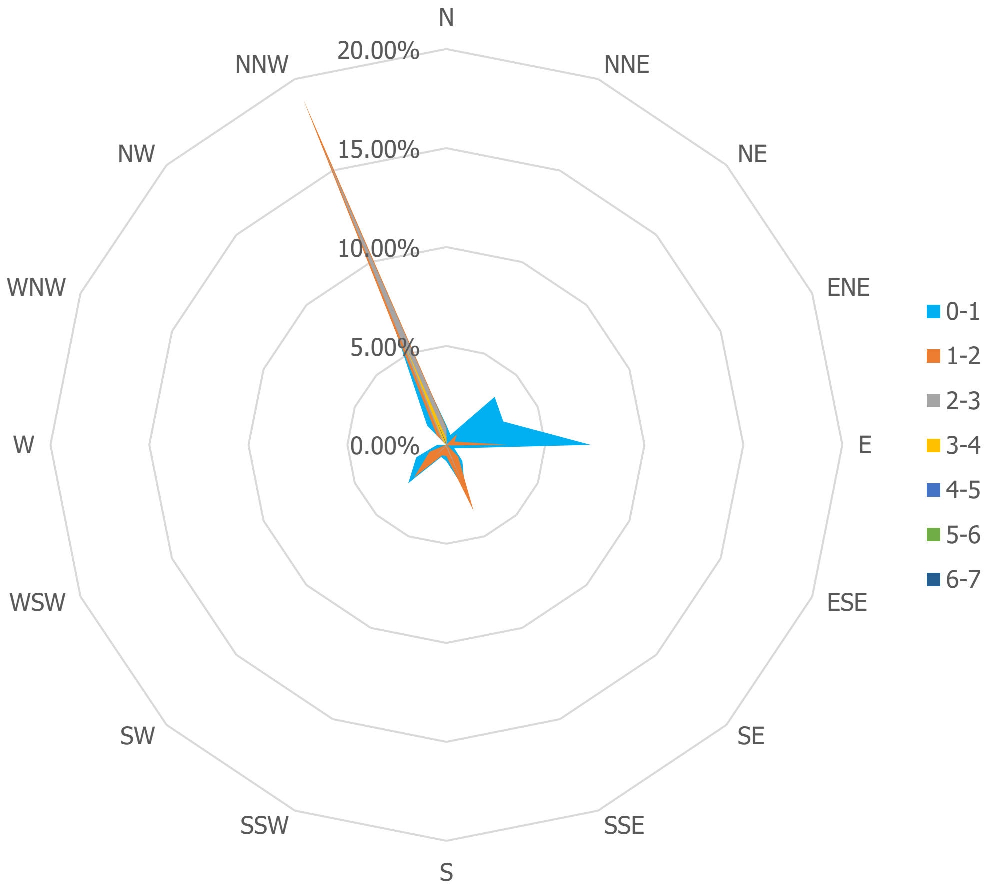

Figure 20. Wind speed (m/s) and direction during the 1-year monitoring period (percentage shown is count of wind speed).

5.4.2 Temperature on the test building

Table 10 summarises the temperature monitoring results in each building position.

Table 10. Temperature on the test building in Wellington.

Wall	Position	Distance from eave (mm)	Temperature (°C)	
			Average	Range
North	Sheltered (N_S)	50	16.1	1.4–38.6
	Boundary (N_B)	640	17.0	-0.4–62.8
	Exposed (N_E)	2,330	18.1	-0.2–58.6
South	Sheltered (S_S)	50	15.6	1.2–35.7
	Boundary (S_B)	640	15.3	-0.2–33.6
	Exposed (S_E)	2,330	14.5	-0.3–31.9
East	Exposed-High (E_{EH})	640	17.1	-0.9–64.7
	Exposed- Low (E_{EL})	2,330	16.9	-0.2–56.6
West	Exposed-High (W_{EH})	640	15.8	-0.5–62.0
	Exposed-Low (W_{EH})	2,330	15.8	0.9–53.7
Atmosphere			13.8	-0.3–27.4

To show the temperature profile on this building, a temperature comparison was made between four positions during the 1-year period starting from 15 December 2015 (see Figure 21). These positions include north-boundary (N_B), south-boundary (S_B), east-exposed-high (E_{EH}) and west-exposed-high (W_{EH}). They have the same distance from the eave. The temperature of the surrounding atmospheric environment was also included for comparison. To show temperature differences and variations, comparisons were also made within two short periods: 29 June 2016 – 29 July 2016 and 16 November 2016 – 16 December 2016 (see Figures 22 and 23).

From Table 10 and Figures 21–23, the following can be observed:

- Both ambient temperature and surface temperature on the building envelope showed variations. However, the temperatures on the building envelope had larger variations than the ambient temperature.
- Among the four walls, the south wall appeared to show the lowest yearly average temperature.
- Among all positions on the building, the three positions on the south wall showed the smallest temperature variation. The sheltered position on the north wall also showed small temperature variations, 1.4–38.6°C, during the 1-year monitoring period. All other positions on the north, east and west walls showed similar temperature variations.
- The lowest hourly surface temperature measured in the building wall positions was -0.9°C, which was similar to the lowest value of the surrounding atmospheric environment, -0.3°C.
- The maximum hourly temperatures measured were 62.8°C, 33.6°C, 64.7°C and 62.0°C on the north, south, east and west walls respectively. The highest ambient temperature was 27.4°C.
- The yearly average temperature showed a trend of sheltered < boundary < exposed on the north wall. This was opposite to the trend on the south wall, sheltered > boundary > exposed. The yearly average temperature in the exposed-high position was similar to that in the exposed-low position on the east and west walls.

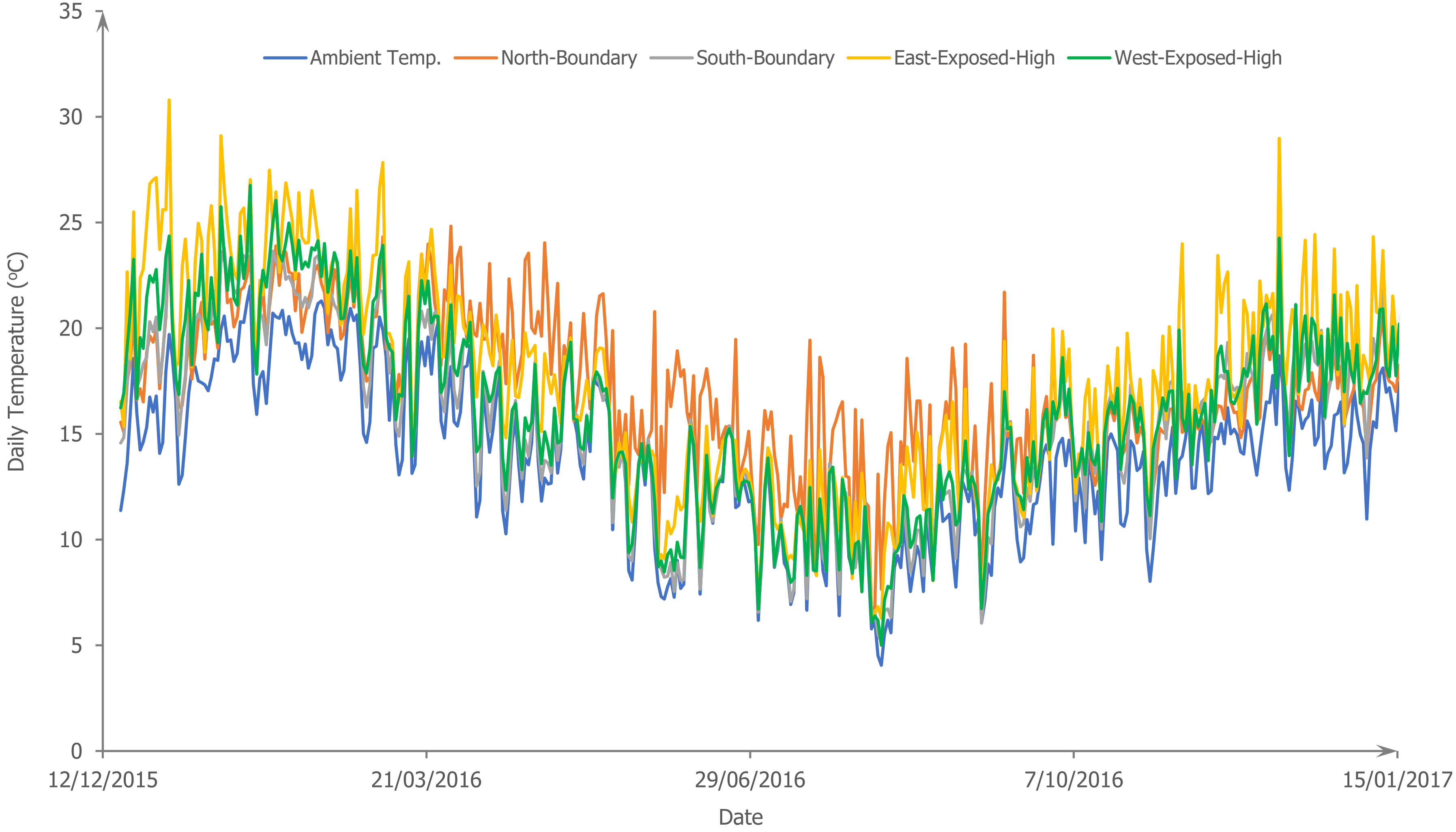

Figure 21. Comparison of daily surface temperature on four walls of the test building in Wellington.

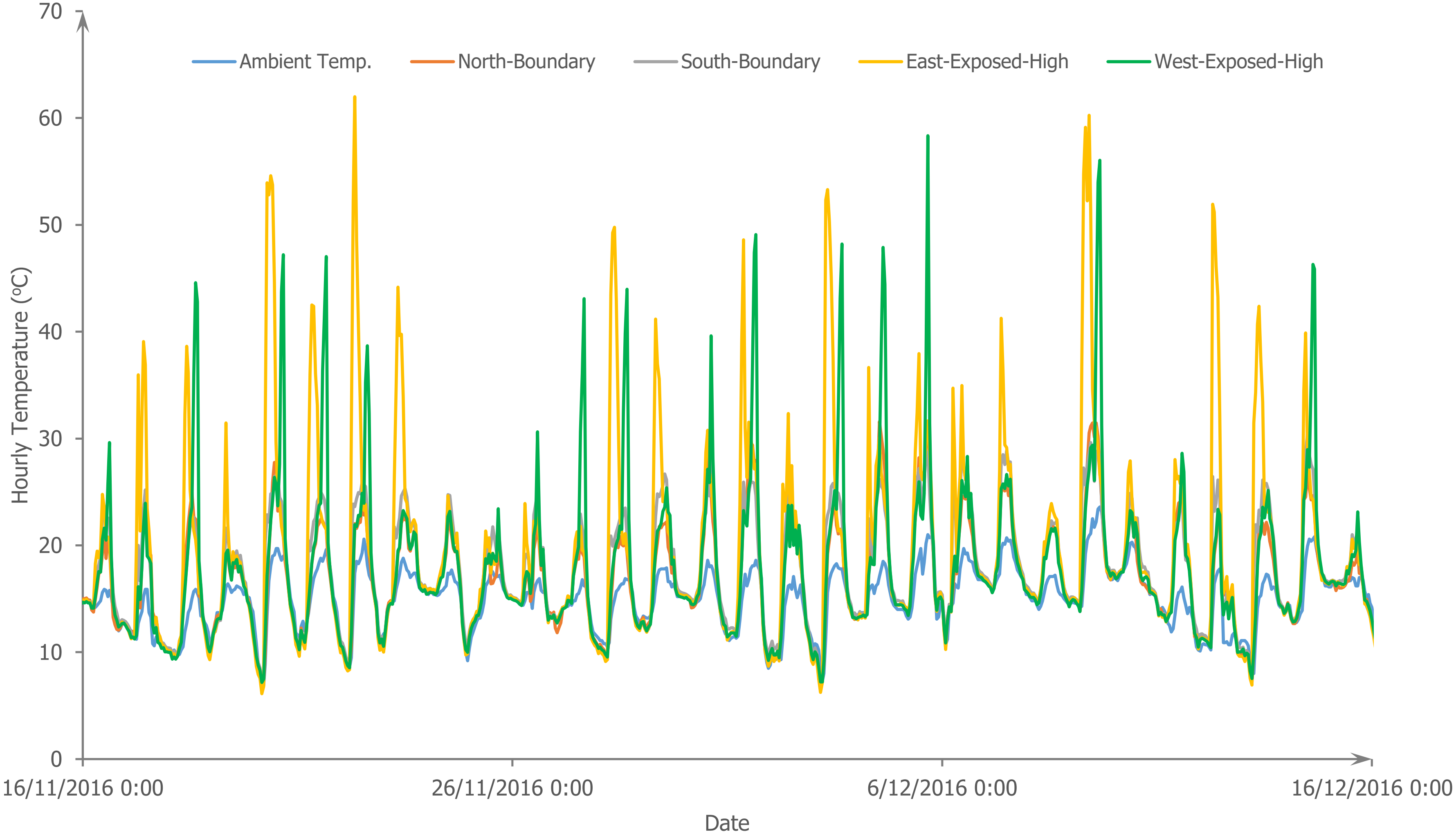

Figure 22. Comparison of hourly surface temperature on four walls (July 2016) of the test building in Wellington.

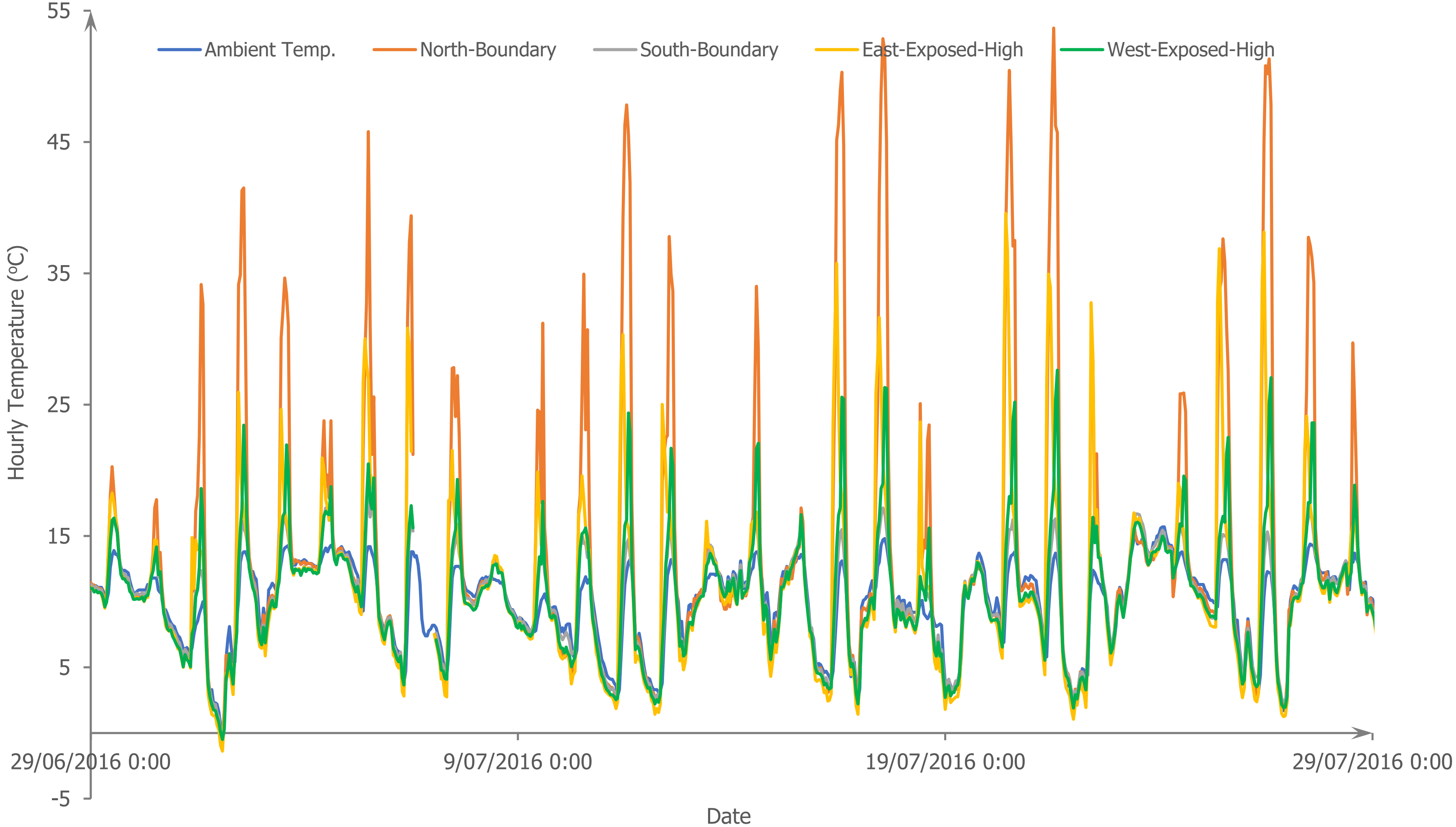

Figure 23. Comparison of hourly surface temperature on four walls (November–December 2016) of the test building in Wellington.

5.4.3 ToW on the test building

ToW was calculated and shown in Table 11, which shows the following:

- The ToW values of the sheltered positions on both north and south walls could be approximately 1,300–1,400 hrs smaller than that of the boundary and exposed positions.
- The ToW values measured in other positions (i.e. boundary and fully exposed) were similar, around 4,200–4,700 hrs. An exception is the fully exposed position on the south wall, SE. It had a ToW of approximately 5,200 hrs.
- ToW measured in the surrounding atmospheric environment is 5,339 hrs, which could be 850–2,150 hrs higher than the ToW values on the building envelope.

Table 11. Total ToW values in positions on the test building in Wellington.

Distance from eave (mm)	Total ToW (hours)								Atmosphere
	North		South		East		West		
50	N_S	3,180	S_S	3,727	x	x	x	x	
640	N_B	4,442	S_B	4,394	E_{EH}	4,489	W_{EH}	4,247	5,339
2,330	N_E	4,151	S_E	5,195	E_{EL}	4,674	W_{EL}	4,483	

x = no position was selected at this height for monitoring.

5.4.4 Wind-driven rain on the test building

Wind-driven rain was monitored in boundary and exposed positions on each wall.

Table 12. Wind-driven rain on the test building in Wellington.

Period	Wind-driven rain (mm)								Atmosphere
	North		South		East		West		
	Boundary	Exposed	Boundary	Exposed	Exposed-High	Exposed-Low	Exposed-High	Exposed-Low	
15/1/16	2.6	3.8	0	0	0.2	0.2	0	0	59.4
17/2/16	0.2	0.4	0	0	0.2	0.6	0	0	40.2
15/3/16	7.6	10	0.4	0	1.6	5.2	0	0	54.8
14/4/16	1.2	1.2	0	0	0.4	0.4	0	0	85.2
16/5/16	8.8	18	0	0.4	2.2	6	0	0.6	144
7/6/16	8.4	20.4	0	0.4	3.4	6	0.6	1.4	153.4
29/6/16	6.8	17.8	0.8	6.2	0.4	1.6	0	1.6	147.6
22/7/16	8	17.8	0	0.8	1.4	3	0	0.4	59.6
18/8/16	15	28.8	12.6	1.6	2	20.8	1.6	7.2	171.2
15/9/16	4.2	5.2	5.8	4.6	0.6	5.8	0	0.2	84.8
11/10/16	9.8	25.6	0	0.8	1.2	1	0.2	1	158.2
9/11/16	2.2	10.6	0	2.4	0	0	0	0	141.2
13/12/16	19.6	138.2	0	2.2	2.8	3.6	0.2	1.6	289.4
Yearly total	94.4	297.8	19.6	19.4	16.4	54.2	2.6	14	1,589

From Table 12, the following can be observed:

- The quantity of wind-driven rain collected on the building was significantly lower than that of the vertical rain. For example, the high position on the west wall only collected 2.6 mm rain, while the total rainfall at this site was 1,589 mm.
- The highest wind-driven rain, 297.8 mm, was measured in the exposed position on the north wall. The boundary position on this wall received the second-highest wind-driven rain, 94.4 mm. The total wind-driven rain decreased in the order of north, east, south and west. The prevailing wind at this site was from the north-northwest (NNW) (see Figure 20). This made the north wall most exposed to rain.
- The fully exposed or exposed-low position received a larger total wind-driven rain than the boundary or exposed-high position on the same wall. The difference was 3–5 times. The exception is the south wall, where the boundary and exposed positions received similar total wind-driven rain, 19.6 mm versus 19.4 mm.

The eaves on the north and south sides of this building are approximately 600 mm wide. Visual observations found no wind-driven rain reached the sheltered area during the 1-year period.

5.4.5 Surface deposition on the test building

Surface soluble deposition on the building is shown in Table 13.

Table 13. Surface deposition on the test building in Wellington.

Wall	Position	Surface deposition (μg/cm^2)					
		Surface on the building			Surface exposed to the atmosphere		
		0°	45°	90°	0°	45°	90°
North	Sheltered (N_S)	101.5	54.7	16.6	22.9	15.7	12.2
	Boundary (N_B)	44.2	25.1	7.7			
	Exposed (N_E)	29.2	19.3	5.3			
South	Sheltered (S_S)	70	52.2	12.3	18.2	18.2	16.1
	Boundary (S_B)	62.3	40.7	10.5			
	Exposed (S_E)	28.8	24.1	8.5			
East	Exposed-High (E_{EH})	47.1	37	20.6	31	17.2	14.4
	Exposed-Low (E_{EL})	28.5	17.2	14.3			
West	Exposed-High (W_{EH})	46.9	38.1	18.9	23	20	13.8
	Exposed-Low (W_{EL})	27.3	19.8	8.4			

From Table 13, the following can be observed:

- The 0° inclined surface, in general, collected the largest amount of soluble deposit among the three inclined surfaces (0°, 45° and 90°). This is also true for the surfaces that were fully exposed to the atmosphere.
- The surfaces in higher positions (sheltered, boundary and exposed-high) collected a larger amount of deposits than the surfaces in lower positions (exposed on the north and south walls and exposed-low on the east and west walls).

- The surfaces on the east and west walls collected similar amounts of deposition if they were installed at the same height and inclined at the same angle.
- The sheltered position on the north wall collected the highest amount of soluble deposits, 101.5 µg/cm^2, during the monitoring period.
- The surfaces that were installed in the exposed positions on the building (N_E, S_E, E_{EL} and W_{EL}) collected similar amounts of soluble deposits. The quantities collected on these surfaces were also similar to those measured on the collection surfaces that were fully exposed to the atmosphere.
- The deposition difference between the 0° and 90° inclined surfaces was found to be related to where they were installed, 2–6 times (on the building) versus 1.1–1.9 times (exposed to the atmosphere).

5.4.6 UVA irradiation on the test building

UVA irradiation (320–400 nm) was monitored half-hourly in one position on each wall. The position was 1,060 mm below the eave, i.e. lower than the boundary position on the north and south walls and the exposed-high position on the east and west walls.

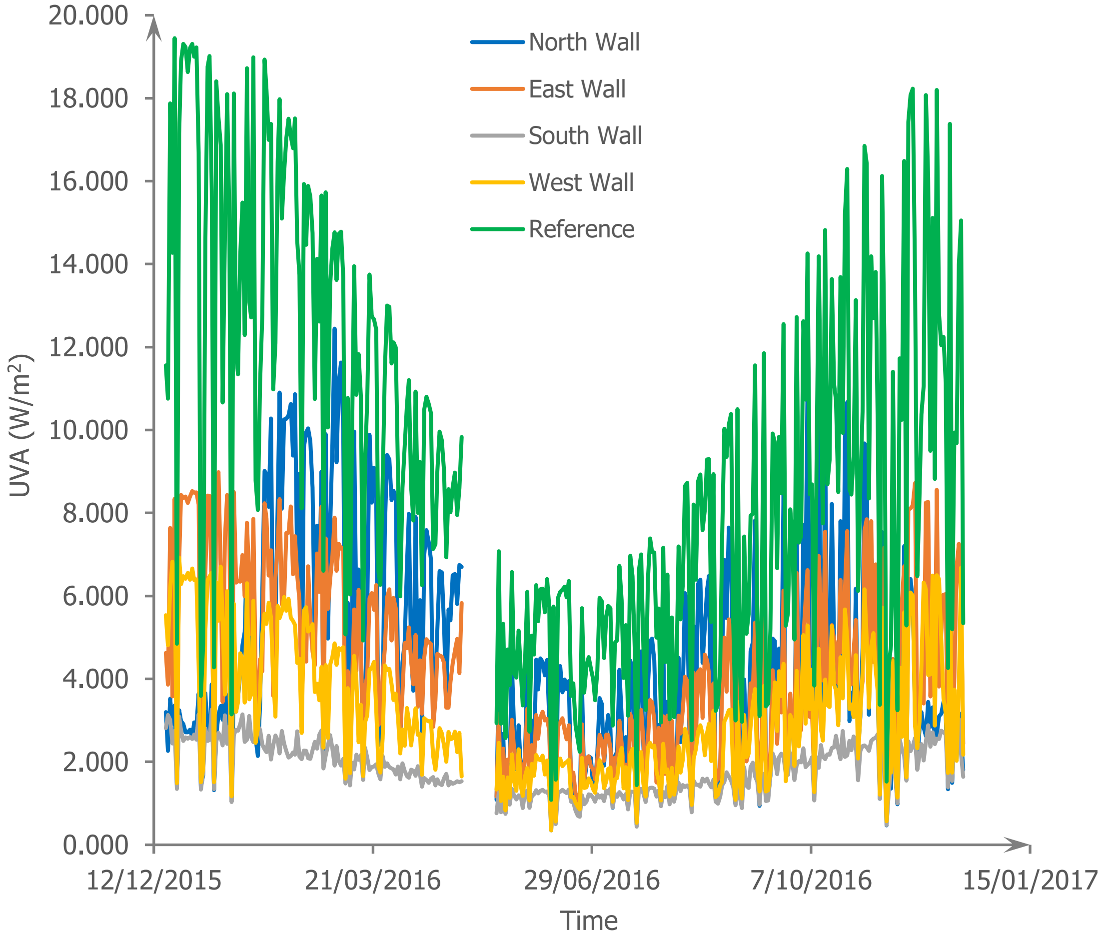

Figure 24. Comparison of daily UVA irradiation on four walls of the test building in Wellington.

From Figure 24, the following can be observed:

- The daily average UVA irradiation intensity had an obvious seasonal variation, strong in summer and weak in winter, and therefore presented a sine-shaped curve over longer periods.

- The south wall received the lowest UVA irradiation and showed the smallest seasonal variation. Daily average UVA irradiation on the south wall was approximately 6 times lower than that on the north wall and 10 times lower than that in the surrounding atmospheric environment.
- The daily average UVA irradiation intensity had an obvious wall orientation dependence: surrounding atmosphere > north > east > west > south.
- The eave on the north provided a sun shelter to the UVA monitoring position in the periods of December 2015 – January 2016 and November 2016 – December 2016. This sheltering effect was not observed on the other three walls.

5.4.7 Corrosion rates of mild steel coupons

The corrosion rates of mild steel coupons installed in different positions on the building is presented in Figure 25.

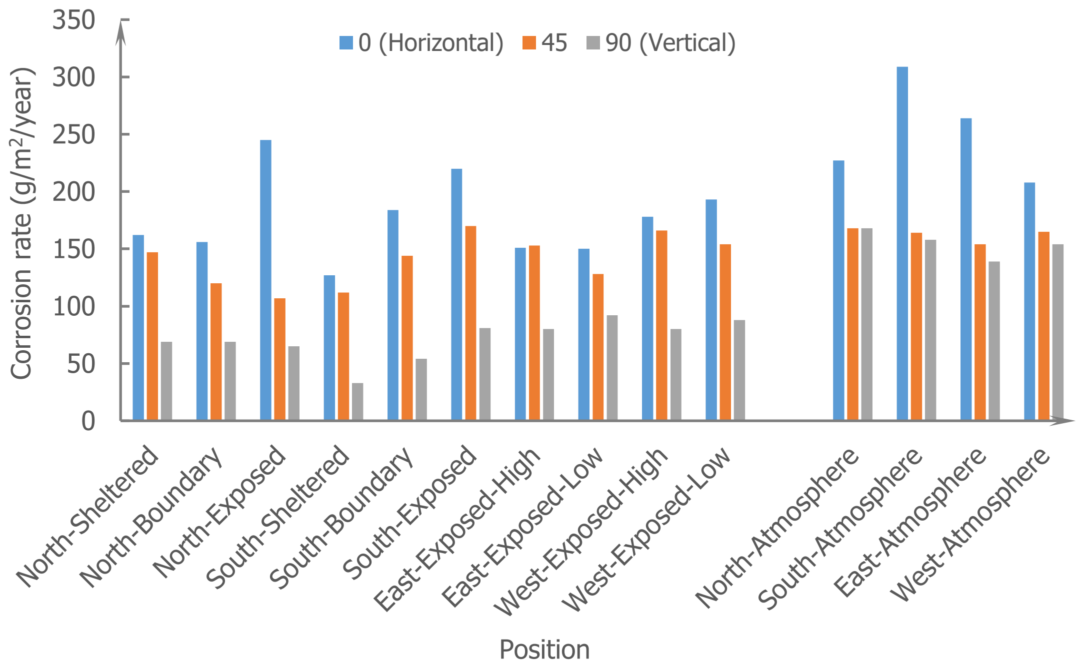

Figure 25. First-year corrosion rates of mild steel coupons on the test building in Wellington.

From Figure 25, the following can be observed:

- The corrosion rates of mild steel coupons followed a trend of 0° > 45° > 90°. This applied to the coupons installed on the building and exposed to the atmosphere.
  - Coupons fully exposed to the atmosphere: the corrosion rates between the 45° and 90° inclined coupons were similar. Meanwhile, the corrosion rates of the 0° inclined coupons were approximately 1.5–2 times higher than those of the 90° inclined coupons. This gave a trend of 0° > 45° >≈ 90°.
  - Coupons installed on the building: The corrosion rates of the 0° inclined coupons were slightly higher than those of the 45° inclined coupons (except N_E and E_{EH}). The corrosion rates of the 45° inclined coupons were approximately 2–3 times higher than those of the 90° inclined coupons. This gave a trend of 0° >≈ 45° > 90°.

  These trends are similar to those observed on the building in Auckland.
- The corrosion rates of the coupons installed on the building were, in general, lower than those of the coupons fully exposed to the atmosphere.

- The coupons installed on the south wall at three inclination angles (0°, 45° and 90°) showed a corrosion rate trend of sheltered < boundary < exposed.
- The coupons on the north wall showed different corrosion rate trends with inclination angles:
  - 0° inclined coupons: sheltered ≈ boundary < exposed.
  - 45° inclined coupons: sheltered > boundary > exposed. However, the corrosion rates in these positions were still similar.
  - 90° inclined coupons: sheltered ≈ boundary ≈ exposed.
- The corrosion rates of the mild steel coupons fully exposed to the atmosphere at an angle of 0° showed a weak dependence on the orientation. The south-facing coupon had the highest corrosion rate, 309 g/m^2/year, which was approximately 1.5 times higher than that of the west-facing coupon. A general trend could be given as: south > east > north >≈ west.
- A corrosion rate dependence on wall orientation was not revealed on the building.

5.4.8 Corrosion rates of mild steel nails in timber

The first-year corrosion rates of mild steel nails in H3.2 CCA-treated timber blocks installed on the building are given in Figure 26.

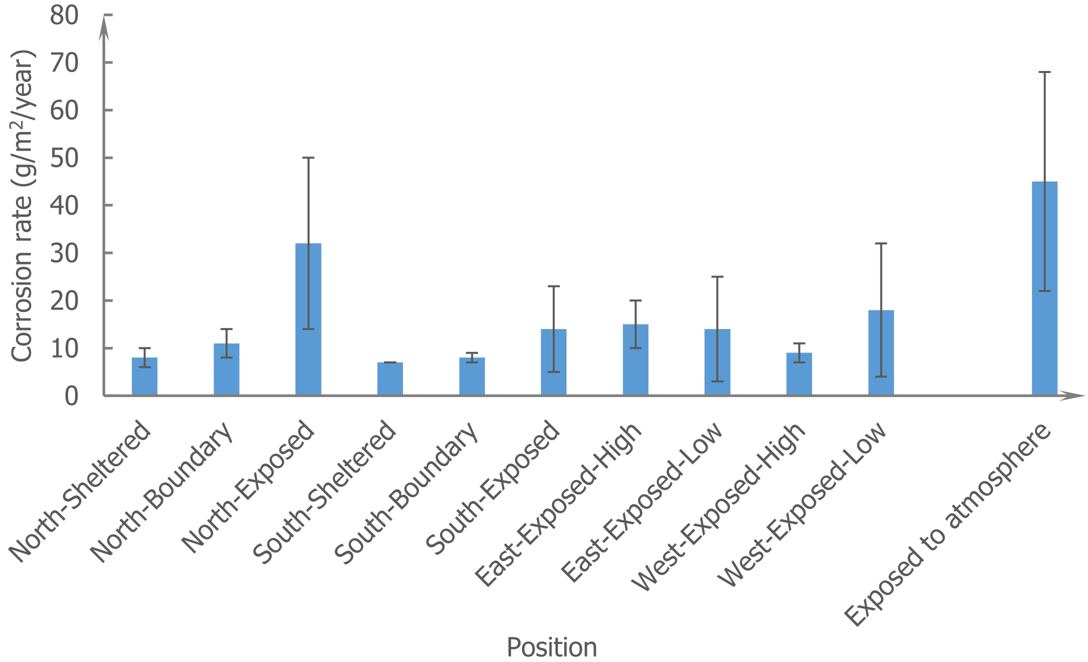

Figure 26. First-year corrosion rates of mild steel nails embedded into H3.2 CCA-treated timber blocks on the test building in Wellington.

From Figure 26, the following can be observed:

- The nails in timber blocks that were fully exposed to the atmosphere had a corrosion rate approximately 1.4–6.4 times higher than those on the building.
- The corrosion rates of the nails on the north and south walls showed a dependence on the position, sheltered < boundary < exposed.
- The nails in the exposed position on the north wall had the highest corrosion rate, 32 g/m^2/year. This position received the highest total wind-driven rain, 297.8 mm.
- The corrosion rate of the nail in the exposed-low position on the west wall was approximately 2 times higher than that of the nail in the exposed-high position. These two positions received 14 mm and 2.4 mm wind-driven rain respectively.

- The corrosion rates of the nails in the two positions on the east wall were similar, 14–15 g/m^2/year. The low and high positions received 54.2 mm and 16.4 mm of wind-driven rain respectively during the 1-year monitoring period.

5.5 Test building in Greymouth

5.5.1 Atmospheric environmental conditions

The highest hourly ambient temperature was approximately 24.2°C while the lowest was approximately 0.4°C at this site during the 1-year monitoring period (June 2018 – June 2019). Time-of-wetness and rainfall during this period were approximately 5,206 hrs (level τ_4) and 1,973 mm respectively. The prevailing wind was from the northeast (NE) – east-northeast (ENE). Wind could also blow from east (E) – east-southeast (ESE) and west-southwest (WSW) – west-northwest (WNW) directions. The maximum wind speed was approximately 14.5 m/s during this period (see Figure 27).

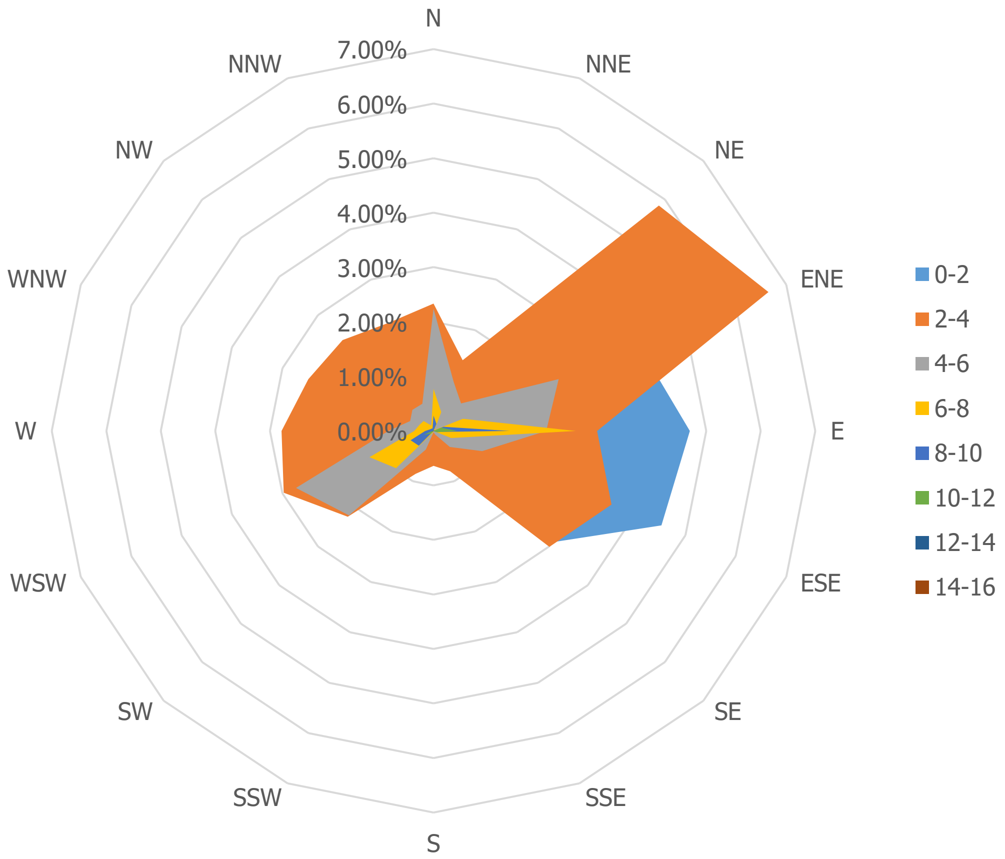

Figure 27. Wind speed (m/s) and direction during the 1-year monitoring period (percentage shown is count of wind speed).

Atmospheric corrosivity of this site was classified by the first-year corrosion rate.

- Mild steel – 193 g/m^2/year as ISO 9223 C2 – Low.
- Copper – 11 g/m^2/year as ISO 9223 C3 – Medium.
- Zinc – 7 g/m^2/year as ISO 9223 C3 – Medium.

This site was not highly corrosive due mainly to its distance from the sea and the sheltering effects offered by the surrounding trees and buildings.

5.5.2 Environmental conditions on the test building

Table 14 summarises the environmental monitoring results in each position on the building. The following can be observed:

- The average temperatures of all positions on the building were similar, 14.3–16.0°C. These were approximately 2–4°C higher than the ambient temperature.
- The exposed position had a larger temperature variation than the sheltered position on the same wall.
- The highest temperature, 54.5°C, measured in the exposed position on the west wall was approximately 30°C higher than the highest ambient temperature.
- The exposed position had a slightly higher average RH than the sheltered position on the same wall.
- The sheltered positions on the building had similar ToW values, approximately 4,600–4,900 hrs (category τ_4).
- The exposed positions on the building had similar ToW values, approximately 5,300–5,700 hrs. The ToW values in the exposed positions on the south, east and west walls were classified as τ_5, the highest category.
- The sheltered position had a smaller ToW than the exposed position on the same wall. The difference was approximately 400–1,000 hrs.
- The ToW measured in the surrounding atmospheric environment was approximately 5,200 hrs, which was 100–500 hrs lower than that of the exposed position and 260–630 hrs higher than that of the sheltered position on the building.

Table 14. Environmental conditions on the test building in Greymouth.

Wall	Position	Temperature (°C)		Average RH (%)	ToW (hours)	
		Average	Range		Value	Category
North	Sheltered	14.9	2.0–32.3	78	4,881	τ_4
	Exposed	16.0	1.1–51.2	79	5,310	τ_4
South	Sheltered	14.5	1.2–31.9	79	4,944	τ_4
	Exposed	14.3	0.5–41.0	83	5,661	τ_5
East	Sheltered	14.5	2.2–28.0	78	4,574	τ_4
	Exposed	14.3	1.2–47.8	82	5,565	τ_5
West	Sheltered	14.7	1.5–31.0	78	4,640	τ_4
	Exposed	15.5	0.8–54.5	82	5,708	τ_5
Atmosphere		12.5	0.4–24.2	81	5,206	τ_4

Note that the ToW of the atmospheric environment was calculated using temperature and RH measured with the weather station in the Greymouth airport. The airport is approximately 1.8 km southwest of the test building and is more open when compared with the test site. This may affect the ToW difference observed.

5.5.3 Surface deposition on the test building

Surface soluble deposits were measured on the painted, nearly vertical timber weatherboard directly. The results are shown in Table 15.

Table 15. Surface deposition on the test building in Greymouth.

Wall	Position	Surface deposition (µg/cm²)					
		Sep 2018	Nov 2018	Feb 2019	Apr 2019	Jun 2019	Yearly total
North	Sheltered	2.0–2.1	0.9–1.1	1.2–1.4	1.7–1.7	3.9–4.1	9.7–10.4
	Exposed	0.9–0.9	0.7–0.7	1.0–1.5	1.3–1.4	1.7–2.0	5.6–6.5
South	Sheltered	5.9–6.9	4.1–4.4	4.7–5.7	4.8–6.0	15.1–16.3	34.6–39.3
	Exposed	1.0–1.3	0.8–1.1	1.5–1.6	1.0–1.1	1.1–1.2	5.4–6.3
East	Sheltered	6.6–7.3	6.3–7.1	8.2–8.7	5.4–5.5	6.5–7.2	33.0–35.8
	Exposed	2.4–2.4	2.5–2.5	5.5–5.6	2.4–2.5	1.0–1.0	13.8–14.0
West	Sheltered	3.5–3.8	2.5–3.0	4.3–4.4	3.4–3.5	4.7–5.7	18.4–20.4
	Exposed	1.7–1.9	0.9–1.1	0.8–0.8	0.9–0.9	0.9–0.9	5.2–5.6

From Table 15, the following can be observed:

- The highest amount of surface soluble deposition, 34.6–39.3 µg/cm², was measured in the sheltered position on the south wall. This was lower than those on the buildings in Auckland (55.5–59.9 µg/cm²), Waihau Bay (163.8–172.2 µg/cm²) and Wellington (101.5 µg/cm²).
- The sheltered position collected more deposits than the exposed position on the same wall. The difference was approximately 2–6 times.
- The sheltered positions on the south and east walls collected more deposits than sheltered positions on the north and west walls (approximately 2–3 times higher).
- The exposed positions on the north, south and west walls collected similar amount of deposits. Meanwhile, the exposed position on the east wall collected more deposits (approximately 2 times higher).

Note that the sheltered positions on the south and east walls were under the eaves, which are approximately 650 mm wide. The sheltered positions on the north and west walls were under the window awnings, which are approximately 300 mm wide.

5.5.4 Corrosion rates of mild steel coupons

The first-year corrosion rates of mild steel coupons installed on the building are given in Figure 28, from which the following can be observed:

- The corrosion rates of the mild steel coupons installed on the small reference rack and fully exposed to the atmosphere showed no obvious orientation dependence. Further, the corrosion rates of the four mild steel coupons installed at an angle of 45° were similar, ranging from 140 to 180 g/m²/year. These were similar to the corrosion rate of the mild steel coupon facing towards north, 193 g/m²/year.
- The corrosion rates of mild steel coupons followed a trend of 0° > 45° > 90°. This applied to the coupons installed on the building and exposed to the atmosphere.
  - Coupons exposed to the atmosphere: the corrosion rates between the 45° and 90° inclined coupons were similar. Meanwhile, the corrosion rates of the 0° inclined coupons were approximately 1.6–2 times higher than those of the 45° inclined coupons. This gave a trend of 0° > 45° >≈ 90°.
  - Coupons installed on the building: The corrosion rates of the 0° inclined coupons were approximately 1.1–1.7 times higher than those of the 45° inclined

coupons. The corrosion rates of the 45° inclined coupons were approximately 1.9–4.7 times higher than those of the 90° inclined coupons. This gave a trend of 0° >≈ 45° > 90°.

This is similar to that observed on the buildings in Auckland and Wellington.

- The coupons installed on the building were, in general, corroding slower than those fully exposed to the atmosphere. This was particularly true for the 0° and 90° inclined coupons. For example, the corrosion rates of the 90° inclined coupons that were exposed to the atmosphere were approximately 2–5 times higher than those of the coupons installed on the building.
- Mild steel corrosion did not show an obvious dependence on wall orientation.
- The corrosion rate in the exposed position was slightly higher than that in the sheltered position on the same wall.

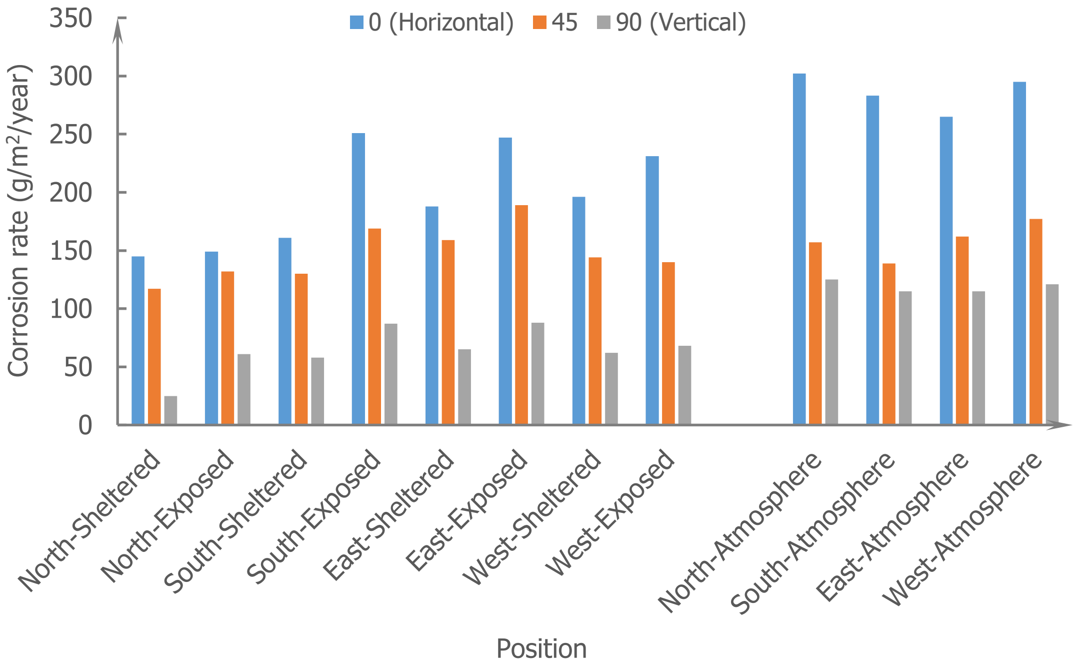

Figure 28. First-year corrosion rates of mild steel coupons on the test building in Greymouth.

5.5.5 Corrosion rates of mild steel nails in timber

The first-year corrosion rates of mild steel nails driven into H3.2 CCA-treated timber blocks are given in Figure 29, from which the following can be observed:

- The nails in timber blocks fully exposed to the atmosphere had a corrosion rate approximately 2–40 times higher than those installed on the building.
- The nail corrosion rates were low in the sheltered positions, 3–6 g/m^2/year.
- The nail corrosion rates in the exposed positions were similar on the north, south and west walls, 35–49 g/m^2/year. A much lower corrosion rate was measured on the east wall, 11 g/m^2/year.
- The nails in the timber blocks in the exposed position had much a higher average corrosion rate than those in the sheltered positions on the same wall. The difference was approximately 2–14 times. This observation is somewhat similar to that observed with the mild steel coupons.

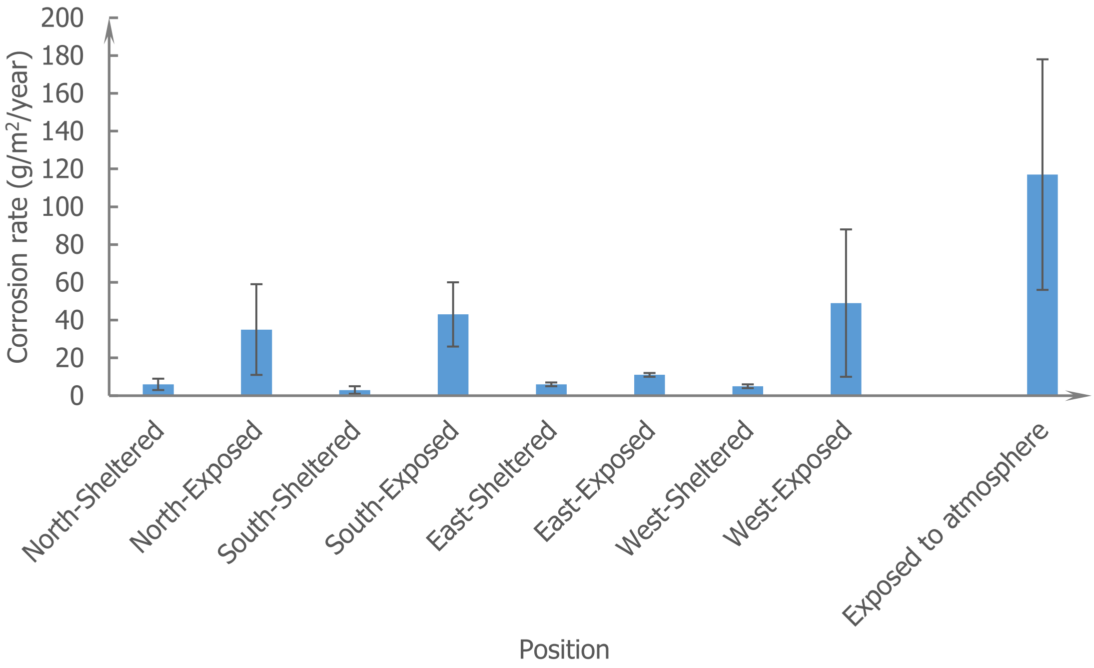

Figure 29. First-year corrosion rates of mild steel nails embedded into H3.2 CCA-treated timber blocks on the test building in Greymouth.

5.6 Test building in Christchurch

5.6.1 Atmospheric environmental conditions

At this site, the highest and lowest hourly ambient temperatures were approximately 38.2°C and -4.0°C respectively during the 1-year monitoring period (September 2018 – September 2019). Time-of-wetness and rainfall were approximately 5,100 hrs (τ_4) and 641 mm respectively. Note that rainfall was measured by the weather station operated within the Christchurch airport, which is approximately 7.6 km southwest of the test building.

Atmospheric corrosivity of the site was classified by the first-year corrosion rate.

- Mild steel – 167 g/m^2/year as ISO 9223 C2 – Low.
- Copper – 11 g/m^2/year as ISO 9223 C3 – Medium.
- Zinc – 4 g/m^2/year as ISO 9223 C2 – Low.

These results showed that this test site was relatively benign (ISO 9223 C2 – Low).

5.6.2 Environmental conditions on the building

Table 16 summarises the environmental monitoring results on the building, from which the following can be observed:

- The average hourly temperatures of all the positions on the building typically ranged from 13.6 to 16.6°C. The two positions on the west wall had slightly higher maximum temperatures than the positions on the other three walls.
- The exposed position had a larger temperature variation than the sheltered position on the same wall.
- The highest hourly temperature was measured in the exposed position on the west wall, namely 55.9°C. The highest ambient temperature was 38.2°C.

- The lowest hourly temperature on this building was -1.7°C in the exposed position on the east wall. This was higher than that in the surrounding atmosphere, -4.0°C.
- The sheltered position had a lower average RH than the exposed position on the same wall, 67–75% versus 73–80%, during the 1-year monitoring period.
- The ToW values in sheltered and exposed positions were approximately 1,600–3,700 hrs and 3,500–4,800 hrs respectively. The south and east walls appeared to experience longer ToW than the north and west wall.
- The exposed position had a larger ToW than the sheltered position on the same wall. The difference was approximately 1,000–2,300 hrs.
- The surrounding atmosphere had a lower average hourly temperature (12.1°C) and a higher average RH (81%) than all the positions on the building.
- The surrounding atmosphere had a ToW of 5,100 hrs, which was higher than all the positions on the building.

Table 16. Environmental condition on the test building in Christchurch.

Wall	Position	Temperature (°C)		Average RH (%)	ToW (hours)	
		Average	Range		Value	Category
North	Sheltered	14.9	2.7–34.9	70	1,764	τ_3
	Exposed	15.0	0.6–49.5	73	3,541	τ_4
South	Sheltered	14.7	1.9–37.0	72	2,561	τ_4
	Exposed	13.7	-0.2–41.9	80	4,753	τ_4
East	Sheltered	14.0	1.1–40.3	75	3,666	τ_4
	Exposed	13.6	-1.7–44.3	79	4,699	τ_4
West	Sheltered	16.6	3.0–46.3	67	1,631	τ_3
	Exposed	16.6	-0.5–55.9	73	3,881	τ_4
Atmosphere		12.1	-4.0–38.2	81	5,100	τ_4

5.6.3 Surface deposition on the test building

Soluble deposits measured on the painted window frame surfaces are shown in Table 17).

Table 17. Surface deposition on the test building in Christchurch.

Wall	Position	Surface deposition (μg/cm^2)				
		Feb 2019	Apr 2019	Jul 2019	Sep 2019	Yearly total
North	Sheltered	12.9–14.7	14.9–15.5	7.9–8.4	3.3–3.5	39.0–42.1
	Exposed	0.9–0.9	0.9–1.0	1.3–1.8	1.0–1.0	4.1–4.7
South	Sheltered	8.3–8.6	12.8–14.1	5.8–6.0	3.8–3.9	30.7–32.6
	Exposed	1.0–1.4	1.4–1.6	1.1–1.4	1.0–1.0	4.5–5.4
East	Sheltered	16.3–17.0	11.5–12.7	10.2–11.3	13.2–14.7	51.2–55.7
	Exposed	1.1–1.2	1.3–1.6	1.0–1.2	1.1–1.5	4.5–5.5
West	Sheltered	10.7–12.7	12.4–13.2	2.7–2.9	2.1–2.2	27.9–31.0
	Exposed	0.9–1.2	0.8–0.8	1.5–1.6	1.0–1.0	4.2–4.6

From Table 17, the following can be observed:

- The four exposed positions collected 4–6 μg/cm^2 in the 1-year period.
- Surface depositions in the sheltered positions varied with the wall. The sheltered position on the east wall collected the highest amount of salt deposits, 51.2–55.7 μg/cm^2, which was approximately 1.8 times higher than the lowest amounts.
- The sheltered position collected more deposits than the exposed position on the same wall. The difference was approximately 6–11 times.

5.6.4 Corrosion rates of mild steel coupons

The first-year corrosion rates of mild steel coupons are given in Figure 30.

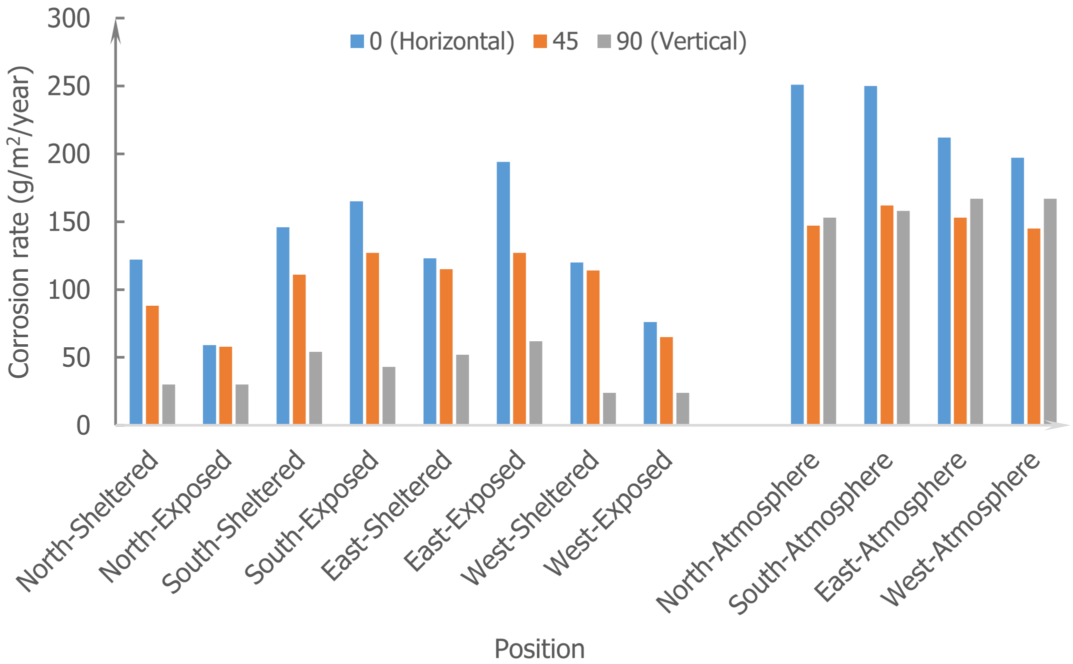

Figure 30. First-year corrosion rates of mild steel coupons on the test building in Christchurch.

From Figure 30, the following can be observed:

- The corrosion rates of the mild steel coupons exposed to the atmosphere showed no obvious orientation dependence.
- The 0° inclined coupons exposed to the atmosphere had higher corrosion rates than the 45° and 90° inclined coupons. The 45° inclined coupons had corrosion rates that were similar to or slightly lower than those of the 90° inclined coupons.
- The corrosion rates of the mild steel coupons on the building did not show an obvious dependence on the wall orientation.
- The 0° and 90° inclined coupons on the building had the highest and lowest corrosion rates respectively. The 45° inclined coupons had corrosion rates that were slightly lower than those of the 0° inclined coupons and higher than those of the 90° inclined coupons (approximately 2–5 times higher). This gave a trend of 0° >≈ 45° > 90°. This trend is similar to that observed on the buildings in Auckland, Wellington and Greymouth and somewhat different from that observed with the coupons fully exposed to the atmosphere at this site.
- The coupons installed on the building were corroding slower than those fully exposed to the atmosphere. For example, the corrosion rates of the 90° inclined

coupons that were exposed to the atmosphere were approximately 3–7 times higher than those of the coupons installed on the building.

- The corrosion rates in the exposed positions on the south and east walls were, in general, higher than the sheltered positions on the building.

Note the following:

- The north wall is close to a fence and trees (less than 2 m). These may provide a shade to the lower section of this wall and protect the coupons in the exposed position from wind and rain. At the west side, trees and plants in the north and south directions may also provide shade to the exposed positions.
- Bird droppings were observed on the 0° and 45° inclined coupons installed in the sheltered positions on the north and west walls. They may accelerate mild steel corrosion under favourable environmental conditions.

5.6.5 Corrosion rates of mild steel nails in timber

Figure 31 shows the first-year corrosion rates of mild steel nails in timber blocks.

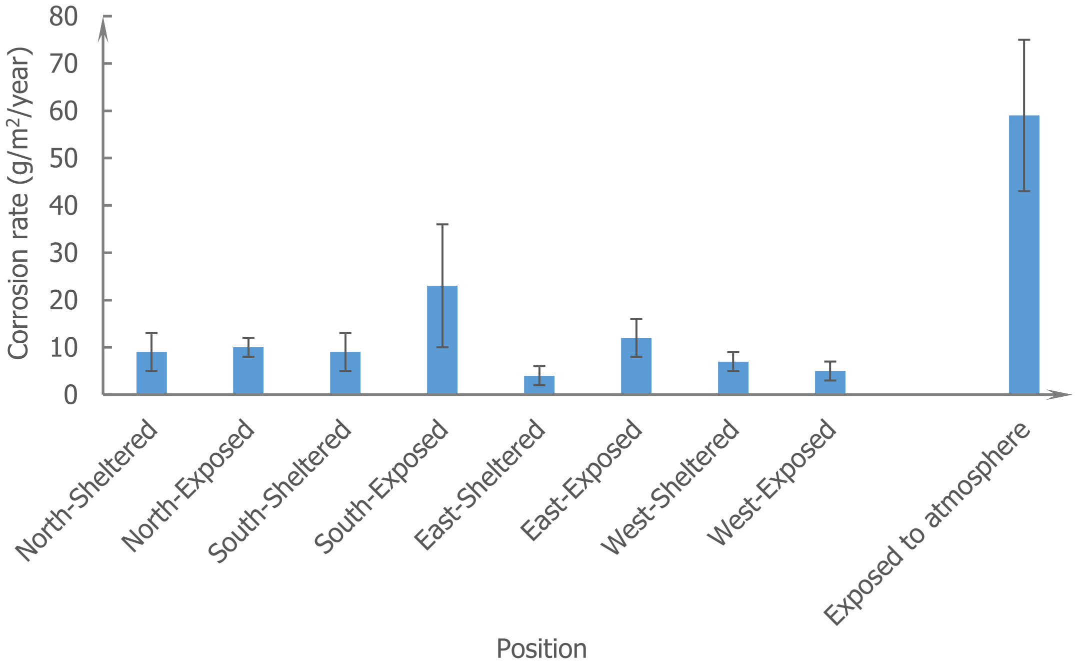

Figure 31. First-year corrosion rates of mild steel nails embedded into H3.2 CCA-treated timber blocks on the test building in Christchurch.

From Figure 31, the following can be observed:

- The corrosion rates of the nails in timber blocks fully exposed to the atmosphere were approximately 3–15 times higher than those of the nails on the building.
- The corrosion rates of the nails on the building did not show an obvious dependence on the wall orientation. However, the exposed position on the south wall had the highest corrosion rate, 23 ± 13 g/m^2/year. This is similar to the observation with mild steel coupons on the building.
- The nails in the timber blocks installed in the exposed positions on the south and east walls had approximately 3 times higher corrosion rates than those installed in the sheltered positions. This is similar to that observed with mild steel coupons.

5.7 Test building in Lauder

5.7.1 Atmospheric environmental conditions

The highest hourly ambient temperature was approximately 32.2°C while the lowest was approximately -6.6°C during the 1-year monitoring period (September 2018 – September 2019). Time-of-wetness and rainfall during this period were approximately 3,166 hrs (level τ_4) and 573 mm respectively. The prevailing wind was from the north-northeast (NNE) – northeast (NE). Wind could also blow from west-southwest (WSW) directions. The maximum wind speed was approximately 15 m/s during this period (see Figure 32).

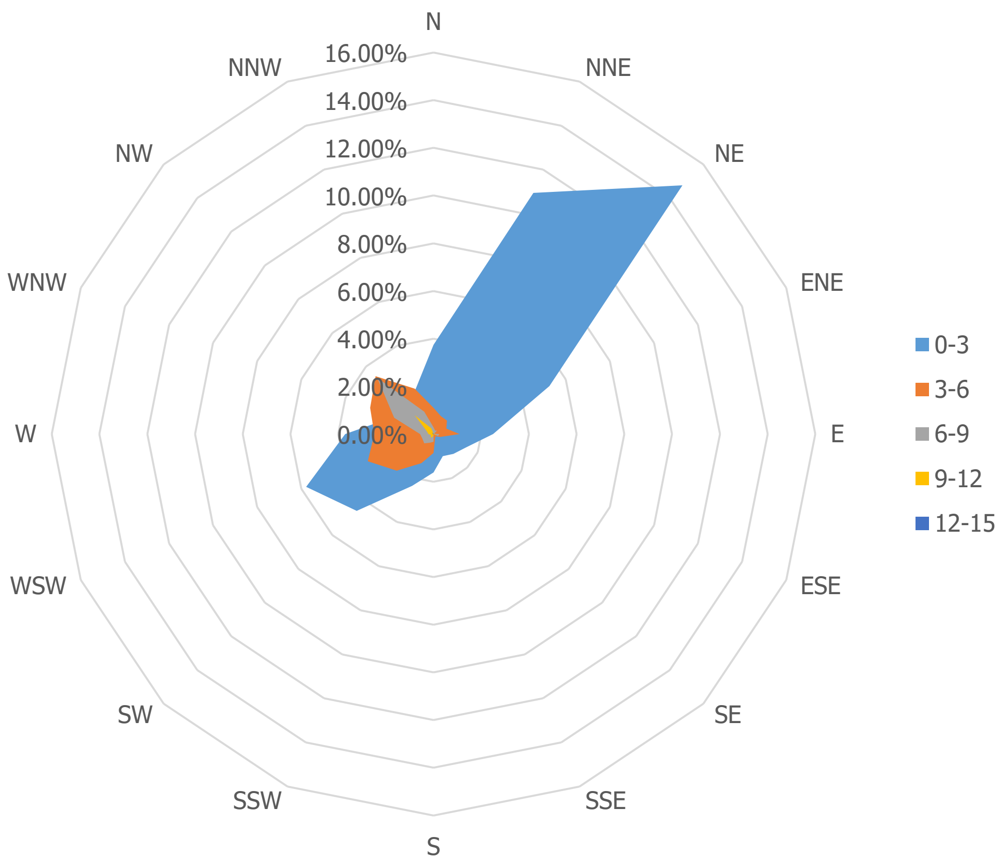

Figure 32. Wind speed (m/s) and direction during the 1-year monitoring period (percentage shown is count of wind speed).

Atmospheric corrosivity of the site was classified by the first-year corrosion rate.

- Mild steel – 26 g/m^2/year as ISO 9223 C2 – Low.
- Copper – 2 g/m^2/year as ISO 9223 C2 – Low.
- Zinc – 3 g/m^2/year as ISO 9223 C2 – Low.

These results showed that the atmosphere of this site is benign (ISO 9223 C2 – Low).

5.7.2 Environmental conditions on the test building

The environmental monitoring results on the building are summarised in Table 18.

Table 18. Environmental condition on the test building in Lauder.

Wall	Position	Temperature (°C)		Average RH (%)	ToW (hours)	
		Average	Range		Value	Category
North	Sheltered	12.3	-4.2–34.0	65	1,681	τ_3
	Exposed	13.6	-5.1–45.5	65	2,469	τ_3
South	Sheltered	11.2	-4.6–33.8	70	2,677	τ_4
	Exposed	10.8	-4.8–35.4	74	3,247	τ_4
East	Sheltered*	13.7	-4.7–37.7	66	1,672	τ_3
	Exposed	12.4	-5.9–45.8	70	2,894	τ_4
West	Sheltered	11.8	-5.0–32.1	68	2,163	τ_3
	Exposed	11.8	-5.3–47.6	73	3,360	τ_4
Atmosphere		10.2	-6.6–32.2	72	3,166	τ_4

* Temperature and RH data for the period July – September 2019 was lost since iButtons were damaged.

From Table 18, the following can be observed:

- The average hourly temperature on the building (sheltered position on the east wall not included) ranged from 10.8–13.6°C. This was higher than the ambient temperature, 10.2°C. The temperature was not obviously dependent on wall orientation.
- The highest hourly temperature, 45.8°C, measured in the exposed position on the east wall was approximately 13°C higher than the highest ambient temperature.
- The sheltered position seemed to have an average temperature similar to the exposed position on the same wall. However, the exposed position showed an obviously larger temperature variation than the sheltered position.
- The sheltered position seemed to have a lower average RH value than the exposed position on the same wall. The exception is the north wall.
- The sheltered and exposed positions on the building had ToW values of approximately 1,700–2,700 hrs and 2,500–3,400 hrs respectively (east wall not included). Therefore, the exposed positions had ToW values approximately 570–1,200 hrs larger than the sheltered positions (east wall not included).
- The surrounding atmosphere had a ToW of 3,166 hrs, which was higher than those of the sheltered positions and approximately 200 hrs lower than the highest ToW measured on the exposed positions on the building.
- ToW values measured on this building and in its surrounding environment were lower than those measured on the buildings in Waihau Bay, Wellington, Greymouth and Christchurch.

5.7.3 Surface deposition on the test building

Surface soluble deposits measured on aluminium window frame surfaces are given in Table 19, from which the following can be observed:

- The total amounts of surface deposition on this building were very low when compared with those on other buildings monitored in the present study. Most positions collected less than 7 μg/cm^2 of deposits during the 1-year period.

- The exposed position on the north wall collected the highest amount of deposits, 18.8–20.5 μg/cm^2. However, the surface used for the initial two measurements was close to the fan of an air conditioning unit. In those two periods, relatively high deposition amounts around 8–10 μg/cm^2 were measured. From February 2019, another surface away from this vent was used and much lower deposition (approximately 1 μg/cm^2) was measured. Therefore, the actual deposition in the exposed position on the north wall could be lower.
- No obvious soluble deposition dependence on wall orientation was revealed. This is in line with expectation since Lauder has the cleanest inland atmospheric environment.
- Marginally, the sheltered position collected more deposits than the exposed position on the same wall.

Table 19. Surface deposition on the test building in Lauder.

Wall	Position	Surface deposition (μg/cm^2)				
		Dec 18	Feb 19	May 19	Sep 19	Yearly total
North	Sheltered	1.1–1.2	1.0–1.1	0.9–1.1	0.8–0.9	3.8–4.3
	Exposed*	8.1–8.9	9.0–9.8	0.9–0.9	0.8–0.9	18.8–20.5
South	Sheltered	1.2–1.4	1.4–1.7	1.3–1.4	1.2–1.3	5.1–5.8
	Exposed	1.0–1.0	0.9–1.1	0.9–0.9	1.0–1.2	3.8–4.2
East	Sheltered	2.1–2.4	1.6–1.8	1.0–1.1	1.0–1.3	5.7–6.6
	Exposed	1.4–1.5	1.3–1.5	0.9–0.9	0.9–1.1	4.5–5.0
West	Sheltered	1.3–1.4	1.0–1.3	0.9–1.0	0.9–1.1	4.1–4.8
	Exposed	1.2–1.2	0.7–0.7	0.9–0.9	0.8–0.9	3.6–3.7

* The surface for measurements in December 2018 and February 2019 was close to an air conditioning system. Measurements in May and September 2019 were then performed on another surface.

5.7.4 Corrosion rates of mild steel coupons

The first-year corrosion rates of mild steel coupons are given in Figure 33, from which the following can be observed:

- The corrosion rates of the mild steel coupons fully exposed to the atmosphere were very low with the highest to be approximately 17 g/m^2/year. This is as expected since Lauder has a dry and clean environment.
- The corrosion rates of mild steel coupons generally followed a trend of 0° > 45° > 90°. This applied to the coupons installed on the building and exposed to the atmosphere. This was similar to that observed in Auckland, Wellington, Greymouth and Christchurch.
- The corrosion rates of the mild steel coupons on the building were also low with the highest to be approximately 39 g/m^2/year. They seemed to be slightly higher than those in the surrounding atmosphere. This was particularly true for the 0° and 45° inclined coupons. However, it should be noted that these high corrosion rates were normally associated with the presence of bird droppings on the coupon surface (particularly in the sheltered positions). Bird droppings can speed up corrosion of steel since they can turn into ammonia and/or salt that are corrosive.
- A corrosion rate dependence on wall orientation was not found on the building and in the surrounding atmosphere.

- It is impossible to determine whether the exposed positions are consistently more or less corrosive than the sheltered positions based on these very low steel corrosion rates.

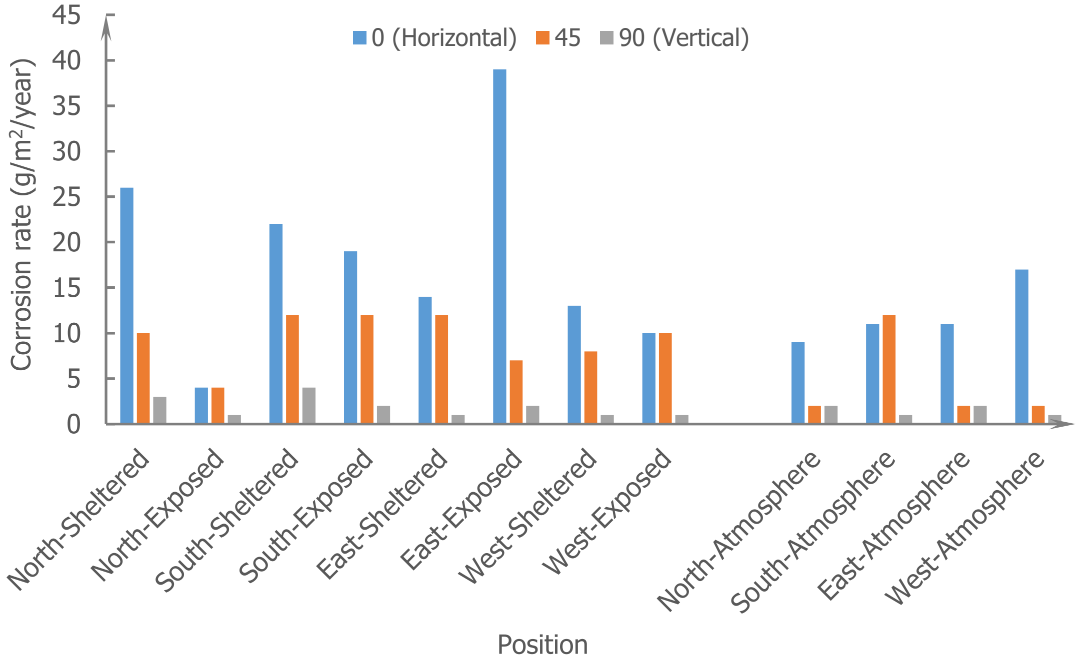

Figure 33. First-year corrosion rates of mild steel coupons on the test building in Lauder.

5.7.5 Corrosion rates of mild steel nails in timber

Figure 34 shows the first-year corrosion rates of mild steel nails driven into H3.2 CCA-treated timber blocks.

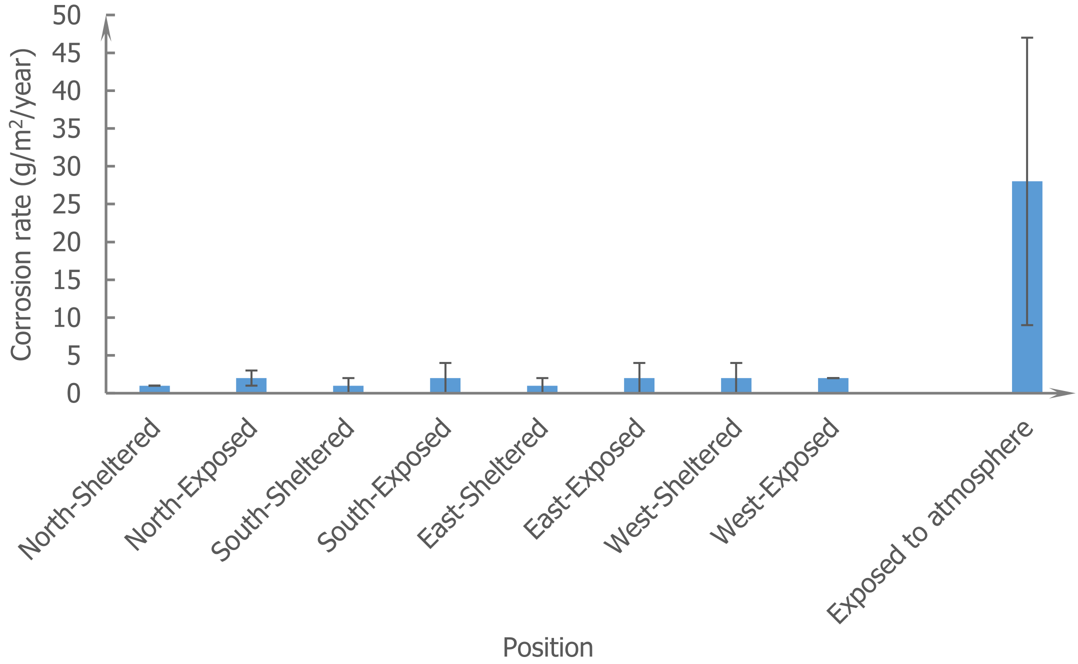

Figure 34. First-year corrosion rates of mild steel nails embedded into H3.2 CCA-treated timber blocks on the test building in Lauder.

From Figure 34, the following can be observed:

- The corrosion rates of nails in timber blocks installed on the building were very low, approximately 1–2 $g/m^2/year$. This was more than 14 times lower than that measured with the nails in timber blocks fully exposed to the surrounding atmospheric environment, 28 ± 19 $g/m^2/year$.
- A mild steel nail corrosion rate dependence on wall orientation was not observed. This was somewhat similar to that observed with the mild steel coupons installed on the building.
- The nails in the timber blocks in the exposed positions seemed to have higher corrosion rates than those in the sheltered positions. However, it should be noted that these corrosion rates were very low, and therefore this comparison could not be made confidently.

6. Discussion

6.1 Environmental conditions on test buildings

6.1.1 Temperature, humidity and time-of-wetness

The surface temperature profile on the building envelope can be quite different from that in the atmospheric environment. For example, the maximum surface temperature measured on the building in Wellington with fibre-cement weather boards was 64.7°C. This was approximately 40°C higher than the maximum ambient temperature, 27.4°C. On the building in Christchurch with brick veneer wall cladding, the maximum temperature was 55.9°C, this being approximately 18°C higher than the maximum ambient temperature, 38.2°C. In addition, the temperature variations on the building were larger than those of the atmosphere.

Surface temperature on the building envelope can be influenced by a variety of factors:

- Different cladding materials have different thermal capacity and heat transfer capability. For example, the specific heat capacities for steel, pine and clay brick are 0.88, 2.05 and 4.19 J/(g·K) respectively (Zhang, 2011).
- Cooling effects provided by winds may play a role in temperature and its variation over the building envelope. In comparison with the surrounding atmospheric environment, the building envelope would tend to have a larger response to solar heating due mainly to its smaller mass.
- Building orientation would inherently lead to the formation of somewhat different temperature variations and extremes on the same building. This is mainly related to the relative position to the sun during the day, which acts as the major heat source to the cladding materials. In addition, construction features, such as eaves, can have obvious influences on wall temperature profile.

Surface temperatures measured on the building envelope were higher than the ambient temperature. An increase of temperature normally leads to a decrease in relative humidity. This could contribute to lower ToW values measured on the building envelope (such as on the buildings in Waihau Bay, Wellington and Christchurch). Meanwhile, temperature and humidity variations in the sheltered positions were normally smaller than those in the exposed positions. The sheltered positions were not directly exposed to weather conditions due mainly to the protection provided by the eave above. These tended to provide a relatively stable micro-scale environment, which may contribute to a smaller ToW as well. ToW is arguably regarded as one of the critical variables that can influence atmospheric corrosion of metals and steels (Norberg, 2002; Chico, de la Fuente, Diaz, Simancas & Morcillo, 2017). This is particularly evident in areas without heavy airborne pollution, such as exposure zone B of NZS 3604:2011.

6.1.2 Wind-driven rain

Wind-driven rain is recognised as an important source of moisture that can influence the hygrothermal performance of building façades and contribute to material deterioration over the building envelope (Blocken, Abuku, Roles & Carmeliet, 2009; Orr, Young, Stelfox, Curran & Viles, 2018).

Wind-driven rain is highly dependent on wall orientation. For example, on the building in Wellington, the highest amount of wind-driven rain was measured in the exposed position on the north wall. This aligned with the direction of the prevailing northwest wind. However, the wind-driven rain quantity on the building envelope was significantly lower than the reference rainfall at the site. For example, the highest wind-driven rain on the Wellington building was 297.8 mm, which was approximately 5 times lower than the reference.

A comparison of wind-driven rain at different heights on the wall confirms that an eave could protect the areas below. However, the actual size of this protected area is related to not only the width of the eave but also the direction and severity of the prevailing/common winds. For example, the eaves on the north and south sides of the Wellington building are approximately 600 mm. The position of 600 mm below the eave on the north wall had a wind-driven rain recording of 94.4 mm, which was approximately 3 times lower than that measured at the lower, fully exposed position, 297.8 mm. However, with extremely strong winds from the north, a limited amount of rain can still penetrate into the sheltered area under the eave. In consideration of the topography in some New Zealand areas, this might be common on some buildings in hilly locations and facing towards strong prevailing winds. On the walls not subject to prevailing/common winds, an eave may protect much larger areas below.

6.1.3 Surface deposition

Most buildings recruited for the present study were influenced in some way by marine environments. Excluding the test building in Rotorua, the highest surface deposition measured in the sheltered positions on six buildings was plotted against the distance from the sea (see Figure 35).

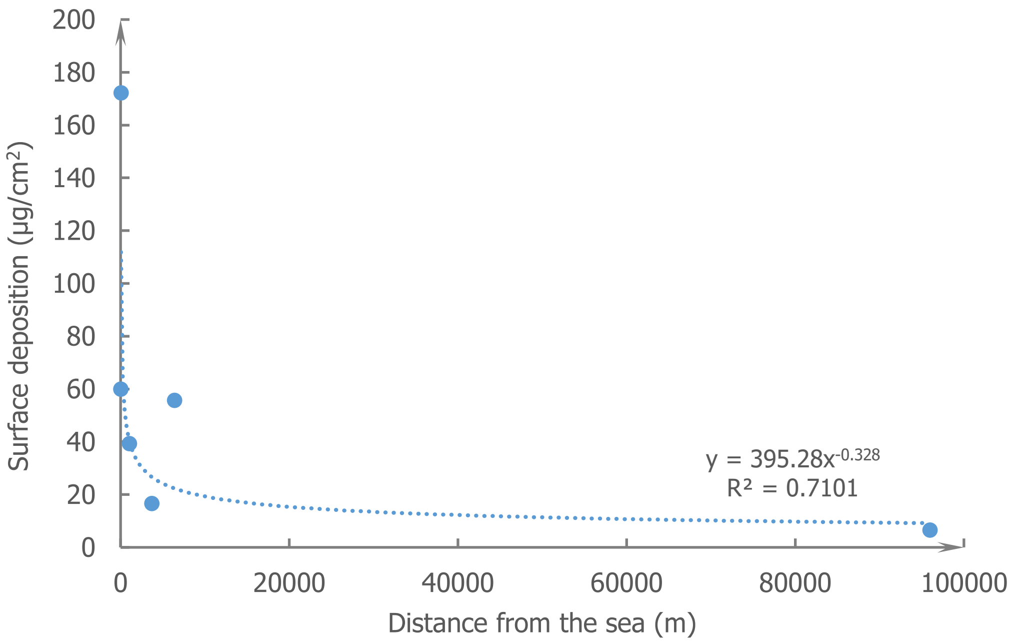

Figure 35. Correlation between the highest surface deposition in sheltered position on the building and distance from the sea.

Surface deposition on the building decreased quickly with distance from the sea. This trend is similar to that observed with a purpose-built shelter (see Figure 3).

The quantity of surface deposits can be affected by many factors, typically including distance from the source (such as the sea), quantity of particles in the air, wind direction and speed and rainwater washing (Castañeda, Corvo, Howland & Marrero, 2018; Pham et al., 2019).

However, surface deposition on the building can be affected by several factors and shows its own features when compared with that exposed to the atmosphere:

- Surface deposition is significantly dependent on the inclination angle of the collection surface. The 0° inclined surface always collects the highest amount of deposits among the three inclined surfaces (0°, 45° and 90°). However, the deposition differences between the 0° and 90° inclined surfaces can be larger when they are installed on the building. For example, on the building in Wellington, the differences were determined to 2–6 times and 1.1–1.9 times for the surfaces on the building and exposed to the atmosphere respectively.
- Surface deposition on the building is dependent on a variety of factors, such as location of pollution source, distance from the source, building orientation and direction/speed of prevailing/common winds. In strong marine environments, the wall facing towards the sea could have a higher chance to collect more salt particles than other walls. However, the wall facing towards the sea normally faces towards the prevailing wind. The prevailing wind may have some negative effects on salt accumulation. Firstly, strong prevailing winds could introduce a larger amount of wind-driven rain to wash away more deposits. Secondly, wind may also have a cleaning effect by itself. It has been predicted that winds with a speed exceeding a critical value have the ability to blow dust and/or dry salt off material surfaces (Cole, Lau, Chan & Paterson, 2004). For example, on the building in Waihau Bay, the highest surface deposition was not observed on the west wall that was directly facing towards to the sea.
- Rain-washing effect is obvious on the building, evidenced by the large difference between sheltered and exposed positions. Rain washing could also be very effective to remove deposits from certain material surfaces.

Salt is considered to be a main contributor to material deterioration on buildings exposed to marine influences (Duncan & Balance, 1988; Delgado et al., 2016; Morillas et al., 2020). The highest surface deposition measured on the six buildings (the Rotorua building was excluded) was plotted with the corrosion rates of the 90° inclined coupons in the sheltered positions (see Figure 36). It is supposed that all soluble deposits will contribute to mild steel corrosion in the present study.

Figure 36 shows that the highest deposition in the sheltered position and the mild steel corrosion rate (90° inclined) on the building can be correlated to each other. Two trends can be derived with these data – linear and polynomial. Both trends show that mild steel corrosion increases with surface deposition.

Atmospheric corrosion of mild steel in these monitoring areas can be affected by climatic factors (temperature, humidity, ToW, wind and rain) and airborne pollutants (sea salt particles). Some of them will play more important roles than others, depending on the actual environmental conditions of a specific area. As such, the atmospheric corrosion processes and/or mechanisms in different areas might be somewhat different. For example, in Lauder, which is virtually free of marine influences, the factor key to atmospheric corrosion of mild steel will be the moisture on the surface. Therefore, ToW should be considered to be more significant. In Waihau Bay, chloride-containing salt particles sourced from the sea will contribute to corrosion significantly. However, they still need to work with the water/moisture layer formed and sitting on the metal surface synergistically to accelerate the corrosion.

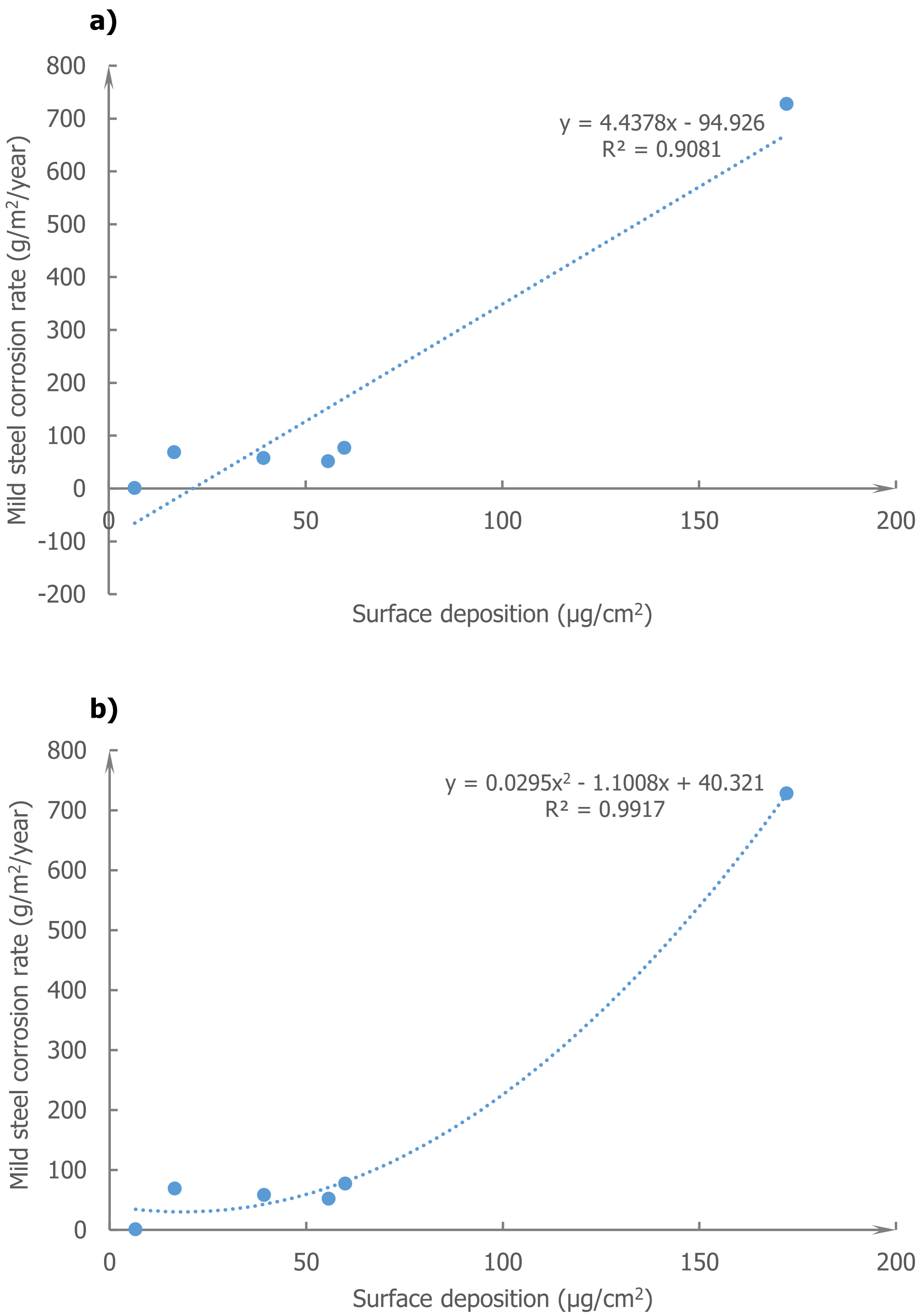

Figure 36. Correlation between the highest surface deposition in the sheltered position on the building and the corrosion rate of 90° inclined mild steel coupon: (a) linear fitting and (b) polynomial fitting.

6.2 Comparative corrosivity between building and the atmosphere

The comparative corrosivity on the test building and of the surrounding atmosphere was determined by the first-year corrosion rates of mild steel coupons and nails driven into H3.2 CCA-treated timber blocks.

6.2.1 Mild steel coupons

In general, the following comparative corrosivity between positions (exposed and sheltered) on the building and atmospheric environment can be observed in Auckland, Rotorua, Wellington, Greymouth and Christchurch:

- surrounding atmosphere >≈ positions on the building.

In Lauder, the corrosivity on the building was broadly similar to that of the surrounding atmosphere, which is clean and dry. However, the following should be taken into account for this judgement:

- The mild steel corrosion rates were generally low.
- Bird droppings were found on the top surface of some coupons installed on the building. This may accelerate corrosion and lead to some higher corrosion rates.

Atmospheric corrosion of mild steel is governed by climatic factors (humidity and rainfall) and air pollution (salt, SO_2 and/or NO_x) (Syed, 2006; Morcillo, de la Fuente, Diaz & Cano, 2011). In Auckland, Wellington, Greymouth and Christchurch, mild steel corrosion would be influenced by environmental humidity (ToW) and, to a lesser extent, by airborne salt. Measurements performed in Wellington and Christchurch showed that ToW values on the buildings were significantly lower than those measured in the surrounding atmosphere. The difference was up to 3,000 hrs. This indicates that the mild steel surfaces on the buildings were drier for longer periods than those fully exposed to the atmosphere. This may slow down corrosion since chemical or electrochemical reactions could only happen in shorter wet periods. The sheltered positions on the buildings could retain more salt particles on their surfaces. However, since the surfaces are drier, these salt particles might not be fully activated to attack the metal.

In Waihau Bay, the comparative corrosivity between the building and its surrounding environment was more complicated:

- surrounding atmosphere > positions on the north and east walls
- surrounding atmosphere < positions on the south and west walls.

This building is approximately 60 m east of the sea. The prevailing wind was from the west during the 1-year monitoring period. The west and south walls could be influenced by the marine environment when considering the actual orientation of this building. High salt deposition was observed in some positions on these two walls. For example, the sheltered position on the south wall collected 163.8–172.2 $\mu g/cm^2$ deposits during the 1-year monitoring period. Relatively high deposition was also observed in the sheltered position on the west wall, 89.4–96.9 $\mu g/cm^2$. The amount of deposition in the exposed position on this wall was the lowest on this building, 27.3–31.1 $\mu g/cm^2$.

High corrosion rates were observed, particularly with the 0° and 45° inclined coupons on the south and west walls of this building. Corrosion rates of the mild steel coupons inclined at these two angles in the exposed positions were approximately 3.2 and 3.7 times higher than those fully exposed to the atmosphere.

The surface deposition in the sheltered position on the north wall of the Waihau Bay building was 124.4 $\mu g/cm^2$, i.e. the second highest on this building. However, mild steel corrosion rates measured on this wall were low – even lower than the surrounding environment.

These indicate that the surface deposition measured can be correlated to metal corrosion rate on the building in the Waihau Bay. However, the correlation is not simple.

Surface deposition can be affected by a number of factors. The total amount of deposits on a corroding mild steel surface might be expressed as below:

- Total deposit = deposit measured + deposit washed away + deposit dissolved and consumed by corrosion.

It is highly possible that the quantity measured on the wall cladding might not reflect the amount of salt arriving at the metal surface:

- Material type and surface condition: mild steel on the building in Waihau Bay experienced severe corrosion, and its surface was covered with thick corrosion products. This rough surface provided a large effective area to receive and retain salt particles. This might be intensified by the barrier effect provided by the wall behind. This is because salt particles tend to be released when the wind flow is forced to change its direction and/or decrease its speed (see Figure 37).

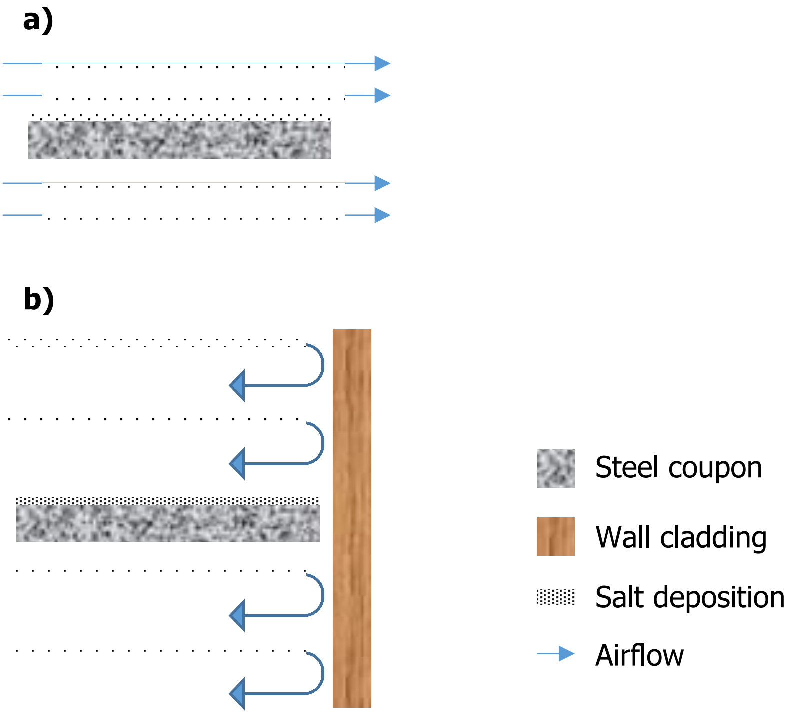

Figure 37. A schematic of surface deposition on the 0° inclined surfaces: (a) fully exposed to the atmosphere and (b) installed on the building.

- Rainwater: the 0° inclined surfaces can retain more water for longer periods than the 90° inclined surfaces. This may remove more salt particles in some situations. However, rainwater sitting on the corroding mild steel surface could enhance the dissolution of salt particles received. Therefore, the salt particles could be involved into the electrochemical corrosion processes rapidly. This amount of salt cannot be quantified appropriately and easily with the method used.
- Wind: it may have a more pronounced cleaning and drying effect to the surface fully exposed to the atmosphere. Meanwhile, the rain driven by the wind can wash away more loosely attached deposits from the surface. This may explain why the exposed position on the west wall had the lowest deposition.

6.2.2 Nails in timber

Nail corrosion results derived from monitoring at six sites showed the following comparative corrosivity between the test building and the atmosphere. These results include Auckland, Waihau Bay, Wellington, Greymouth, Christchurch and Lauder.

- surrounding atmosphere > positions on the building.

These two exposure environments could be different, particularly in terms of rainwater received:

- Fully exposed to the atmosphere: these timber blocks receive the highest amount of rainwater and are subject to irregular dry-wet cycles that are influenced by air temperature, RH and wind pattern. They may have high moisture content within extended periods.
- Positions on the building: the timber blocks, when installed in the exposed positions, could be wet when receiving wind-driven rain. However, the total amount of rain received would be much lower than that fully exposed to the atmosphere. Further, this wind-driven rain quantity would be dependent on building wall orientation. Meanwhile, the timber blocks installed in the sheltered positions would normally receive no rain.

The degradation of nails in timbers is more complicated when compared with atmospheric corrosion of metallic coupons. For example, nails always have direct, tight contacts with timber and only their head surfaces can be directly influenced by the atmosphere during service.

Most timber used on buildings is treated with preservative. For example, radiata pine weatherboards should be treated to H3.1 level to achieve a 15-year durability. Moisture or water can initiate hydrolysis, mobilisation and redistribution of preservation chemicals originally fixed onto wood structures. Free, active species (such as copper ions) can then attack susceptible metals (Kear, Wu & Jones, 2009; Li, Marston & Jones, 2011; Zelinka, Glass & Derome, 2014).

The corrosion of a nail is then dependent on timber moisture content and its duration above the threshold, 18–20%.

- The equilibrium moisture content of timber is dependent on the temperature and relative humidity of the air (Dinwoodie, 2001; Rowell, 2005). For example, a timber in an atmosphere of 20°C and 22% RH will have a moisture content of 6%. This will be double if the same timber is moved to an atmosphere of 40°C and 64% RH.
- Timber exposed directly to the atmosphere can receive rain. Its moisture content can go up significantly since water can be absorbed into its structure due to its hygroscopic nature.

Therefore, rainwater will be the primary driver for high moisture contents in timber and contribute to nail corrosion. Based on the findings of the present study, it would be expected that a nail's corrosion rate could be correlated with the quantity of rainwater received by the timber block.

Figure 38 shows the correlation between annual rainfall and corrosion rate of nails in timber blocks that were fully exposed to the atmosphere. A higher annual rainfall is generally linked with a higher nail corrosion rate. For example, Lauder and Greymouth have the lowest and highest annual rainfall, 573 mm and 1,973 mm. These two sites also have the lowest and the highest nail corrosion rate, 28 ± 19 g/m^2/year and 117 ± 61 g/m^2/year respectively.

However, some exceptions can be observed:

- Wellington had the third-highest annual rainfall, 1,589 mm. However, its nail corrosion rate was the second lowest, 45 ± 23 g/m^2/year.
- Waihau Bay had the third lowest annual rainfall, 1284 mm. However, its nail corrosion rate was the second highest, 92 ± 44 g/m^2/year.

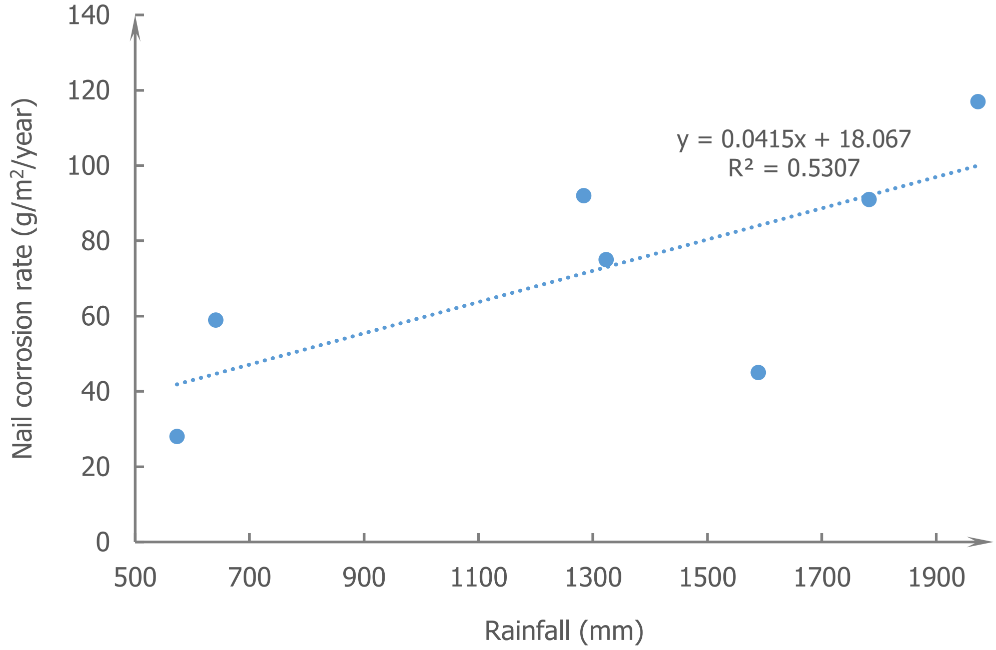

Figure 38. Correlation between annual rainfall and corrosion rate of the nail in timber fully exposed to the atmosphere.

Although rainfall is important, it is not the only factor when considering nail corrosion in timber. How the rainwater will be absorbed to wet the timber and how long the timber moisture content will stay above the threshold (18–20%) to sustain corrosion are more important.

Obviously, these two situations are significantly dependent on the drying-wetting cycles and kinetics in timber. Temperature and humidity of the surrounding air and local rain and wind patterns (direction, speed, quantity and wind run) will exert their influences.

In areas with heavy air pollution, the corrosion in timber could be more complicated:

- Timber blocks might receive and accumulate salt particles on their surfaces when exposed to severe marine environments. These salt particles may absorb moisture from the surrounding atmosphere, increasing surface timber moisture content. Meanwhile, they could attack the exposed nail heads. This may contribute to the high nail corrosion rates measured in Waihau Bay. However, the contribution from salt deposition might be limited, particularly in areas with light or moderate marine influences such as Auckland, Wellington and Greymouth.
- In geothermal areas such as Rotorua, high contents of H_2S and SO_2 in the air may contribute to the high nail corrosion rates. These two sulphur-containing species

could either directly attack the exposed nail head or attack the embedded shaft through inward transportation together with moisture. However, the synergistic effects of wind-induced timber drying on inwards transportation and interactions of wind-carried sulphur-containing species with timber and metal should be considered.

6.3 Comparative corrosivity between sheltered and exposed building positions

The corrosivity between sheltered and exposed positions on the building was compared by using the first-year corrosion rates of mild steel coupons installed at 0°, 45° and 90° angles and mild steel nails embedded into H3.2 CCA-treated timber blocks.

6.3.1 Mild steel coupons

In general, the following comparative corrosivity between sheltered and exposed positions on the building can be observed:

- exposed position >≈ sheltered position: Auckland, Wellington, Greymouth and Christchurch
- exposed position >> sheltered position: Rotorua.

In Waihau Bay, the situation is more complicated, and the comparative corrosivity is observed to be relevant with coupon inclination angle and wall orientation:

- exposed position > sheltered position: 0° inclined coupons on the north wall, 0° and 45° inclined coupons on the south wall, 45° inclined coupons on the west wall
- exposed position ≈ sheltered position: 90° inclined coupons on the north wall, 0°, 45° and 90° inclined coupons on the east wall, 0° inclined coupons on the west wall
- exposed position < sheltered position: 45° inclined coupons on the north wall, 90° inclined coupons on the south wall, 90° inclined coupons on the west wall.

This observation was a result of the complicated interactions between sea salt, rain/moisture and the mild steel surface. For example, the surface of the corroding mild steel surface in this severe marine environment is very rough. This rough surface of the 0° and 45° inclined coupons could collect salt particles easily. Meanwhile, rainwater or moisture condensation can persist on these surfaces within longer periods, which could:

- enhance dissolution and inward transportation of salt particles into the porous fast-growing corrosion product layers, accelerating corrosion, and
- help capture more salt particles from the air.

On the building in Rotorua, the gaseous sulphur-containing emissions (H_2S and SO_2) from active geothermal sources would be the main contributor to metal corrosion. H_2S and SO_2 can be involved into the chemical and/or electrochemical corrosion of susceptible metals through dry and/or wet processes. However, the presence of moisture or water on the material could significantly accelerate this attack:

- H_2S is weakly acidic when dissolved in water and is therefore corrosive because it can be involved in a series of chemical and/or electrochemical reactions. It has been shown that most copper alloys are resistant to dry H_2S but will have relatively poor performance when in contact with moist H_2S (Craig & Anderson, 2002).

- SO_2 does not react strongly with most metals in the absence of water. However, it has an extremely high solubility in water and can react with water and oxygen in wet atmosphere to form sulphuric acid (H_2SO_4). This substance is very corrosive to many building materials, including ferrous and non-ferrous metals, paints and stones (Gillette, 1975). For example, dissolution of SO_2 into rainwater or moisture layer on the mild steel surface would significantly accelerate corrosion attack.

Compared with the coupons installed in the exposed positions, the coupons installed in the sheltered positions were completely protected from direct rain. This drier micro-environment tended to reduce the dissolution of airborne H_2S and SO_2 and made their attack to metal more difficult. In this sense, a physical cover/shelter would be good to slow down corrosive attack to susceptible metallic components or structures in geothermal environments.

6.3.2 Nails in timber

Results derived from monitoring at all seven sites showed the following comparative corrosivity with nails in H3.2 CCA-treated timbers:

- exposed position > sheltered position.

As discussed in section 6.2.2, nail corrosion will be initiated and sustained only when the timber moisture is higher than the threshold (18–20%) and stays above this for extended periods.

The timber blocks in the sheltered building positions received none or extremely limited amounts of rainwater. Their moisture contents were governed by the equilibrium between temperature and the humidity of the air. This monitoring indicated that air temperature and humidity in the sheltered positions were relatively stable. Therefore, a high moisture content in timber was unlikely.

The timber blocks in the exposed positions can be wet when receiving wind-driven rain. This could increase timber moisture content to the levels that cannot be achieved by the equilibrium between temperature and humidity of the air.

On the other hand, the timber blocks in the sheltered positions may retain more deposits on their surfaces when compared with those in the exposed positions on the building. The deposits may absorb moisture from the air, increasing surface timber moisture content. Meanwhile, they could attack the exposed nail heads. However, this contribution to nail corrosion might be very limited, particularly when considering the actual nail head area exposed.

In general, it is expected that timbers in the exposed positions would have higher moisture contents over longer periods when compared with those in the sheltered positions. This leads to higher nail corrosion rates.

7. Concluding remarks

Some studies have been carried out to investigate material degradation under exposed and sheltered conditions using purpose-built testing structures. However, observations could be different with different tests. Therefore, it is difficult to understand the exact sheltering influences on material degradation.

Micro-environmental conditions over building envelopes can be different from those of the surrounding atmosphere. However, previous studies mainly focused on wind-driven rain and surface deposition.

In this study, monitoring has been carried out on seven buildings across New Zealand to investigate micro-environmental conditions over the building envelope. The following has been observed:

- The temperature on the building envelope had a larger variation than that of the surrounding atmosphere. The maximum temperatures measured on the building could be up to 40°C higher than the maximum ambient temperature.
- The temperature on the building envelope was position dependent. The exposed position would have a temperature higher than the sheltered position on the same wall. The temperature in the sheltered position generally had a smaller variation than that in the exposed position on the same wall.
- Time-of-wetness (ToW) showed a general trend of sheltered position on the building < exposed position on the building < surrounding atmosphere. ToW is an important factor that is extensively used in atmospheric corrosion studies and environmental corrosivity classification.
- The quantity of wind-driven rain collected on the building had an obvious dependence on prevailing/common wind direction, wall orientation and position on the wall. It was significantly lower than that of the reference rainfall. For example, the exposed-high position on the west wall of the building in Wellington received 2.6 mm rain. The total rainfall at this site was approximately 1,589 mm during the 1-year period.
- Surface deposition was dependent on the inclination angle of the collection surface and its position on the building. The 0° inclined (horizontal) surface always collected more deposits than the 45° and 90° inclined (vertical) surfaces no matter where they were installed (on the building or fully exposed to the atmosphere). The sheltered position always collected a larger amount of deposits than the exposed position on the same walls. This could be partially explained by the rain-washing effect. On the building in Wellington, the exposed positions on the building retained similar amounts of deposits with those fully exposed to the atmosphere although they received limited amounts of wind-driven rain. Surface deposition on the building decreased rapidly and could be correlated with the distance from the sea.
- UVA irradiation on the Wellington building was lower than that in the surrounding atmosphere. It also showed an obvious dependence on wall orientation. For example, the daily average UVA irradiation on the south wall was approximately one-sixth of that on the north wall and one-tenth of that in the open atmosphere.
- Corrosion rate of mild steel coupons showed a dependence on the inclination angle. The followings were observed in the present study:
  - On the building: 0° >≈ 45° > 90°.
  - Fully exposed to the atmosphere: 0° > 45° >≈ 90°.

It has been experimentally observed that the 0° inclined (horizontal) surface could retain more water for longer periods. This, together with a larger surface deposition, could contribute to a higher corrosion rate.

- The corrosivity of the surrounding atmosphere was slightly greater than or similar to that on the buildings in Auckland, Rotorua, Wellington, Greymouth, Christchurch and Lauder. The Rotorua site has strong geothermal influences, while the other sites (except Lauder) had light to moderate marine influences.
- The comparative corrosivity between the building and its surrounding atmosphere was complicated in Waihau Bay, a severe marine environment (ISO 9223 C4 – High). The corrosivity was observed as south and west walls > surrounding atmosphere > north and east walls. The south and west walls were more open to the severe marine environment than the north and east walls when considering the actual orientation of this building.
- Surface deposition on the buildings could be correlated to mild steel corrosion rate. In general, a higher deposition indicated a higher corrosion rate. However, this did not imply that marine-sourced salt is the only factor key to mild steel atmospheric corrosion in the present study. In areas with light marine influences, environmental moisture might play a more important role.
- Corrosion of nails in H3.2 CCA-treated timbers showed a general trend of fully exposed to the atmosphere > exposed positions on the building > sheltered positions on the building. This trend could be explained by the difference in the quantity of wind-driven rain in these positions.
- Corrosion rates of the mild steel coupons in the sheltered position were generally lower than or similar to those of the mild steel coupons in the exposed position on the same wall. This was particularly evident on the buildings that are located in areas with light to moderate marine influences and in areas with geothermal influences. In severe marine environments such as Waihau Bay, the situation was more complicated. Corrosion rates of mild steel coupons in the exposed position on the wall that was directly subject to marine influences could be lower than those of the coupons in the sheltered position. However, the opposite could still be observed.

These findings indicated that more attention should be paid to identify environmental factors key to material degradation on the building envelope. These factors should be included into and simulated appropriately by specific testing schemes.

Furthermore, sample arrangement and preparation details must be carefully controlled. This may include material type, surface finish, installation angle, position on the building and surface exposed (skyward or groundward).

In addition, the structures built for simulated or accelerated tests must be able to reflect the in-service conditions on actual buildings. For example, the wall cladding behind the sample could potentially affect wind flow and therefore salt deposition on the sample surface. This might be quite different from that occurring on the surface of the sample fully exposed to the atmosphere.

The present study improved our understanding of the micro-environments defined by NZS 3604:2011. This may provide better support to the material specification scheme used in relevant regulation documents and to the design of accelerated/simulated material performance testing methodology.

References

Alcantara, J., Chico, B., Diaz, I., de la Fuente, D. & Morcillo, M. (2015). Airborne chloride deposit and its effect on marine atmospheric corrosion of mild steel. *Corrosion Science*, 97, 74–88.

Axarli, K. N. (2005). *The influence of building design features on microclimatic modification in the warm periods of the year: Discussion based on temperature measurement*. Paper presented at the International Conference on Passive and Low Energy Cooling for the Built Environment, Santorini, Greece, 19–21 May 2005.

Badea, G. E., Setel, A., Sebesan, M., Cret, P., Lolea, M. & Covaci, H. (2011). *Corrosion study in atmospheric environment*. Paper presented at the 17th Building Services, Mechanical and Building Industry Days International Conference, Debrecen, Hungary, 13–14 October 2011.

Blocken, B., Abuku, M., Roles, S. & Carmeliet, J. (2009). *Wind-driven rain on building facades: Some perspectives*. Paper presented at the 5th European and African Conference on Wind Engineering (EACWE 5), Florence, Italy, 19–23 July 2009.

Carter, J. P., Linstrom, P. J., Flinn, D. R. & Cramer, S. D. (1987). *Effects of sheltering and orientation on the atmospheric corrosion of structural metals*. Paper presented at Corrosion'87, San Francisco, CA, 9–13 March 1987.

Castañeda, A., Corvo, F., Howland, J. J. & Marrero, R. (2018). Penetration of marine aerosol in a tropical coastal city: Havana. *Atmósfera*, 31(1), 87–104.

Chen, Y. S., Chiu, H. J., Chan, Y. W., Chang, Y. C. & Yang, C. C. (2013). The correlation between air-borne salt and chlorides cumulated on concrete surface in the marine atmosphere zone in North Taiwan. *Journal of Marine Science and Technology*, 21(1), 24–34.

Chen, Z. Y., Liang, D., Ma, G., Frankel, G. S., Allen, H. C. & Kelly, R. G. (2010). Influence of UV irradiation and ozone on atmospheric corrosion of bare silver. *Corrosion Engineering, Science and Technology*, 45(2), 169–180.

Chico, B., de la Fuente, D., Diaz, I., Simancas, J. & Morcillo, M. (2017). Annual atmospheric corrosion of carbon steel worldwide: An integration of ISOCORRAG, ICP/UNECE and MICAT databases. *Materials*, 10(6), 601.

Cole, I. S., Paterson, D. A. & Ganther, W. D. (2003). Holistic model for atmospheric corrosion – Part 1: Theoretical framework for production, transportation and deposition of marine salts. *Corrosion Engineering, Science and Technology*, 38(2), 129–134.

Cole, I. S., Lau, D., Chan, F. & Paterson, D. A. (2004). Experimental studies of salts removal from metal surfaces by wind and rain. *Corrosion Engineering, Science and Technology*, 39(4), 333–338.

Cole, I. S. & Ganther, W. D. (2006). Experimental determination of time taken for openly exposed metal surfaces to dry. *Corrosion Engineering, Science and Technology*, 41(2), 161–167.

Cole, I. S. & Paterson, D. A. (2007). Holistic model for atmospheric corrosion – Part 7: Cleaning of salt from metal surfaces. *Corrosion Engineering, Science and Technology*, 42(2), 106–111.

Craig, B. D. & Anderson, D. B. (2002). *Handbook of corrosion data* (2nd ed). Materials Park, OH: ASM International.

Delgado, J. M. P. Q., Guimaraes, A. S., de Freitas, V. P., Antepara, I., Koci, V. & Cerny, R. (2016). Salt damage and rising damp treatment in building structures. *Advances in Building Technologies and Construction Materials*, 1280894.

Deloitte Access Economics. (2018). *Cost of residential housing development: A focus on building materials*. Auckland, New Zealand: Deloitte Touche Tohmatsu.

Dinwoodie, J. M. (2001). Structure of timber and the presence of moisture. In J. M. Illston & P. L. J. Domone (Eds.), *Construction materials – their nature and behavior* (3rd ed.). London and New York: Spon Press.

Drozdz, S. A., Abbott, W. H. & Jackson, J. L. (2007). *Measuring the rate and impact of corrosion on DoD equipment and facilities*. Final Report on Project AR-F-311 for FY05. DoD Corrosion Prevention and Control Program. ERDC/CERL TR-07-18. Vicksburg, MS: US Army Corps of Engineers, Engineer Research and Development Center.

Duncan, J. R. & Balance, J. A. (1988). Marine salts contribution to atmospheric corrosion. In S. W. Dean & T. S. Lee (Eds.), *Degradation of metals in the atmosphere* (pp. 316–326). ASTM STP 965. Philadelphia, PA: American Society of Testing and Materials.

Ganther, W. D., Cole, I. S., Helal, A. M., Chan, W., Paterson, D. A., Trinidad, G., Corrigan, P., Mohamed, R., Sabah, N. & Al-Mazrouei, A. (2011). Towards the development of a corrosion map for Abu Dhabi. *Materials and Corrosion*, 62(11), 1066–1073.

Ge, H. & Krpan, R. (2007). Field measurement of wind-driven rain on a low-rise building in the coastal climate of British Columbia. Paper presented at the 11th Canadian Conference on Building Science and Technology, Banff, Canada, 21–23 March 2007.

Ge, H. & Krpan, R. (2009). *Wind-driven rain study in the coastal climate of British Columbia*. Burnaby, Canada: Building Science Centre of Excellence, British Columbia Institute of Technology.

Ghali, E. (2010). *Corrosion resistance of aluminium and magnesium alloys: Understanding, performance, and testing*. Hoboken, NJ: John Wiley & Sons.

Gillette, D. G. (1975). Sulfur dioxide and material damage. *Journal of the Air Pollution Control Association*, 25(12), 1238–1243.

Griffin, R. B. (2006). Corrosion in marine atmospheres. In S. D. Cramer & B. S. Covino, Jr. (Eds.), *ASM Handbook Volume 13C: Corrosion: Environments and industries* (pp. 42–60). Materials Park, OH: ASM International.

Hubbs, B. & Hircock, M. (2003). *Building envelope performance monitoring*. Paper presented at the 9th Canadian Conference on Building Science and Technology, Vancouver, Canada, 27–28 February.

Jett, O., Andrews, K., Barfield, W., Jett, R. & Abbott, W. H. (2007). *A preliminary evaluation of the effects of sheltering on corrosion*. Paper presented at the Tri-service Corrosion Conference, Denver, Colorado, 3–7 December 2007.

Jordan, D. L. (2010). Atmospheric corrosion testing. In R. W. Revie (ed.), *Uhlig's corrosion handbook* (3rd ed.) (pp. 1095–1100). Hoboken, NJ: John Wiley & Sons.

Kear, G., Wu, H. Z. & Jones, M. S. 2009. Weight loss studies of fastener materials corrosion in contact with timbers treated with copper azole and alkaline copper quaternary compounds. *Corrosion Science*, 51, 252–262.

King, G. A. & O'Brien, D. J. (1995). The influence of marine environments on metals and fabricated coated metal products, freely exposed and partially sheltered. In W. Kirk & H. H. Lawson (Eds.), *Atmospheric corrosion* (pp. 167–194). ASTM STP 1239. Philadelphia, PA: American Society for Testing and Materials.

Klassen, R. D. & Roberge, P. R. (2001). *The effects of wind on local atmospheric corrosivity*. Paper presented at CORROSION 2001, Houston, Texas, 11–16 March 2001.

Kreislova, K., Knotkova, D., Krivy, V. & Podjuklova, J. (2009). *The effect of differentiated exposure conditions on corrosion behaviour of weathering steel on bridges*. Paper presented at EUROCORR 2009, Nice, France, 6–10 September 2009.

Lenglet, M., Lopitaux, J., Leygraf, C., Odnevall, I., Carballeira, M., Noualhaguet, J. C., Guinement, J., Gautier, J. & Boissel, J. (1995). Analysis of corrosion products formed on copper in $Cl_2/H_2S/NO_2$ exposure. *Journal of the Electrochemical Society*, 142(11), 3690–3696.

Leonard, R. W. (2003). Continuous hot dip coatings. In S. D. Cramer & B. S. Covino, Jr. (Eds.), *ASM Handbook Vol 13A: Corrosion: Fundamentals, testing, and protection* (pp. 786–793). Materials Park, OH: ASM International.

Li, Z. W., Marston, N. J. & Jones, M. S. (2011). *Corrosion of fasteners in treated timber*. BRANZ Study Report SR241., Judgeford, New Zealand: BRANZ Ltd.

Li, Z. W., Marston, N. J. & Stokes, K. (2018). *Materials within geothermal environments*. BRANZ Study Report SR393. Judgeford, New Zealand: BRANZ Ltd.

Ma, Y. T., Li, Y. & Wang, F. H. (2009). Corrosion of low carbon steel in atmospheric environments of different chloride content. *Corrosion Science*, 51, 997–1006.

Macdonald, D. D., Sikora, E., Balmas, M. W. & Alkire, R. C. (1996). The photo-inhibition of localized corrosion on stainless steel in neutral chloride solution. *Corrosion Science*, 38(1), 97–103.

Mansfeld, F. (1979). Atmospheric corrosion rates, time-of-wetness and relative humidity. *Materials and Corrosion*, 30(1), 38–42.

Martins, T., Adolphe, L. & Bastos, L. (2014). *DOE sensitivity analysis of urban morphology factors regarding solar irradiation on buildings envelope in the*

Brazilian tropical context. Paper presented at the 30th International PLEA Conference, CEPT University, Ahmedabad, India, 16–18 December 2014.

McCafferty, E. (2010). *Introduction to corrosion science*. New York, NY: Springer.

Mohaddes Foroushani, S. S. (2013). *A numerical study of the effects of overhangs on the wind-driven rain wetting of building facades* (Master's thesis). Ryerson University, Toronto, Canada.

Morcillo, M., de la Fuente, D., Diaz, I. & Cano, H. (2011). Atmospheric corrosion of mild steel. *Revista de Metalurgia*, 47(5), 426–444.

Morillas, H., de Mendonca Filho, F. F., Derluyn, H., Maguregui, M., Gregoire, D. & Madariaga, J. M. (2020). Decay processes in buildings close to the sea induced by marine aerosol: Salt depositions inside construction materials. *Science of The Total Environment*, 721, 137687.

Moussa, S. O. & Hocking, M. G. (2001). The photo-inhibition of localized corrosion of 304 stainless steel in sodium chloride environment. *Corrosion Science*, 43(11), 2037–2047.

Nguyen, M. N., Wang, X. M. & Leicester, R. H. (2012). *Climate change impacts on corrosion of metal fasteners in timber construction*. Paper presented at the World Conference on Timber Engineering, Auckland, New Zealand, 15–19 July 2012.

Norberg, P. (2002). Surface moisture and time of wetness measurements. In J. W. Martin & D. R. Bauer (Eds.), *Service life prediction methodology and metrologies* (pp. 23–36). ACS Symposium Series 805. Washington, DC: American Chemical Society.

Oesch, S. & Heimgartner, P. (1996). Environmental effects on metallic materials: Results of an outdoor exposure programme running in Switzerland. *Materials and Corrosion*, 47, 425–438.

Orr, S. A., Young, M., Stelfox, D., Curran, J. & Viles, H. (2018). Wind-driven rain and future risk to built heritage in the United Kingdom: Novel metrics for characterising rain spells. *Science of the Total Environment*, 640–641, 1098–1111.

Pham, N. D., Kuriyama, Y., Kasai, N., Okazaki, S., Suzuki, K. & Nguyen, D. T. (2019). A new analysis of wind on chloride deposition for long-term aerosol chloride deposition monitoring with weekly sampling frequency. *Atmospheric Environment*, 198, 46–54.

PricewaterhouseCoopers. (2016). *Valuing the role of construction in the New Zealand economy*. Auckland, New Zealand: PricewaterhouseCoopers.

Qu, Q., Yan, C. W., Zhang, L., Wan, Y. & Cao, C. N. (2002). Influence of NaCl deposition on atmospheric corrosion of A3 steel. *Journal of Materials Science and Technology*, 18(6), 552–555.

Reserve Bank of New Zealand. (2020). *House prices and values*. Retrieved from https://www.rbnz.govt.nz/statistics/key-graphs/key-graph-house-price-values.

Riazi, H. R., Danaee, I. & Peykari, M. (2013). Influence of ultraviolet light irradiation on the corrosion behavior of carbon steel AISI 1015. *Metals and Materials International*, 19, 217–224.

Roberge, P. R. (1999). *Handbook of corrosion engineering*. New York, NY: McGraw-Hill.

Rowell, R. M. (2005). Moisture properties In *Handbook of wood chemistry and wood composites* (pp. 77–98). Boca Raton, FL: CRC Press.

Schindelholz, E., Risteen, B. E. & Kelly, R. G. (2014). Effect of relative humidity on corrosion of steel under sea salt aerosol proxies II. $MgCl_2$, artificial seawater. *Journal of the Electrochemical Society*, 161(10), C460–C470.

Schweitzer, P. A. (2006). Atmospheric corrosion. In *Fundamentals of metallic corrosion: Atmospheric and media corrosion of metals* (pp. 39–66). Boca Raton, FL: CRC Press.

Syed, S. (2006). Atmospheric corrosion of materials. *Emirates Journal for Engineering Research*, 11(1), 1–24.

Tran, T. T. M., Fiaud, C., Sutter, E. M. M. & Villanova, A. (2003). The atmospheric corrosion of copper by hydrogen sulphide in underground conditions. *Corrosion Science*, 45, 2787–2802.

Tzanis, C., Varotsos, C., Christodoulakis, J., Tidblad, J., Ferm, M., Ionescu, A., Lefevre, R. A., Theodorakopoulou, K. & Kreislova, K. (2011). On the corrosion and soiling effects on materials by air pollution in Athens, Greece. *Atmospheric Chemistry and Physics*, 11, 12039–12048.

WBK & Associates Inc. (2003). *Sulphur dioxide: Environmental effects, fate and behaviour*. Edmonton, Canada: Alberta Environment.

Wypych, G. (2013). *Handbook of materials weathering* (5th ed.). Scarborough, Canada: ChemTec Publishing.

Yousif, E. & Haddad, R. (2013). Photodegradation and photostabilization of polymers, especially polystyrene: Review. *SpringerPlus*, 2, Article number: 398.

Zelinka, S. L., Glass, S. V. & Derome, D. (2014). The effect of moisture content on the corrosion of fasteners embedded in wood subjected to alkaline copper quaternary treatment. *Corrosion Science*, 83, 67–74.

Zhang, H. M. (2011). *Building materials in civil engineering*. Cambridge, UK: Woodhead Publishing.

Zhang, X. G. (2005). Corrosion of zinc and zinc alloys. In S. D. Cramer & B. S. Covino, Jr. (Eds.), *ASM Handbook Vol 13B: Corrosion: Materials* (pp. 402–417). Materials Park, OH: ASM International.

Appendix A: Test buildings

Auckland

Two positions on each wall were chosen for monitoring on this building:

- Exposed positions: appropriately 0.23 m from the bottom of the wall cladding. Note the height of subfloor is approximately 0.76–1.03 m.
- Sheltered positions:
  - north and south walls: under the eave.
  - east and west walls: under window awning.

Figure 39. Monitoring positions on the test building in Auckland.

North - Sheltered
SD_{90}: 31.6-34.2µg/cm^2
$CR_{0(S)}$: 210g/m^2/yr
$CR_{0(G)}$: 129g/m^2/yr
CR_{45}: 188g/m^2/yr
CR_{90}: 132g/m^2/yr
$CR_{(Nail)}$: 11.9±4.2g/m^2/yr

N

North - Exposed
SD_{90}: 5.3-6.1µg/cm^2
$CR_{0(S)}$: 181g/m^2/yr
$CR_{0(G)}$: 142g/m^2/yr
CR_{45}: 171g/m^2/yr
CR_{90}: 125g/m^2/yr
$CR_{(Nail)}$: 32.6±11.1g/m^2/yr

West - Sheltered
SD_{90}: 27.9-32.2µg/cm^2
$CR_{0(S)}$: 148g/m^2/yr
$CR_{0(G)}$: 63g/m^2/yr
CR_{45}: 125g/m^2/yr
CR_{90}: 53g/m^2/yr
$CR_{(Nail)}$: 8.3±1.2g/m^2/yr

East - Sheltered
SD_{90}: 34.7-39.6µg/cm^2
$CR_{0(S)}$: 155g/m^2/yr
$CR_{0(G)}$: 89g/m^2/yr
CR_{45}: 147g/m^2/yr
CR_{90}: 86g/m^2/yr
$CR_{(Nail)}$: 11.9±2.4g/m^2/yr

West - Exposed
SD_{90}: 3.5-4.0µg/cm^2
$CR_{0(S)}$: 223g/m^2/yr
$CR_{0(G)}$: 120g/m^2/yr
CR_{45}: 167g/m^2/yr
CR_{90}: 77g/m^2/yr
$CR_{(Nail)}$: 41.4±16.3g/m^2/yr

East - Exposed
SD_{90}: 4.9-5.2µg/cm^2
$CR_{0(S)}$: 333g/m^2/yr
$CR_{0(G)}$: 170g/m^2/yr
CR_{45}: 193g/m^2/yr
CR_{90}: 101g/m^2/yr
$CR_{(Nail)}$: 47.2±28.8g/m^2/yr

South - Sheltered
SD_{90}: 55.5-59.9µg/cm^2
$CR_{0(S)}$: 157g/m^2/yr
$CR_{0(G)}$: 56g/m^2/yr
CR_{45}: 143g/m^2/yr
CR_{90}: 77g/m^2/yr
$CR_{(Nail)}$: 5.6±1.8g/m^2/yr

South - Exposed
SD_{90}: 14.8-18.4µg/cm^2
$CR_{0(S)}$: 281g/m^2/yr
$CR_{0(G)}$: 124g/m^2/yr
CR_{45}: 209g/m^2/yr
CR_{90}: 116g/m^2/yr
$CR_{(Nail)}$: 27.4±8.1g/m^2/yr

Atmospheric environment
T_{max}: 27.3°C
T_{min}: -0.6°C
ToW: 5147hrs
Rain: 1323mm

North
$CR_{0(S)}$: 346g/m^2/yr
$CR_{0(G)}$: 293g/m^2/yr
CR_{45}: 143g/m^2/yr
CR_{90}: 120g/m^2/yr
$CR_{(Nail)}$: 75.2±29.1g/m^2/yr

South
$CR_{0(S)}$: 330g/m^2/yr
$CR_{0(G)}$: 369g/m^2/yr
CR_{45}: 166g/m^2/yr
CR_{90}: 144g/m^2/yr

East
$CR_{0(S)}$: 322g/m^2/yr
$CR_{0(G)}$: 316g/m^2/yr
CR_{45}: 167g/m^2/yr
CR_{90}: 145g/m^2/yr

West
$CR_{0(S)}$: 330g/m^2/yr
$CR_{0(G)}$: 440g/m^2/yr
CR_{45}: 172g/m^2/yr
CR_{90}: 140g/m^2/yr

Figure 40. A summary of monitoring results obtained on the test building in Auckland.

Rotorua

Monitoring was performed in two positions on each of northeast and southeast walls without eaves or other sheltering structures:

- Low position: approximately 1 m from the ground
- High position: approximately 2.65 m from the ground.

Monitoring was performed in three positions on the southwest wall with a wide overhang:

- Low position: approximately 1 m from the ground
- High-exposed position: approximately 2.65 m from the ground
- High-sheltered position: approximately 2.65 m from the ground.

Monitoring was not performed on the northwest wall due to health and safety concerns.

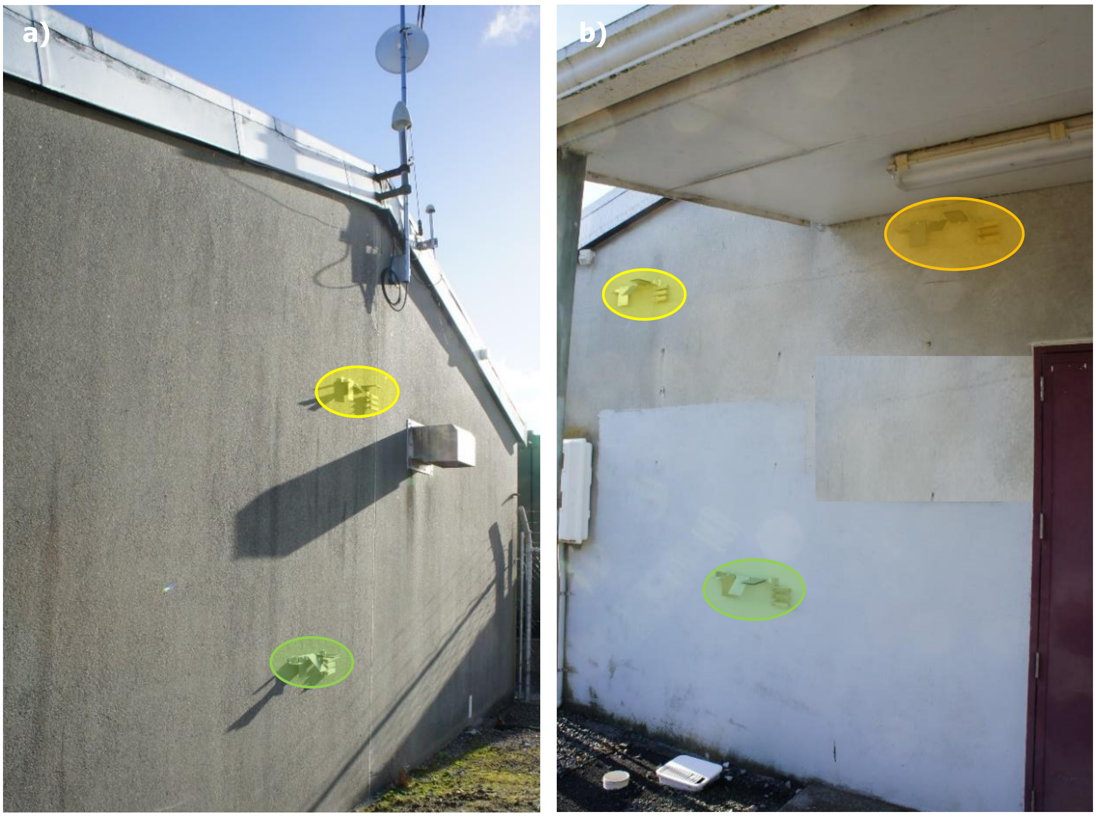

Figure 41. Monitoring positions on the test building in Rotorua.

Southwest – High – Exposed
H_2S: 4.2ppb
SO_2: 21.6ppb
$CR_{0(S)}$: 2568g/m^2/yr
$CR_{0(G)}$: 2541g/m^2/yr
CR_{45}: 710g/m^2/yr
CR_{90}: 261g/m^2/yr
$CR_{(Nail)}$: 36.5±15.0g/m^2/yr

Southwest – High – Sheltered
H_2S: 4.9ppb
SO_2: 26.1ppb
$CR_{0(S)}$: 266g/m^2/yr
$CR_{0(G)}$: 134g/m^2/yr
CR_{45}: 213g/m^2/yr
CR_{90}: 127g/m^2/yr
$CR_{(Nail)}$: 12.3±1.4g/m^2/yr

Northeast – High – Exposed
H_2S: 4.0ppb
SO_2: 24.9ppb
$CR_{0(S)}$: 1953g/m^2/yr
$CR_{0(G)}$: 3039g/m^2/yr
CR_{45}: 1897g/m^2/yr
CR_{90}: 578g/m^2/yr
$CR_{(Nail)}$: 160.0±21.7g/m^2/yr

Southwest – Low – Exposed
H_2S: 3.4ppb
SO_2: 31.4ppb
$CR_{0(S)}$: 2967g/m^2/yr
$CR_{0(G)}$: 2420g/m^2/yr
CR_{45}: 785g/m^2/yr
CR_{90}: 289g/m^2/yr
$CR_{(Nail)}$: 37.4±8.1g/m^2/yr

Southeast – High – Exposed
H_2S: 4.1ppb
SO_2: 28.3ppb
$CR_{0(S)}$: 3018g/m^2/yr
$CR_{0(G)}$: 1838g/m^2/yr
CR_{45}: 722g/m^2/yr
CR_{90}: 288g/m^2/yr
$CR_{(Nail)}$: 56.1±20.1g/m^2/yr

Northeast – Low – Exposed
H_2S: 4.8ppb
SO_2: 31.7ppb
$CR_{0(S)}$: 2626g/m^2/yr
$CR_{0(G)}$: 3356g/m^2/yr
CR_{45}: 1872g/m^2/yr
CR_{90}: 717g/m^2/yr
$CR_{(Nail)}$: 165.4±61.7g/m^2/yr

Southeast – Low – Exposed
H_2S: 5.1ppb
SO_2: 27.2ppb
$CR_{0(S)}$: 3763g/m^2/yr
$CR_{0(G)}$: 2312g/m^2/yr
CR_{45}: 1069g/m^2/yr
CR_{90}: 410g/m^2/yr
$CR_{(Nail)}$: 111.7±40.3g/m^2/yr

Atmospheric environment
T_{max}: 28.3°C
T_{min}: -2°C
ToW: 5139hrs
Rain: 1783mm

Southwest	Southeast	Northeast	Northwest
$CR_{0(S)}$: 3149g/m^2/yr	$CR_{0(S)}$: 3155g/m^2/yr	$CR_{0(S)}$: 2946g/m^2/yr	$CR_{0(S)}$: 2784g/m^2/yr
$CR_{0(G)}$: 3254g/m^2/yr	$CR_{0(G)}$: 2826g/m^2/yr	$CR_{0(G)}$: 3966g/m^2/yr	$CR_{0(G)}$: 3016g/m^2/yr
CR_{45}: 1655g/m^2/yr	CR_{45}: 1431g/m^2/yr	CR_{45}: 1387g/m^2/yr	CR_{45}: 1998g/m^2/yr
CR_{90}: 2079g/m^2/yr	CR_{90}: 1828g/m^2/yr	CR_{90}: 1634g/m^2/yr	CR_{90}: 1510g/m^2/yr

$CR_{(Nail)}$: 91.4±52.8g/m^2/yr

Figure 42. A summary of monitoring results obtained on the test building in Rotorua.

Waihau Bay

Monitoring was performed in two positions on each wall on this test building, which that is approximately 60 m east of the coastline:

- Sheltered positions: approximately 0.2 m below the eave
- Exposed positions: approximately 1.5 m below the eave.

Figure 43. Monitoring racks and devices on the north wall of the test building in Waihau Bay.

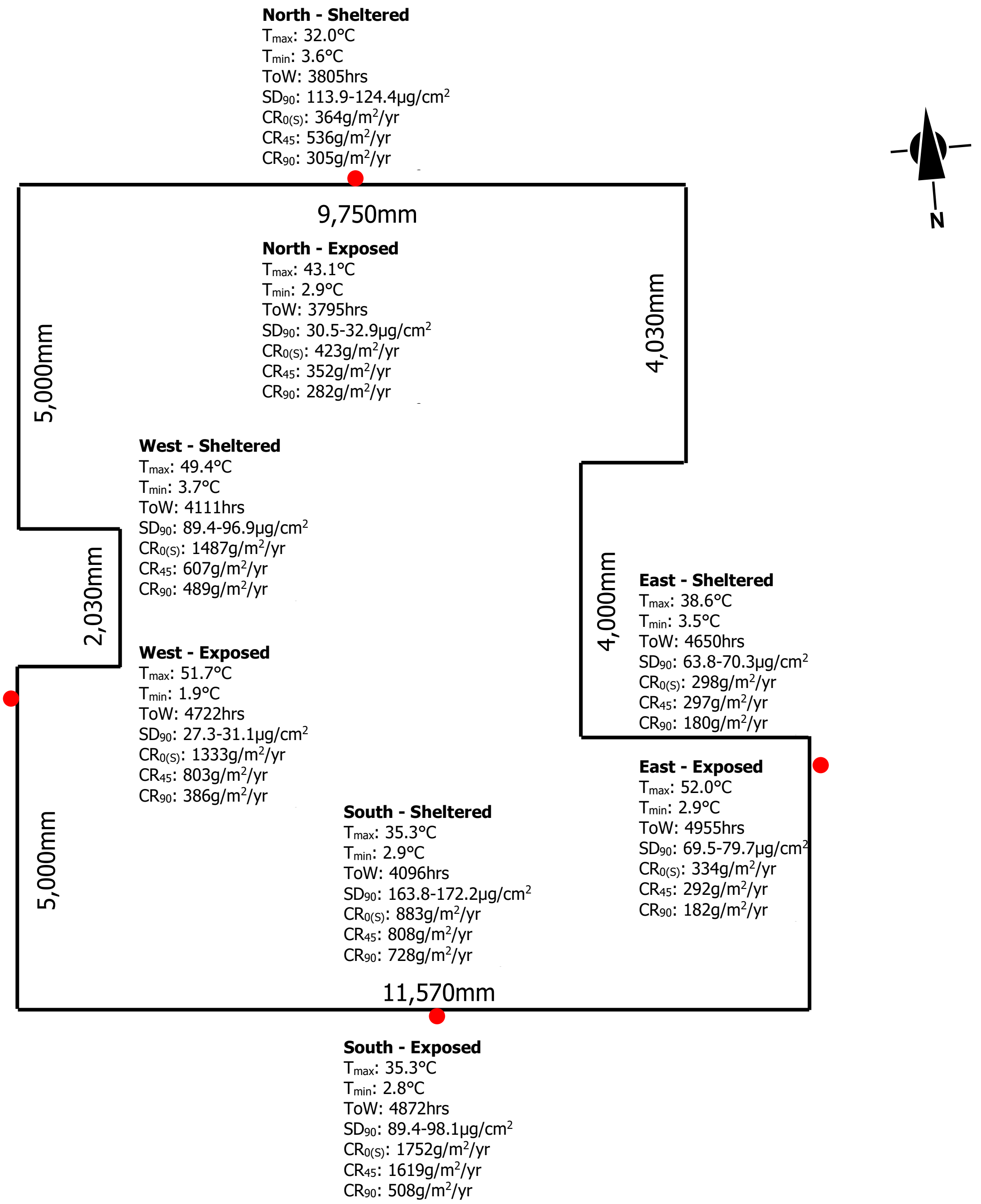

Atmospheric environment
T_{max}: 26.9°C
T_{min}: 2.5°C
ToW: 5526hrs
Rain: 1284mm

North	South	East	West
$CR_{0(S)}$: 694g/m^2/yr	$CR_{0(S)}$: 550g/m^2/yr	$CR_{0(S)}$: 533g/m^2/yr	$CR_{0(S)}$: g/m^2/yr
CR_{45}: 615g/m^2/yr	CR_{45}: 442g/m^2/yr	CR_{45}: 566g/m^2/yr	CR_{45}: 417g/m^2/yr
CR_{90}: 409g/m^2/yr	CR_{90}: 457g/m^2/yr	CR_{90}: 458g/m^2/yr	CR_{90}: 509g/m^2/yr

$CR_{(Nail)}$: 92±44g/m^2/yr

Figure 44. A summary of monitoring results obtained on the test building in Waihau Bay.

Wellington

Several positions have been selected for monitoring on this building (see Table 20 and Figures 45 and 46).

Table 20. Monitoring positions on the test building in Wellington.

Distance from eave (mm)	Wall			
	North	**South**	**East**	**West**
0	Sheltered	Sheltered	×	×
	N_S	S_S	×	×
640	Boundary	Boundary	Exposed - High	Exposed - High
	N_B	S_B	E_{EH}	W_{EH}
1,060	UVA	UVA	UVA	UVA
2,330	Exposed	Exposed	Exposed - Low	Exposed - Low
	N_E	S_E	E_{EL}	W_{EL}

x = no position was selected at this height for monitoring.

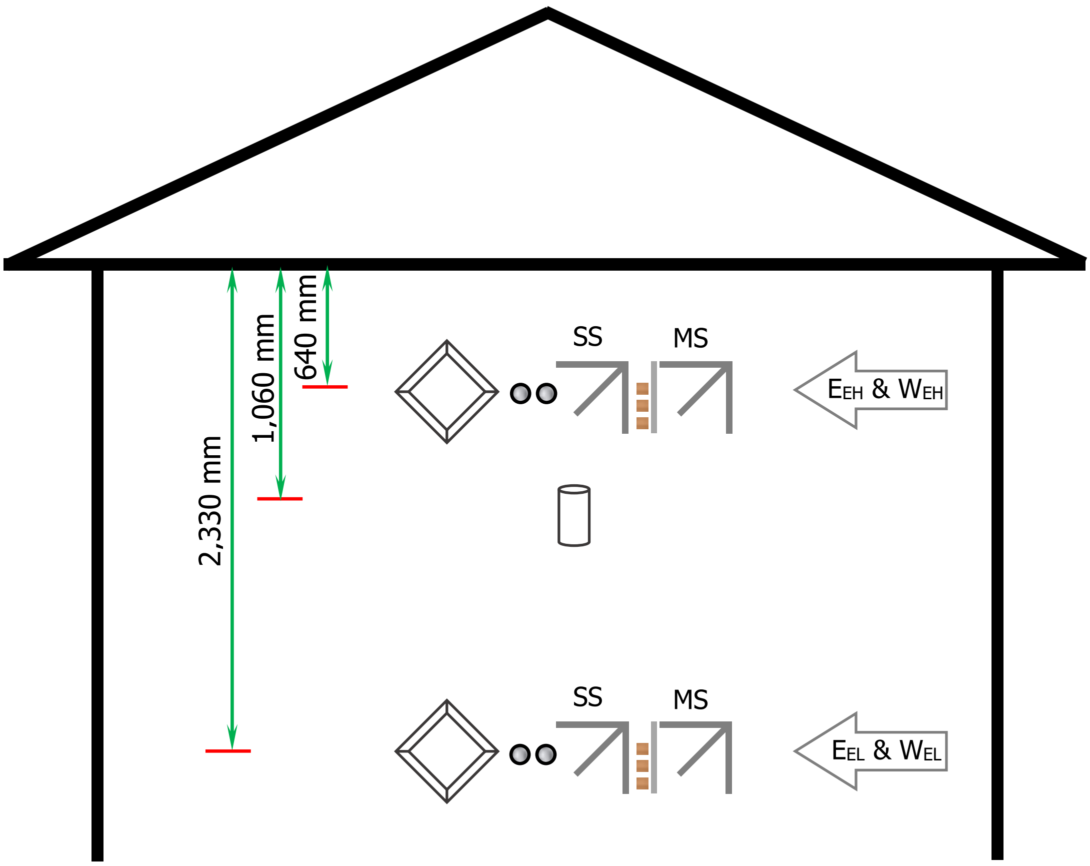

Figure 45. A schematic of positions of the coupons and monitoring devices installed on the west and east walls (not to scale).

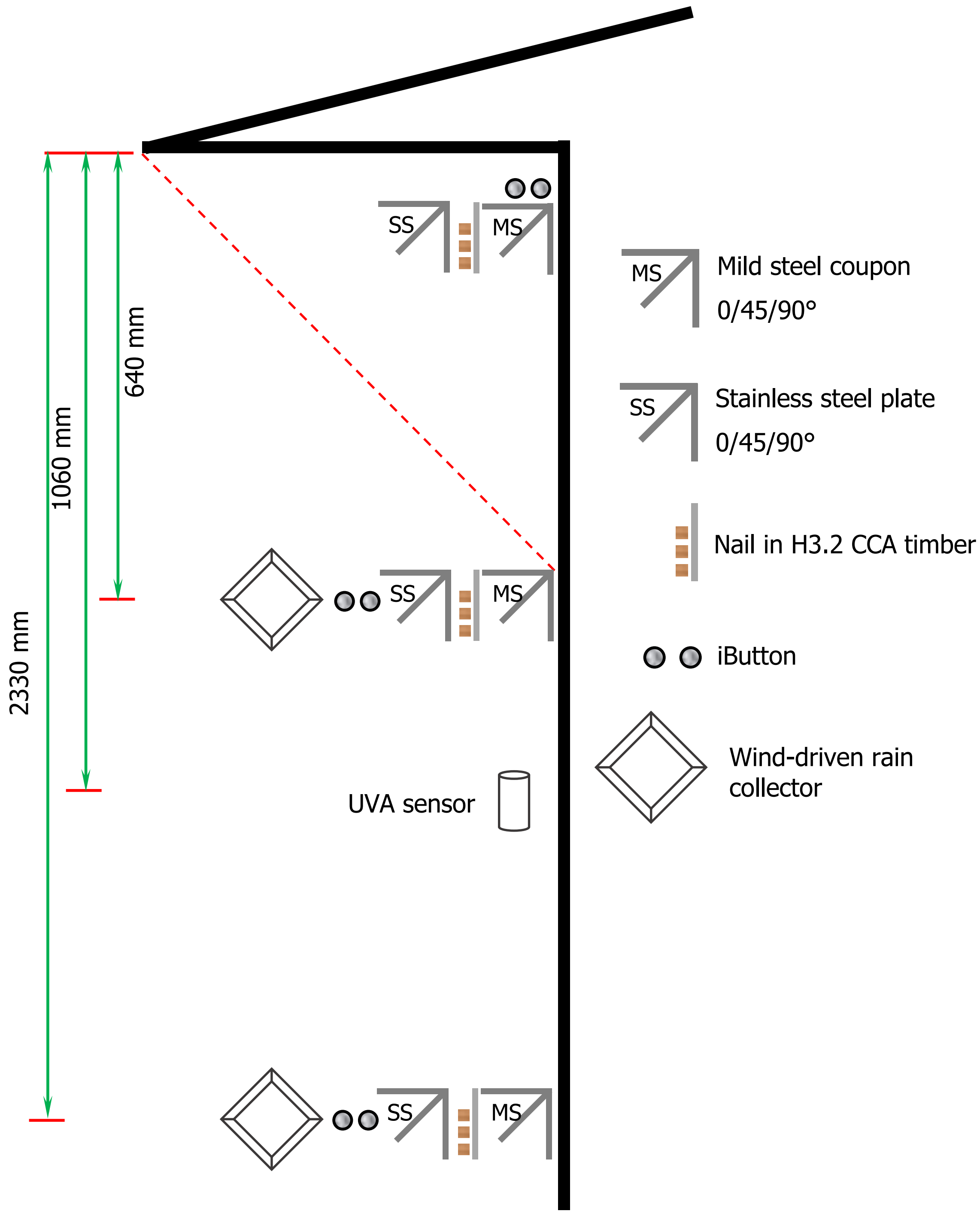

Figure 46. A schematic of positions of the coupons and monitoring devices installed on the north and south walls (not to scale).

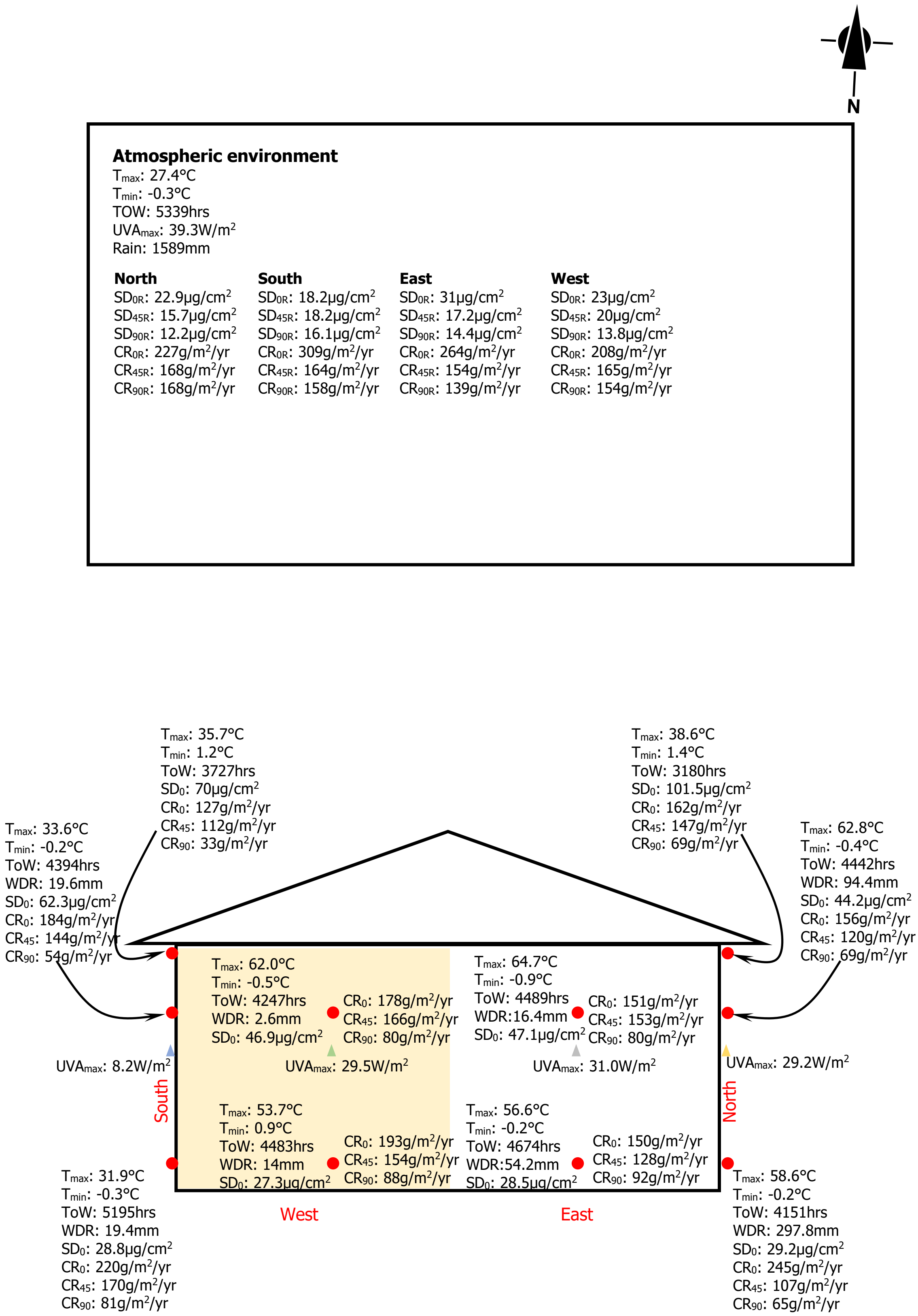

Figure 47. A summary of monitoring results obtained on the test building in Wellington.

Greymouth

Monitoring was performed in two positions on each wall:

- Sheltered positions: on the north and west walls, the sheltered positions were under the window awnings (see Figure 48a), and on the east and south walls, the sheltered positions were under the eaves (see Figure 48b).
- Exposed positions: approximately 1.1 m from the ground.

Figure 48. Monitoring positions on the (a) north and (b) east walls of the test building in Greymouth.

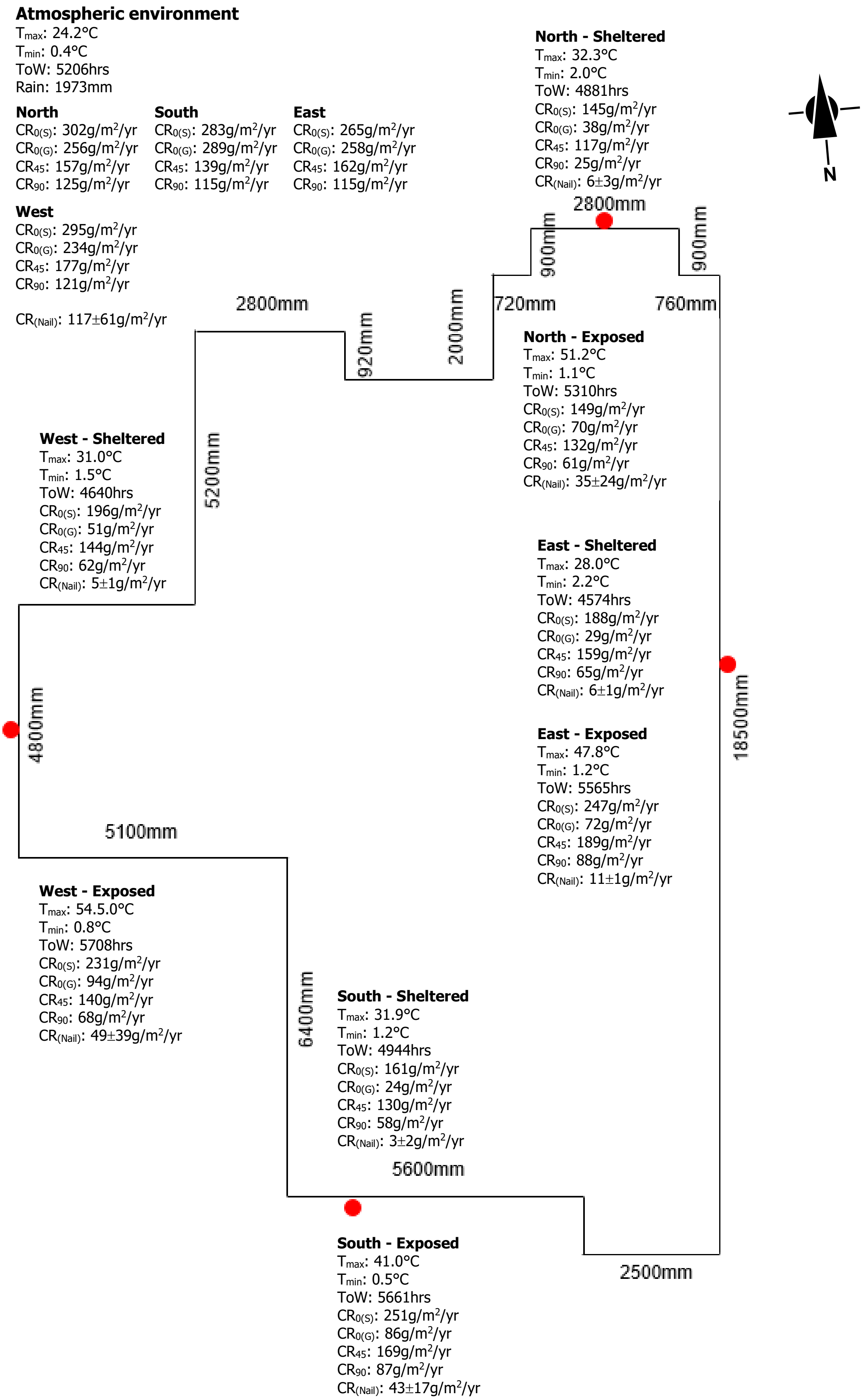

Figure 49. A summary of monitoring results obtained on the test building in Greymouth.

Christchurch

Monitoring was performed in two positions on each wall:

- Sheltered positions: under the eaves (approximately 0.44 m wide) and approximately 2.6 m from the top of the subfloor space
- Exposed positions: approximately 1 m from the top of the subfloor space.

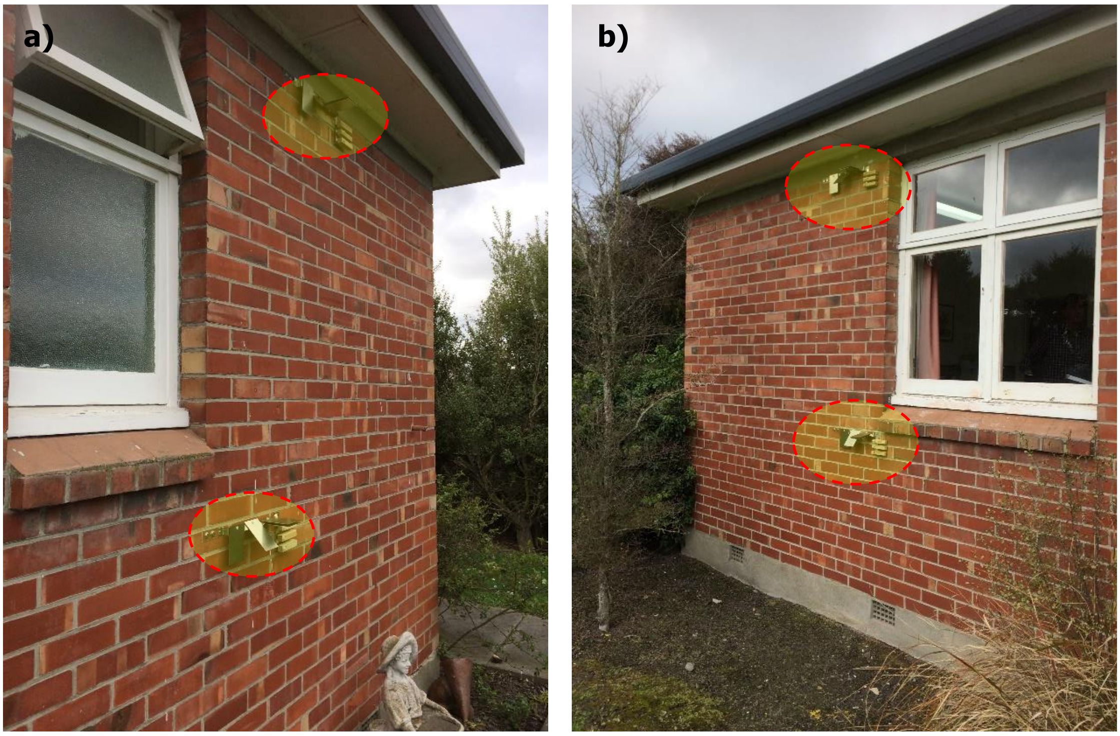

Figure 50. Monitoring positions on the (a) east and (b) west walls of the test building in Christchurch.

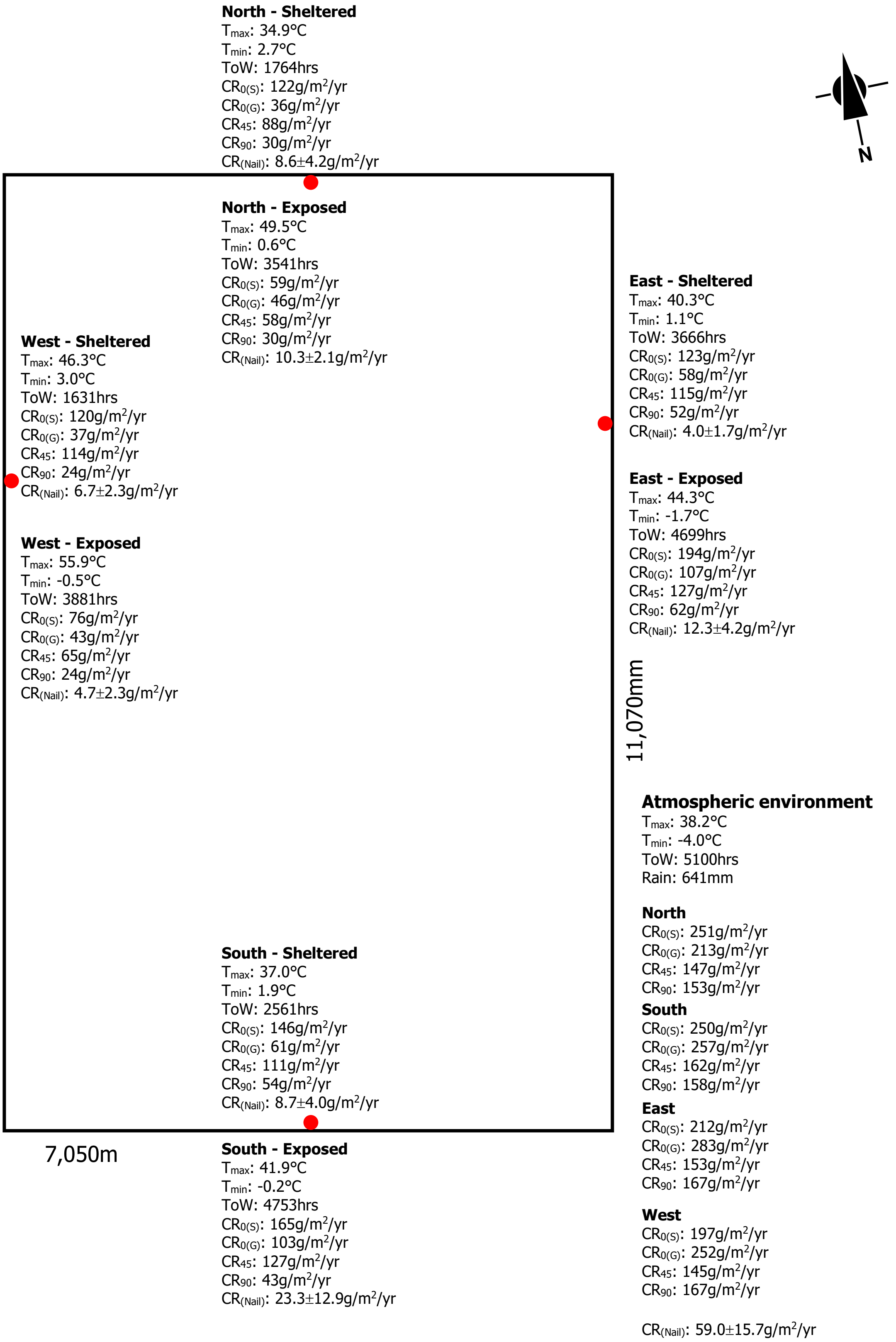

Figure 51. A summary of monitoring results obtained on the test building in Christchurch.

Lauder

Monitoring was performed in two positions on each wall:

- Sheltered positions: approximately 0.2 m from the bottom of the eave (approximately 0.6 m wide)
- Exposed positions: the same distance to the bottom of the brick veneer wall but distances to the ground varied:
  - north: 1.2 m
  - south: 1 m
  - east: 1.45 m
  - west: 0.8 m.

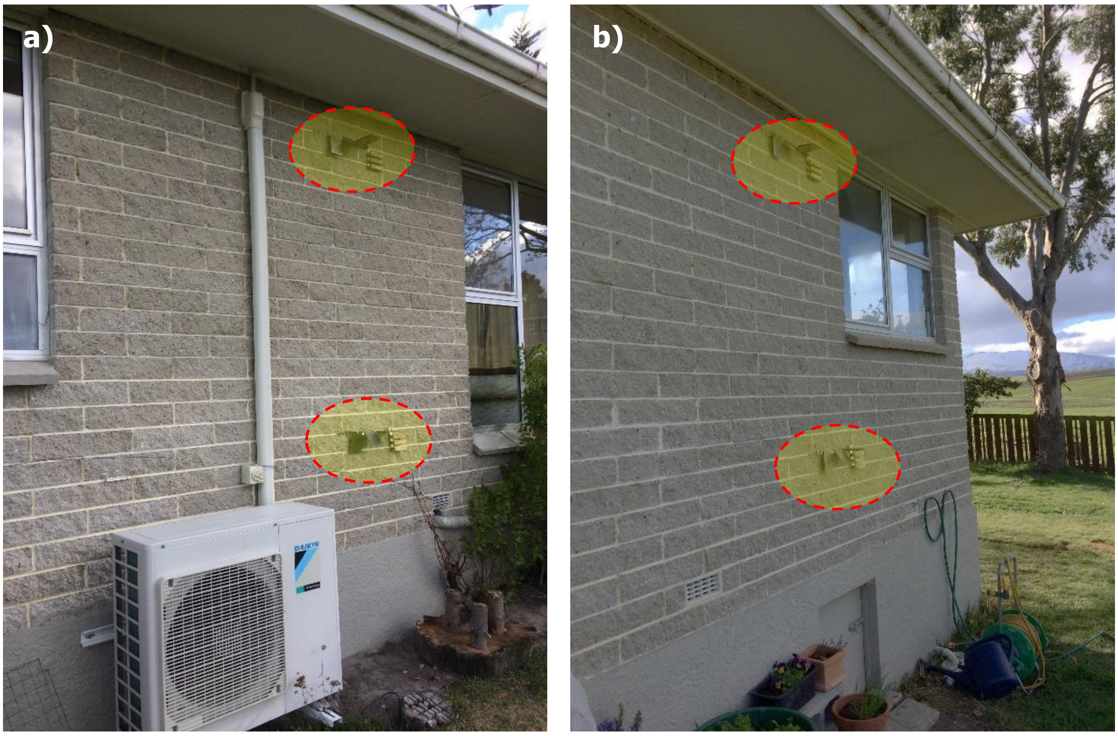

Figure 52. Monitoring positions on the (a) north and (b) east wall of the test building in Lauder.

Atmospheric environment
T_{max}: 32.2°C
T_{min}: -6.6°C
ToW: 3166hrs
Rain: 573mm

North
$CR_{0(S)}$: 9g/m^2/yr
$CR_{0(G)}$: 7g/m^2/yr
CR_{45}: 2g/m^2/yr
CR_{90}: 2g/m^2/yr

South
$CR_{0(S)}$: 11g/m^2/yr
$CR_{0(G)}$: 7g/m^2/yr
CR_{45}: 12g/m^2/yr
CR_{90}: 1g/m^2/yr

East
$CR_{0(S)}$: 11g/m^2/yr
$CR_{0(G)}$: 7g/m^2/yr
CR_{45}: 2g/m^2/yr
CR_{90}: 2g/m^2/yr

West
$CR_{0(S)}$: 17g/m^2/yr
$CR_{0(G)}$:
17g/m^2/yr
CR_{45}: 2g/m^2/yr

$CR_{(Nail)}$: 28±19g/m^2/yr

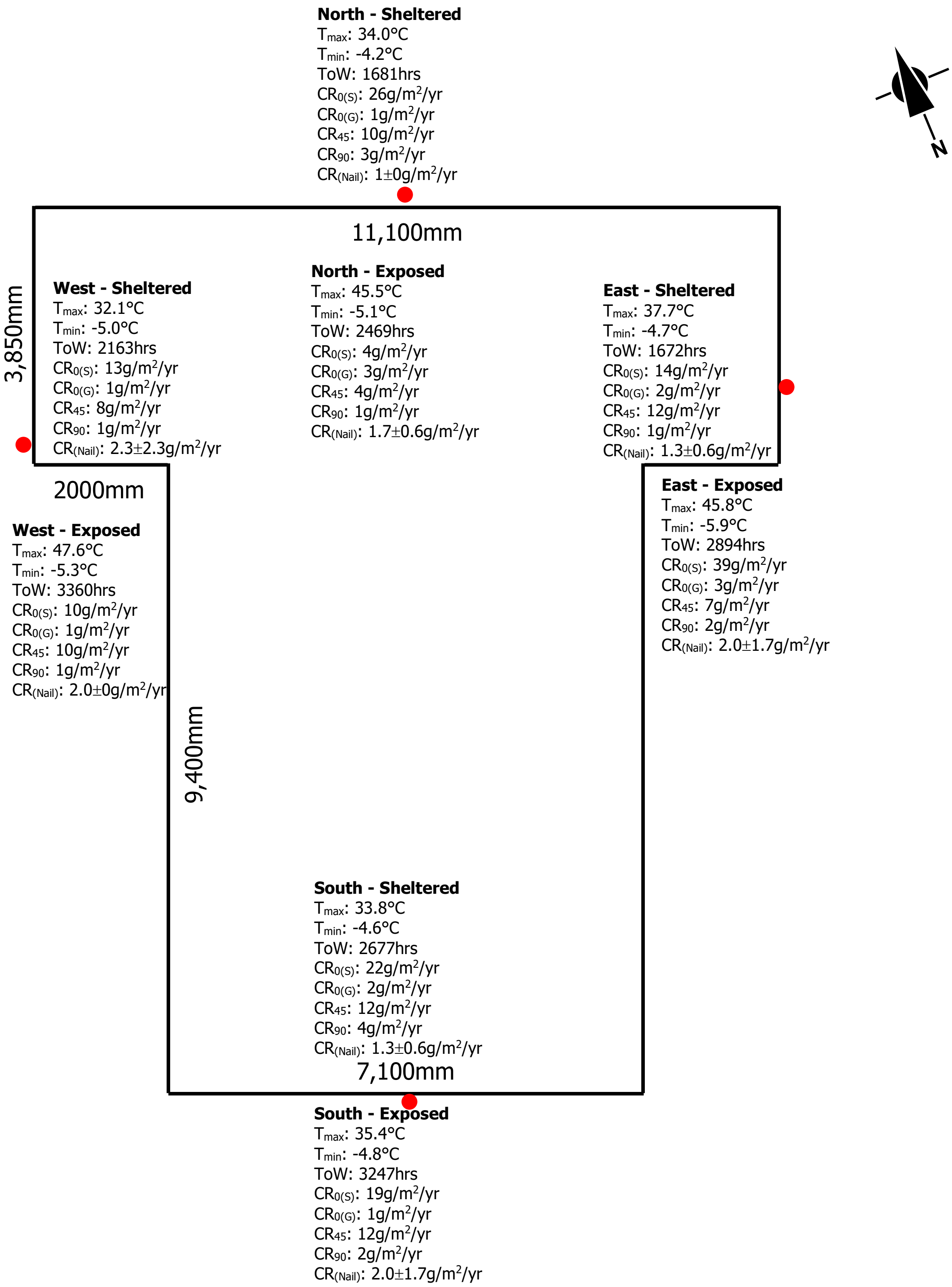

Figure 53. A summary of monitoring results obtained on the test building in Lauder.